In presenting the dissertation as a partial fulfillment of the requirements for an advanced degree from the Georgia Institute of Technology, I agree that the Library of the Institute shall make it available for inspection and circulation in accordance with its regulations governing materials of this type. I agree that permission to copy from, or to publish from, this dissertation may be granted by the professor under whose direction it was written, or, in his absence, by the Dean of the Graduate Division when such copying or publication is solely for scholarly purposes and does not involve potential financial gain. It is understood that any copying from, or publication of, this dissertation which involves potential financial gain will not be allowed without written permission.

7/25/68

THE DAMPING EFFECTS OF VISCOELASTIC MATERIALS ON THE TRANSVERSE VIBRATIONS OF BEAMS AND PLATES

A THESIS

Presented to

The Faculty of the Graduate Division

by

Britt Kendall Pearce

In Partial Fulfillment

of the Requirements for the Degree

Doctor of Philosophy

in the School of Mechanical Engineering

Georgia Institute of Technology

February, 1969

THE DAMPING EFFECTS OF VISCOELASTIC MATERIALS ON

THE TRANSVERSE VIBRATIONS OF BEAMS AND PLATES

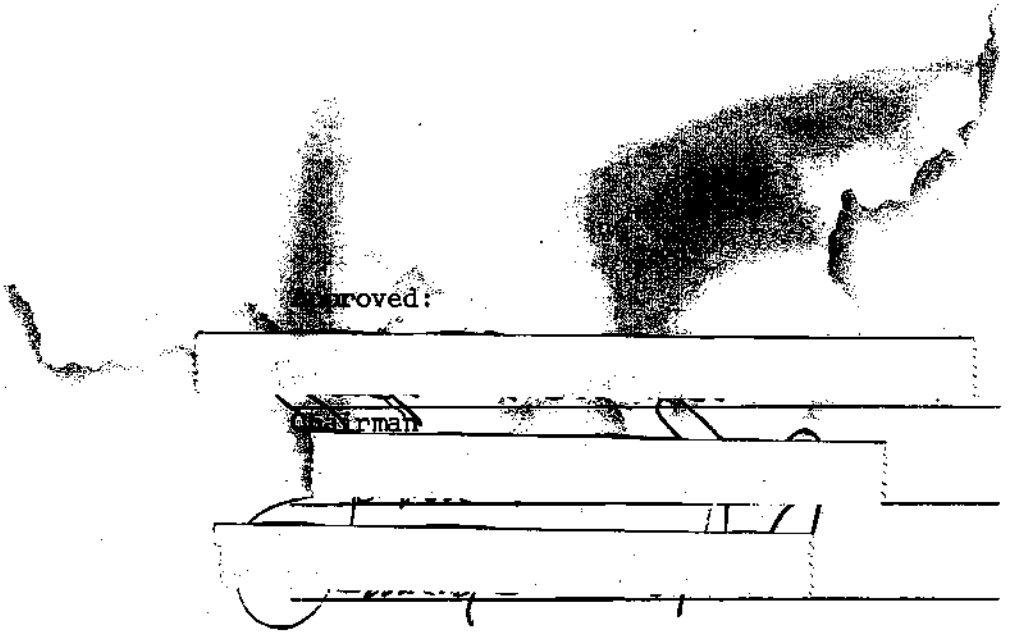

Date approved by Chairman: Feb 20, 1969

This thesis is dedicated to my parents

and my devoted wife, Carey.

ACKNOWLEDGMENTS

Special thanks go to the thesis advisor, Dr. Joseph R. Baumgarten, without whose encouragement, enthusiasm, generous contribution of time, and competent advice this thesis would not have been possible. Thanks are also due the other members of the reading committee: Dr. Edward R. Wood, Dr. John H. Murphy, Dr. W. M. Williams, and Dr. H. L. Johnson.

The author is grateful to the School of Mechanical Engineering of Georgia Institute of Technology for the support given him in the form of (1) a three-year NASA Traineeship, (2) a one-year NDEA Fellowship, and (3) a NASA Research Grant NsG657 Project B 1104.

Thanks are also expressed for the encouragement and support given by the author's wife and parents.

TABLE OF CONTENTS

LIST OF TABLES

Table | Page

LIST OF ILLUSTRATIONS

NOMENCLATURE

English Symbols		Units
a	length of beam or plate	in.
A	area	$in.^2$
b	width of beam or plate	in.
E_b	Young's modulus of elastic (metal) beam material	psi
E_c	complex modulus of viscoelastic material (see Equations 7 and 17)	psi
E_d	dynamic (loss) modulus of viscoelastic material	psi
E_p	Young's modulus of elastic (metal) plate material	psi
E_s	Young's (static) modulus of viscoelastic material	psi
$F_m(x)$	characteristic beam function	
g	acceleration of gravity	$in./sec.^2$
$G_m(x)$	characteristic beam function	
h	thickness of viscoelastic coating	in.
L	energy dissipated	in.-lb.
t	thickness of elastic (metal) beam or plate material	in.
T	kinetic energy	in.-lb.
u,v,w	displacement of a point of the system in the x,y,z directions, respectively	in.

English Symbols		Units
$\bar{u},\bar{v},\bar{w}$	displacement of neutral axis in the x,y,z directions, respectively	in.
U_m,V_m,W_m	undetermined coefficients of the deflections	
V	strain (potential) energy	in.-lb.
x,y,z	Cartesian coordinates	
$\bar{z}$	distance of neutral axis from the interface of coating and metal (see Figure 7)	in.
z_1,z_2,z_3	distances of coating and metal surfaces from the neutral axis (see Figure 7)	in.

Greek Symbols		
α	exponential damping constant	1/sec.
α_m,β_m	constants depending on mode and end conditions	-,1/in.
γ	weight per unit volume	lb./in.^{3}
δ	logarithmic decrement	
ε	strain	in./in.
η	loss factor	
ν	Poisson's ratio	
ρ	mass per unit area	lb.-sec.^{2}/in.^{3}
σ	stress	psi
τ	time	sec.
ϕ	damping coefficient	psi-sec.
ω	undamped natural frequency	rad./sec.
$\bar{\omega}$	damped natural frequency	rad./sec.

Subscripts

b	elastic (metal) beam material
c	viscoelastic material
m,n	mode numbers
p	elastic (metal) plate material

SUMMARY

It has been found that a number of materials, such as plastics, resins, adhesives, and rubbers have the ability to dissipate energy in a mechanical system by converting energy of motion into heat energy. These materials exhibit both viscous and elastic behavior and are consequently termed viscoelastic materials. Incorporation of such a material with an elastic structure is often beneficial in abating troublesome vibration. However, a designer needs some criteria for determining the damping effects that a given amount of viscoelastic coating produces other than pure guesswork.

The primary objective of this investigation is to relate the damping produced by an unconstrained layer of viscoelastic material (in terms of logarithmic decrement) to the thickness of the viscoelastic layer applied to a beam or plate and to the properties and dimensions of the two materials. It is of primary importance to present this relation in the form of equations or curves from which design data may be easily obtained. This had previously been done for beams subject to "light" damping; however, the problem is here approached using a different method in order to consider not only beams but also plates in addition to considering damping of higher magnitude.

Other considerations are: (1) further investigation concerning the existence of an optimum thickness ratio beyond which addition of viscoelastic material results in a decrease in damping, (2) relation of

damping to the "viscoelasticity" of a material, (3) comparison of coatings on one side only with two symmetric coatings. The investigation is limited to a study of the free vibration (in the fundamental mode) of beams and plates with no constraints. The effects of rotary inertia and vertical shear are neglected, and thin beam and plate theory applies in the derivations.

The analytical solution is formulated using an energy method which is quite similar to Rayleigh's method for determining the natural frequencies of vibration of homogeneous, undamped beams. However, in this case, the beams (and plates) are nonhomogeneous and damped. (It is assumed that the damping is linear.) An expression is developed which accounts for the energy dissipated by the coating, then the principle of conservation of energy is applied. This results in a relationship between the exponential damping constant and the dimensions and properties of the beam (or plate) and, therefore, the solution desired.

The solutions developed include:

(1) Computer solutions. The logarithmic decrement and damped natural frequency of a given composite beam or plate may be calculated for light or heavy damping and for coatings on one or both sides.

(2) Curves. An approximate value of the logarithmic decrement may be obtained for a given composite beam or plate with light or heavy damping and for coatings on one or both sides.

(3) Approximate solutions. The logarithmic decrement and natural frequency of a given composite beam or plate subject to "light" damping may be calculated for coatings on one or both sides.

Experimental measurement of the natural frequencies and logarithmic decrements of a number of different composite beams and plates verifies that the relations developed allow one to predict both quantities accurately knowing the properties and dimensions of the materials employed.

It was also found that an optimum thickness ratio actually exists. If additional coating material is applied above this point, damping decreases rather than increases. (This results because of the shift of the neutral axis.) The value of the optimum thickness ratio may be found analytically for beams and plates with coatings on one side only (for light damping); however, no optimum thickness ratio exists for beams and plates with symmetric coatings.

The damping of a beam composed of two given materials and having a given ratio of coating thickness to metal thickness is comparable in magnitude to that of a plate composed of the same two materials and having the same thickness ratio.

For small (and moderate) thickness ratios, it is more efficient to employ all the viscoelastic coating on one side of a beam or plate rather than split it equally between the two sides. However, for large thickness ratios it is sometimes more effective to use two symmetric coatings.

Damping depends directly upon only three dimensionless ratios: coating thickness divided by metal thickness, loss modulus of the viscoelastic coating divided by the Young's modulus of the coating, Young's modulus of the coating divided by Young's modulus of the metal.

The results of this investigation can be extended to consider higher modes and other end conditions with very little effort.

CHAPTER I

INTRODUCTION

Background

Mechanical vibration deals with the oscillatory motion of a physical system and is determined by three properties: the mass, stiffness, and damping of the system. At certain frequencies the restoring forces (stiffness) and inertia forces (mass) balance each other and the system is said to be in resonance. In many structures, such as those in airplanes and guided missiles, undesirable vibrations are transmitted from the jet engine or from the turbulence of the air to the parts of the device carrying sensitive electronic instruments. Naturally, such vibration must be minimized to as great a degree as possible.

There are three general methods which may be used in the design of a system to avoid or control resonant response:

(a) The system may be detuned by designing the components in such a way that the natural frequencies of adjacent elements differ by as large a magnitude as possible.

(b) The system may be strengthened by increasing the stiffness at critical points.

(c) The system may be damped by converting some of the mechanical energy to heat energy.

The use of structural damping (c) offers a greater degree of flexibility in the control of resonant response when vibrations in a structure are random in amplitude and frequency.

The increased need for reducing vibrations in structural members produced by broad-band sources, such as the response of aircraft and missile frames to rocket excitation, has led to the employment of viscoelastic coatings. Such coatings serve to damp out the induced motion helping to prevent fatigue and eliminate annoyance while making little contribution to the weight of the structure. A clear understanding of the dynamic behavior of such a system is, of course, necessary for its proper application.

There are two methods of employing viscoelastic materials to dissipate energy—*unconstrained* and *constrained* layer damping. The unconstrained system (Figure 1) consists of a base member, used for its structural characteristics, and a viscoelastic layer, used for its damping ability. When the base undergoes flexure, dissipation of energy is produced by the extension and compression of the damping layer. The constrained-layer system or so-called "sandwich" (Figure 2) consists of two stiff members separated by a viscoelastic layer. Relative motion between the two stiff layers causes shearing of the viscoelastic material dissipating some of the vibrational energy of the system. Constrained-layer damping is actually more efficient than unconstrained. However, there are reasons for interest in the latter:

(a) In practical applications a single layer is much simpler to apply, especially when not a step in the original construction.

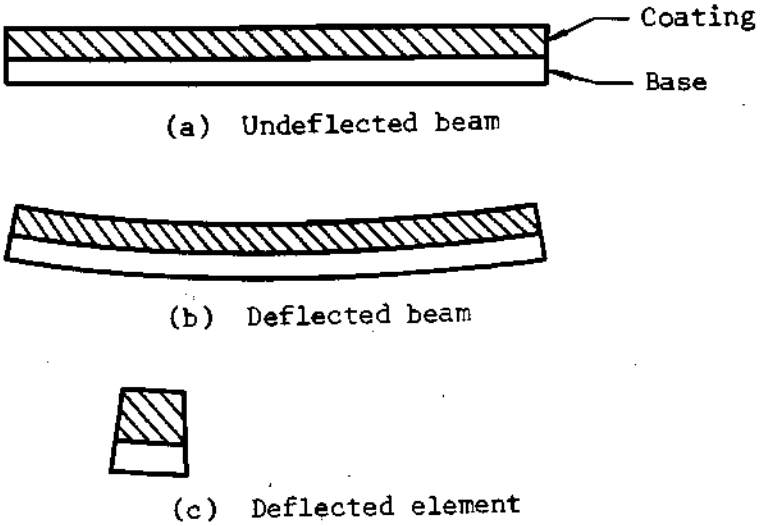

Figure 1. Unconstrained Viscoelastic Coating

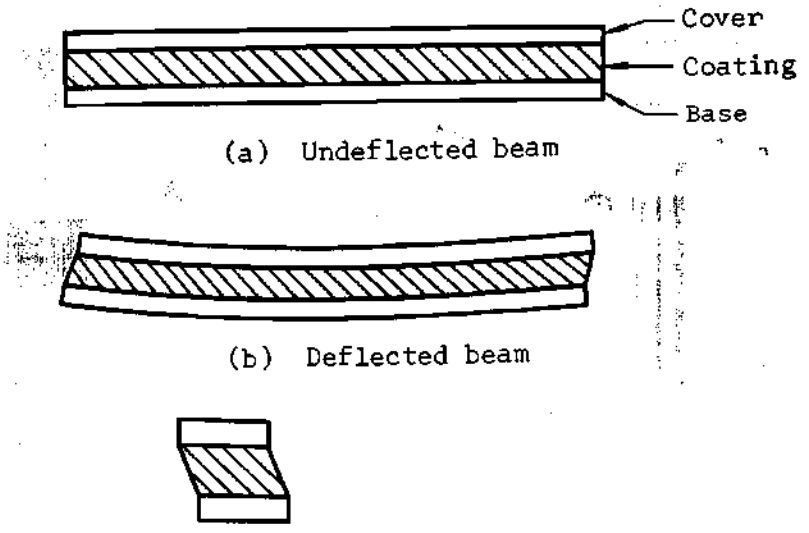

Figure 2. Constrained Viscoelastic Coating

(b) Excessive weight is a most undesirable burden in the majority of cases.

This investigation involves only the case of *unconstrained* viscoelastic layers.

Review of Literature

There have been a number of investigations to determine the damping effects produced by viscoelastic materials for both the constrained and unconstrained cases. The majority are concerned with beams only and experimental results, in comparison to analytical, have not been convincing in most cases.

Constrained Case

Probably the most significant work in this area is that of Kerwin (1)* who studied the damping effectiveness or loss factor, η, of a single constrained viscoelastic layer. (Loss factor is one of the most common measures of damping. When multiplied by π it is equivalent to logarithmic decrement or δ as it is often denoted.) The definition of η in terms of the fractional decay rate in space of the bending-wave power was the basis for the energy approach used. An expression was developed for decay rate of power based on the dissipation of power through the shear motion of the damping layer. Then loss factor was related to the dimensions and properties of the three layers making up the bar. Kerwin and other investigators made the following assumptions (unless otherwise specified) which are of special importance in the area

---

*Numbers in parentheses refer to references in Literature Cited.

of viscoelastic damping:

(a) The viscoelasticity may be represented by a complex modulus, i.e., $E_c = E_s + iE_d$.

(b) E_d is much smaller than E_s, i.e., $\eta_c \leq 0.1$.

Ungar and Ross (2) extended this work by considering multiple constrained layers of damping tapes rather than a single one. It was found that a single tape covered by a thick constraining layer is more effective than several thin layers involving the same amount of material. The results of neither investigation are easily applied by a designer.

Whittier (3) investigated a single constrained layer separated from the base by a spacing layer, the purpose of the spacer being to increase the extension of the viscoelastic material. The analysis involved setting up and solving a fifth order differential equation. Experimental and analytical values were not in good accord.

The damping of an aluminum honeycomb beam was evaluated by Mead (4). An energy approach showed that damping in the core arises not only by virtue of the shearing strains but also by virtue of the bending strains.

Thorn's contribution (5) was to take the theory developed by Kerwin (1) and discuss in detail the application of this to the design of typical structures. It was assumed that the theory was valid for both beams and plates.

Free vibration of sandwich beams with butyl rubber and polyvinyl chloride cores was evaluated by Jones, Salerno, and Savacchio (6). Hamilton's Principle was employed to derive the equations of motion.

These were solved by assuming η_c was small (a common assumption mentioned previously). Experimental and analytical results showed fair agreement. These men are presently investigating plates of the same composition.

DiTaranto (7) also used a differential equations approach, but assumed a finite series solution. This led to an expression for composite loss factor, η. It was found that η is independent of end conditions and mode shapes.

Unconstrained Case

(a) Beams. The most impressive work done related to the subject of viscoelastic damping has been Oberst's study (8) of the bending vibrations of thin beams covered on one side by a layer of damping material. Experimental and analytical results were in excellent agreement and the results were presented in a form readily usable by a designer. Simple flexure theory was used and it was assumed that damping was small ($\eta_c \leq 0.1$). This led to an expression for loss factor as a function of the properties and dimensions of the beam. Theoretically, an optimum coating thickness was shown to exist. However, this was not verified by experiment.

An energy approach by Lienard (9) investigated both linear and non-linear damping; however, it yielded little of design value.

An analysis of round bars coated with a viscoelastic material was formulated by Plass (10). The differential equation of motion of the system was combined with the equation describing the viscoelastic behavior yielding a third order differential equation. A solution was assumed which led to a third power polynomial in α, the damping constant of the system, upon substitution in the differential equation. Solution

of this gave the amount of damping which results. Plass compared his theoretical results with the experimental results of another investigator and found agreement to be fair. A unique feature of this investigation was the use of a combination Kelvin-Maxwell model to describe viscoelastic behavior.

Lal (11) attempted to extend Plass' work by accounting for the effects of rotary inertia and transverse shear in the beam. In this case, a fifth order differential equation resulted; this was solved by finite Fourier transforms.

(b) Plates. A purely experimental investigation of the damping of steel plates coated with a layer of bitumen emulsion containing schist powder or similar products was conducted by Van Itterbeek and Myncke (12). This was limited to coatings which were thin in relation to the thickness of the metal plate.

Another experimental investigation by Giddens (13) probed the effect of damping materials on dynamic stresses in flat panels. The stresses at various points in the plates were measured for different thicknesses of viscoelastic coatings and over a wide range of frequencies. It was found that, generally, the stresses were reduced significantly with the addition of viscoelastic materials.

Hertelendy and Goldsmith (14) presented a purely analytical investigation for a plate with symmetrical coatings (Figure 3). In this investigation three approaches were employed:

(a) An exact solution by the Rayleigh-Lamb equations;

(b) an approximate solution by the Timoshenko beam equation;

(c) an approximation by a perturbation solution assuming the coating to be a membrane.

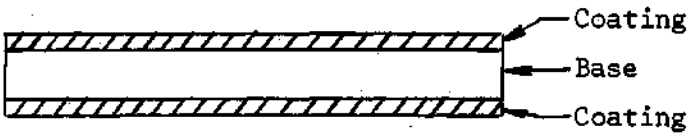

Figure 3. Symmetrical Coatings

The three methods were found to agree for low wave number (ratio of thickness of plate to wavelength), but there was no experimental verification.

A number of other references related to viscoelastic damping in general are available concerning such subjects as properties of viscoelastic materials, damping with partial coverage, and damping at joints and supports. It is believed that those of primary concern to the problem at hand have been mentioned; therefore, the remainder will not be discussed, but are included at the end of the thesis under the heading Other References.

Objectives and Scope

The main objective of this investigation is to relate the damping produced by an unconstrained layer of viscoelastic material (in terms of logarithmic decrement) to the thickness of the viscoelastic layer applied to a metal beam or plate and to the dimensions and properties of the two materials. It is of prime concern to present this relation in the form of equations or curves from which design data is readily attainable. (Much of the work in previous investigations is

not easily interpreted.) For the case of beams with small damping (loss factor of the viscoelastic material less than or equal to 0.1), Oberst (8) has accomplished this quite well using simple flexure theory. The results of the energy method used here will be compared with Oberst's for small damping. Large damping ($\eta_c > 0.1$) will also be considered for both beams and plates. In the case of plates coated with viscoelastic materials, there is a lack of reference literature; it is believed that work in this area is original.

Several other important considerations will be investigated. One of these is the determination of the ratio of coating thickness to base thickness which produces maximum damping. Several of the previous investigations indicate that, theoretically, an optimum amount of damping is attained when the coating thickness reaches a certain value. However, none verified experimentally that this is, in fact, the case. Therefore, the question is investigated further. In addition, the design data is tabulated not only to relate damping to the thickness of the coating, but also to the viscoelasticity index or loss factor, η_c, of the coating. Finally, beams and plates with symmetric coatings are to be considered and the effectiveness of these compared to that of coatings applied to one side only.

The investigation is restricted to free vibrations of beams and rectangular plates with no end or edge constraints. As the first or fundamental mode is usually of greatest concern, the study is also limited to this mode although it could easily be extended to include other modes as well as other end conditions.

CHAPTER II

VISCOELASTIC BEHAVIOR

The dynamic behavior of viscoelastic materials differs distinctly from that of ordinary elastic materials. In classical theory of elasticity it is always assumed that the stress-strain relations are linear and independent of time, i.e., $\sigma = E\varepsilon$. However, it has been discovered that a number of materials—plastics, resins, adhesives, and rubbers—have time dependent properties also. This is accounted for by considering the material as a combination of two media: one which is perfectly elastic, the other having the properties of a viscous fluid (hence the name "viscoelastic" material). The term viscoelastic is restricted in this investigation to those materials whose response to stress obeys the superposition principle. In other words, the material properties can be represented by a model constructed from elements which obey Hooke's elastic law and elements which obey Newton's viscosity law (15).

A system of springs and dashpots must be chosen to describe the behavior of each particular material. There are two basic models from which any number of others may be fashioned through the incorporation of additional elements. These two models are the Maxwell or liquid model (Figure 4(a) and Equation 1) and the Voigt or solid model (Figure 4(b) and Equation 2). From Figure 4(a),

$$\varepsilon = \varepsilon_{spring} + \varepsilon_{dashpot}$$

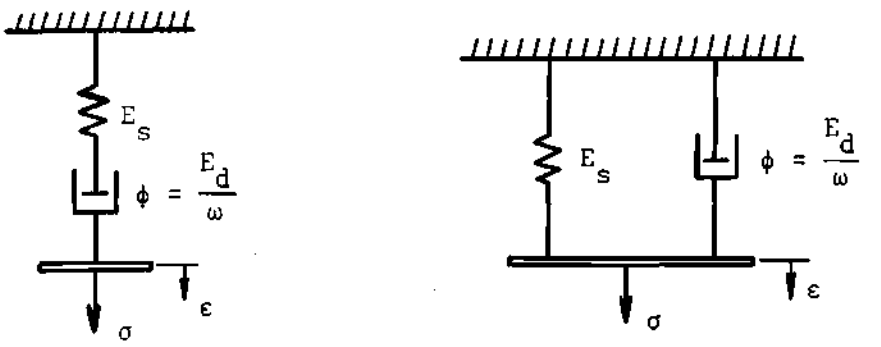

(a) Maxwell model (b) Voigt or Kelvin model

Figure 4. Viscoelastic Models

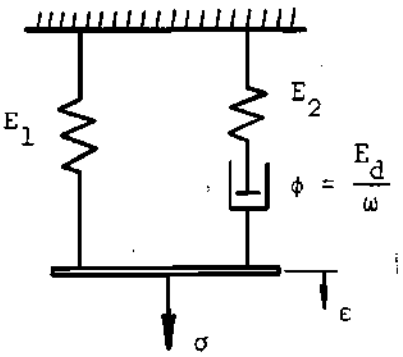

Figure 5. Maxwell-Voigt Combination Model

$$\sigma_s = E_s \varepsilon_s \qquad \sigma_d = \phi \frac{\partial \varepsilon_d}{\partial \tau}$$

$$\sigma = \sigma_s = \sigma_d$$

$$\frac{\partial \varepsilon}{\partial \tau} = \frac{\partial \varepsilon_s}{\partial \tau} + \frac{\partial \varepsilon_d}{\partial \tau} = \frac{1}{E_s} \frac{\partial \sigma}{\partial \tau} + \frac{1}{\phi} \sigma$$

Thus,

$$\sigma = \phi \frac{\partial \varepsilon}{\partial \tau} - \frac{\phi}{E_s} \frac{\partial \sigma}{\partial \tau} \tag{1}$$

From Figure 4(b),

$$\sigma = \sigma_{\text{spring}} + \sigma_{\text{dashpot}}$$

$$\sigma_s = E_s \varepsilon_s \qquad \sigma_d = \phi \frac{\partial \varepsilon_d}{\partial \tau}$$

$$\varepsilon = \varepsilon_s = \varepsilon_d$$

Therefore,

$$\sigma = E_s \varepsilon + \phi \frac{\partial \varepsilon}{\partial \tau} \tag{2}$$

The Voigt model is applicable in this investigation since it concerns solid materials. It is found, however, that the spring constant, E_s, and the damping coefficient, ϕ, of this model are not

actually constant for most materials. Both are functions of temperature and frequency as shown by Nolle (16). (Temperature change is not considered in this investigation, but frequency variation is an important consideration.) This suggests the use of a more complex model than the Voigt, for example, a Maxwell-Voigt combination (Figure 5 and Equation 3). From Figure 5,

$$\sigma = \sigma_1 + \sigma_2$$

$$\varepsilon = \varepsilon_1 = \varepsilon_2$$

$$\sigma_1 = E_1 \varepsilon_1$$

From Equation 1,

$$\sigma_2 = \phi \frac{\partial \varepsilon_2}{\partial \tau} - \frac{\phi}{E_2} \frac{\partial \sigma_2}{\partial \tau}$$

Therefore,

$$\sigma = E_1 \varepsilon + \frac{\phi}{E_2} (E_1 + E_2) \frac{\partial \varepsilon}{\partial \tau} - \frac{\phi}{E_2} \frac{\partial \sigma}{\partial \tau} \qquad (3)$$

Actually, using a Voigt model in conjunction with a modulus vs. frequency curve is equivalent to using a more complex model. For example, suppose the curves of Figure 6 describe the dynamic properties of a material. (For any particular value of frequency, the moduli are constants and the Voigt model is valid.) Let the system of Figure 4(b)

be given a sinusoidal motion, i.e.,

$$\varepsilon = \varepsilon_o \sin \omega\tau \tag{4}$$

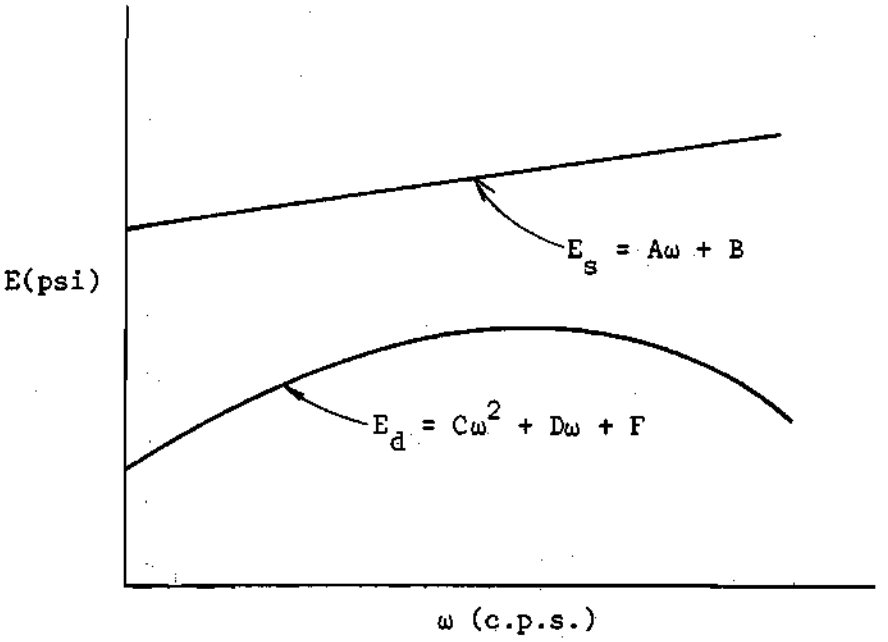

Figure 6. Modulus vs. Frequency Curves

Substituting the moduli of Figure 6 into Equation 2 yields

$$\sigma = A\omega\varepsilon + B\varepsilon + C\omega \frac{\partial\varepsilon}{\partial\tau} + D \frac{\partial\varepsilon}{\partial\tau} + \frac{F}{\omega} \frac{\partial\varepsilon}{\partial\tau} \tag{5}$$

From Equation 4

$$\frac{\partial^2\varepsilon}{\partial\tau^2} = -\omega^2\varepsilon$$

Differentiating Equation 2 with respect to time,

$$\frac{\partial \sigma}{\partial \tau} = -E_d \omega \epsilon + E_s \frac{\partial \epsilon}{\partial \tau}$$

Letting $A = \frac{E_d}{G}$, $D = -\frac{E_s}{G}$, and $G = \frac{E_2}{\phi}$, Equation 5 becomes

$$\sigma = B\epsilon + C\omega \frac{\partial \epsilon}{\partial \tau} + \frac{F}{\omega} \frac{\partial \epsilon}{\partial \tau} - \frac{1}{G} \frac{\partial \sigma}{\partial \tau}$$

Letting $B = E_1$, $C = 0$, and $F = \frac{E_d}{E_2}(E_1+E_2)$,

$$\sigma = E_1 \epsilon + \frac{\phi}{E_2}(E_1+E_2) \frac{\partial \epsilon}{\partial \tau} - \frac{\phi}{E_2} \frac{\partial \sigma}{\partial \tau} \qquad (6)$$

Equations 3 and 6 are identical. Therefore, it is seen that if the modulus vs. frequency curves have the form of those of Figure 6 (with A, B, C, D, and F as given above), they represent the behavior of a Maxwell-Voigt combination model when used in conjunction with the Voigt model. (If the curves of Figure 6 had taken a more complex form they would represent another model more complex in nature than the Maxwell-Voigt combination.) Consequently, it has been shown that the simple mathematics of the Voigt model may be utilized without sacrifice of accuracy in describing the behavior of the system.

It should also be noted that using the Voigt model is equivalent to using a complex modulus, i.e.,

$$\sigma_c = E_c \epsilon = (E_s + iE_d)\epsilon \qquad (7)$$

From Equation 4,

$$\frac{\partial \varepsilon}{\partial \tau} = \omega \varepsilon_o \cos \omega \tau = i\omega \varepsilon$$

Therefore, Equations 2 and 7 are identical.

CHAPTER III

BEAM ANALYSIS

An energy method similar to Rayleigh's method is the basis for determining the amount of energy lost by a system composed of both elastic and viscoelastic materials. Rayleigh's method simply employs the principle of conservation of energy and is used to approximate the natural frequencies of a conservative system. For a conservative system, the total energy of the system at any particular time is the same as at any other instant of time. For a nonconservative system this is not true; over a given interval of time, a certain amount of energy loss occurs. The amount of energy in a nonconservative system at a particular instant of time is equal to the amount of energy remaining in the system at a later instant of time plus the amount of energy dissipated during that interval. In symbolic form:

$$E_1 = E_2 + L_{1\rightarrow 2} \tag{8}$$

These energy terms may be derived in terms of the dimensions and properties of the system and the damping constant of the system. Knowing the properties and dimensions, one can determine the damping for that particular case. The procedure for this derivation will now be explained further.

In this analysis small deflection of both beams and plates is assumed as well as the usual assumptions which accompany it. These are:

(a) Strain in the middle plane may be neglected.

(b) Planes remain plane during deflection.

(c) Vertical shear does not affect deflection.

(d) The slope of the deflected plate in any direction is small; thus, its square may be neglected in comparison with unity.

Other assumptions are:

(1) The base beam or plate as well as the coating is homogeneous and isotropic.

(2) There is no slip at the interface of the base and the coating.

(3) Strain energy includes pure extensional (membrane) and bending strain of both the base and the coating. The effects of vertical shear are neglected.

(4) The kinetic energy includes only the effects of transverse inertia. The effects of rotary inertia are neglected.

Beam with Single Unconstrained Coating

The natural frequency of the system must be determined before solving for the damping constant of the system. In addition, the derivation for natural frequency lends to a better understanding of the damping solution; therefore, it is presented first. The solution presented for this case applies to the free-free beam of Figure 7.

Derivation of Natural Frequency

The Rayleigh method is normally used only for homogeneous, elastic beams. However, it has been shown by Kimel, Kirmser, Patel, and Raville (17) that a method similar to this may be used to predict the natural frequencies of nonhomogeneous (three-layer), undamped, sandwich beams. This approach is now applied to a two-layer, damped beam.

Undamped Natural Frequency. It is assumed, initially, that the composite beam of Figure 7 is undamped. The beam *deflections* for the mode of interest, m, are then assumed to be

$$\bar{u} = U_m F'_m(x) \sin \omega_m \tau \tag{9}$$

$$\bar{w} = W_m F_m(x) \sin \omega_m \tau \tag{10}$$

(Note: Subscripts refer to mode number, not to summation notation.)

U_m, W_m - undetermined coefficients of deflection for mth mode.

$\bar{u}$ - displacement of neutral axis in x-direction.

$\bar{w}$ - displacement of neutral axis in z-direction.

$F_m(x)$ - characteristic beam function (reference 18).

$F_m(x) = (\cosh \beta_m x - \cos \beta_m x) - \alpha_m(\sinh \beta_m x - \sin \beta_m x)$.

α_m, β_m - constants depending on mode and end conditions.

ω_m - undamped natural frequency for mth mode (rad/sec).

and $F'_m(x) = d/dx(F_m(x))$.

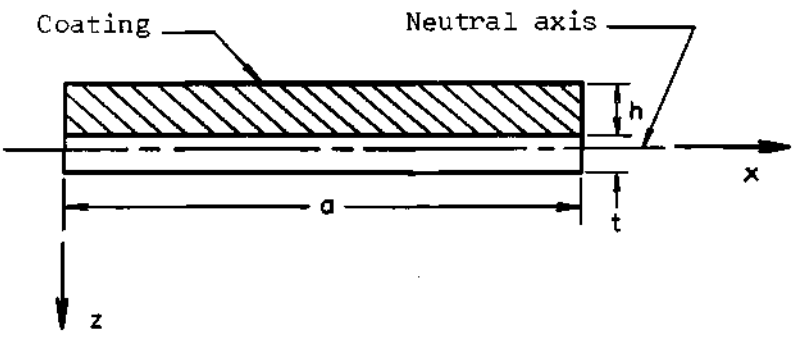

(a) Free-free beam

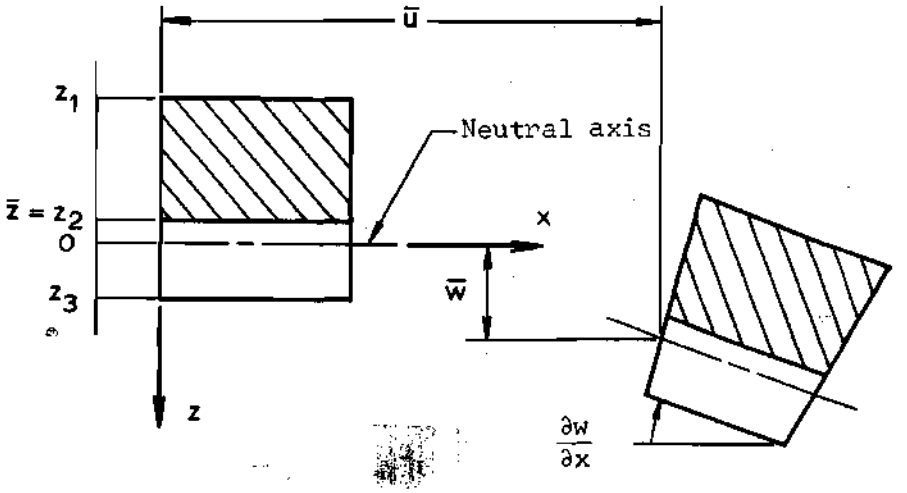

(b) Small element in initial and displaced position

Figure 7. Free-free Beam with Single Unconstrained Coating

Now

$$w = w_b = w_c = \bar{w}$$

and

$$u = u_b = u_c = \bar{u} - z \frac{\partial w}{\partial x}$$

where the subscripts b and c refer to the base beam (metal) and coating, respectively. It is seen that displacement in the x-direction occurs as a result of both extensional ($\bar{u}$) and bending effects $\left(-z \frac{\partial w}{\partial x}\right)$.

The *strains* may be written in terms of the assumed deflections. Thus, the extensional strains in the beam and coating are from theory of elasticity (19)

$$\varepsilon^{*}_{eb} = \varepsilon_{ec} = \frac{\partial \bar{u}}{\partial x} = U_m F''_m(x) \sin \omega_m \tau \tag{11}$$

The bending strains are

$$\varepsilon_{bb} = \varepsilon_{bc} = \frac{\partial}{\partial x}\left(-z \frac{\partial w}{\partial x}\right) = -zW_m F''_m(x) \sin \omega_m \tau \tag{12}$$

The shear strain is

$$\gamma_{xz} = \frac{\partial u}{\partial z} + \frac{\partial w}{\partial x} = \frac{\partial w}{\partial x} - \frac{\partial w}{\partial x} = 0 \tag{13}$$

The *strain* (potential) *energy*, V, is now determined. The

---

*The first subscript refers to type strain, the second to layer.

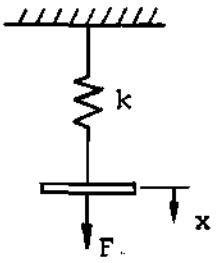

$F = kx$

Figure 8. Force-Displacement Model of Spring

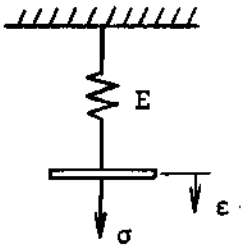

$\sigma = E\varepsilon$

Figure 9. Stress-Strain Model of Spring

materials under consideration are assumed to obey Hooke's law when placed under load. Thus,

$$V = \int_{x_1}^{x_2} F\,dx = \int_{x_1}^{x_2} kx\,dx = \frac{1}{2}kx^2 \quad \text{(Figure 8)}$$

or

$$\frac{d^3V}{dxdydz} = \int_{\varepsilon_1}^{\varepsilon_2} \sigma\,d\varepsilon = \int_{\varepsilon_1}^{\varepsilon_2} E\varepsilon\,d\varepsilon = \frac{1}{2}E\varepsilon^2 \quad \text{(Figure 9)}$$

The strain energy density for a beam is then

$$\frac{d^3V}{dxdydz} = \frac{1}{2}\sigma\varepsilon \tag{14}$$

The extensional strain energies of the base and coating are derived as follows:

$$\frac{d^3V_{eb}}{dxdydz} = \frac{E_b}{2}\epsilon_{eb}^2 = \frac{E_b}{2}U_m^2[F_m''(x)]^2 \sin^2\omega_m\tau$$

$$V_{eb} = \frac{E_b}{2}\int_{z_2}^{z_3}\int_0^b\int_0^a U_m^2[F_m''(x)]^2 \sin^2\omega_m\tau \, dxdydz$$

where z_2 and z_3 are distances of base surfaces from the neutral axis (see Figure 7 and Appendix A).

$$\int_0^a [F_m''(x)]^2 \, dx = a\beta_m^4 \quad \text{(Reference 20)}$$

β_m - constant depending on end conditions.

Therefore,

$$V_{eb} = \frac{E_b(z_3-z_2)}{2} ab\beta_m^4 U_m^2 \sin^2\omega_m\tau \tag{15}$$

Similarly,

$$V_{ec} = \frac{E_c(z_2-z_1)}{2} ab\beta_m^4 U_m^2 \sin^2\omega_m\tau \tag{16}$$

From Equation 7,

$$E_c = E_s + iE_d$$

Therefore,

$$E_c^2 = E_s^2 + E_d^2 \tag{17}$$

The bending strain energies are

$$\frac{d^3V_{bb}}{dxdydz} = \frac{E_b}{2}\epsilon_{bb}^2 = \frac{E_b}{2} z^2 W_m^2 [F_m''(x)]^2 \sin^2\omega_m\tau$$

$$V_{bb} = \frac{E_b(z_3^3-z_2^3)}{6} ab\beta_m^4 W_m^2 \sin^2\omega_m\tau \qquad (18)$$

and

$$V_{bc} = \frac{E_c(z_2^3-z_1^3)}{6} ab\beta_m^4 W_m^2 \sin^2\omega_m\tau \qquad (19)$$

The total elastic strain energy of the system is then

$$V = V_{eb} + V_{ec} + V_{bb} + V_{bc} \qquad (20)$$

The *kinetic energy*, T, arising from transverse inertia is from Timoshenko (21)

$$T = \frac{1}{2}\rho \int_A \left(\frac{\partial w}{\partial \tau}\right)^2 dA \qquad (21)$$

$$\frac{\partial w}{\partial \tau} = \omega_m W_m F_m(x) \cos \omega_m\tau$$

$$T = \frac{1}{2}\rho \int_0^b \int_0^a \omega_m^2 W_m^2 F_m^2(x) \cos^2\omega_m\tau \, dxdy$$

$$\int_0^a F_m^2(x)\, dx = a \quad \text{(Reference 20)}$$

Therefore,

$$T = \frac{1}{2} \rho \, ab\omega_m^2 W_m^2 \cos^2 \omega_m \tau \tag{22}$$

The total amount of energy in this conservative system at any time τ_1 is equal to the energy at any later time τ_2, or

$$E_1 = E_2 \tag{23}$$

where

$$E = T + V$$

For convenience, the times $\tau_1 = 0$ and $\tau_2 = \pi/2\omega_m$ are chosen (reference 22) and Equation 23 becomes

$$T_{max} = V_{max} \tag{24}$$

Substitution yields

$$\frac{1}{2} \rho \, ab\omega_m^2 W_m^2 = \frac{E_b(z_3-z_2)}{2} ab\beta_m^4 U_m^2 + \frac{E_c(z_2-z_1)}{2} ab\beta_m^4 U_m^2 + \tag{25}$$

$$+ \frac{E_b(z_3^3-z_2^3)}{6} ab\beta_m^4 W_m^2 + \frac{E_c(z_2^3-z_1^3)}{6} ab\beta_m^4 W_m^2$$

Employing the principle of virtual work (as done in reference 17) leads to the following equations:

$$\frac{1}{2} \rho \, ab\omega_m^2 = \frac{E_b(z_3^3-z_2^3)}{6} ab\beta_m^4 + \frac{E_c(z_2^3-z_1^3)}{6} ab\beta_m^4 \tag{26}$$

$$0 = \frac{E_b(z_3-z_2)}{2} ab\beta_m^4 + \frac{E_c(z_2-z_1)}{2} ab\beta_m^4 \tag{27}$$

Equation 26 yields a relationship for ω_m in terms of the properties and dimensions of the beam, i.e.,

$$\omega_m^2 = \frac{E_b(z_3^3-z_2^3)\beta_m^4}{3\rho} + \frac{E_c(z_2^3-z_1^3)\beta_m^4}{3\rho} \tag{28}$$

The undamped *fundamental* frequency for the free-free, two layer beam of Figure 7 is then

$$\omega_1^2 = \frac{E_b(z_3^3-z_2^3)\beta_1^4}{3\rho} + \frac{E_c(z_2^3-z_1^3)\beta_1^4}{3\rho} \tag{29}$$

where

$$\beta_1 = 4.730/a$$

Damped Natural Frequency. At this point it is usually assumed that damping is "light"; thus, damped and undamped frequencies are equal. However, this is not always the case; thus, a general system with "heavy" damping is considered.

It has been assumed that the behavior of the viscoelastic material is described by the Voigt model (Figure 10), not Hooke's law (Figure 8). The equation of motion for the single degree of freedom system of Figure 10 is given by Hansen and Chenea (23) as

$$x'' + \frac{\omega^2}{q} x' + \omega^2 x = 0 \tag{30}$$

where

$$x' = \frac{dx}{d\tau} \qquad \text{and} \qquad q = k/c$$

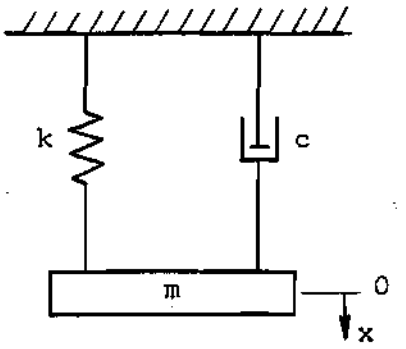

Figure 10. Force-displacement Representation of Voigt Model

The familiar solution is

$$x = (C_1 \cos \bar{\omega}\tau + C_2 \sin \bar{\omega}\tau) e^{-\frac{\omega^2}{2q}\tau} \tag{31}$$

where

$$\bar{\omega}^2 = \omega^2 \left[1 - \left(\frac{\omega}{2q}\right)^2\right] \tag{32}$$

and $\bar{\omega}$ = damped natural frequency.

In the analysis of a beam with damping, the deflection for the mode of interest, m, is assumed to be

$$w = W_m F_m(x) \sin \bar{\omega}_m \tau \, e^{-\alpha\tau} \tag{33}$$

This corresponds to Equation 31; however, $C_1 = 0$, $C_2 = W_m F_m(x)$, and $\alpha = \omega^2/2q$. Rewriting Equation 32 using the notation of Equation 33 yields

$$\bar{\omega}^2 = \omega^2\left[1-\left(\frac{\alpha}{\omega}\right)^2\right]$$

or

$$\bar{\omega}^2 = \omega^2 - \alpha^2 \tag{34}$$

The undamped natural frequency, ω, is known (Equation 29); therefore, the damped natural frequency, $\bar{\omega}$, of the system may be determined if the exponential damping constant, α, is known. Of course, finding α is the crux of the problem since it is directly related to the damping loss of the system (Equation 50). It should be noted that when damping is small, undamped and damped natural frequency are approximately the same.

Derivation of the Damping Equation

If it is assumed that the composite beam of Figure 7 is linearly *damped*, the transverse *deflection* is not given by Equation 10, but is instead

$$w = W_m F_m(x) \sin \bar{\omega}_m \tau \, e^{-\alpha\tau} \tag{35}$$

The deflection is seen to diminish with time and is of a form which satisfies the differential equation of motion.

It was seen in the derivation of undamped natural frequency that consideration of pure extension in the beam makes no contribution to the solution; therefore, only bending effects are considered here in order to simplify the derivation.

The *bending strains* of the beam and coating are

$$\varepsilon_{bb} = \varepsilon_{bc} = \frac{\partial}{\partial x}\left(-z\,\frac{\partial w}{\partial x}\right) = -zW_m F_m''(x)\,\sin\bar{\omega}_m\tau\; e^{-\alpha\tau} \qquad (36)$$

The strain energy density is (Equation 14)

$$\frac{d^3V}{dxdydz} = \frac{1}{2}E\varepsilon^2$$

Thus, the bending *strain energies* of the base, V_{bb}, and coating, V_{bc}, are:

$$\frac{d^3V_{bb}}{dxdydz} = \frac{E_b}{2}z^2W_m^2[F_m''(x)]^2\,\sin^2\bar{\omega}_m\tau\; e^{-2\alpha\tau}$$

$$V_{bb} = \frac{E_b(z_3^3-z_2^3)}{6}ab\beta_m^4W_m^2\,\sin^2\bar{\omega}_m\tau\; e^{-2\alpha\tau} \qquad (37)$$

$$V_{bc} = \frac{E_c(z_2^3-z_1^3)}{6}ab\beta_m^4W_m^2\,\sin^2\bar{\omega}_m\tau\; e^{-2\alpha\tau} \qquad (38)$$

$$V = V_{bb} + V_{bc} \qquad (39)$$

The *kinetic energy* is again (from Equation 21)

$$T = \frac{1}{2}\rho \int_A \left(\frac{\partial w}{\partial \tau}\right)^2 dA$$

$$\frac{\partial w}{\partial \tau} = \bar{\omega}_m W_m F_m(x) \cos \bar{\omega}_m \tau \, e^{-\alpha\tau} - \alpha W_m F_m(x) \sin \bar{\omega}_m \tau \, e^{-\alpha\tau}$$

$$T = \frac{1}{2}\rho \, abW_m^2 \left[\bar{\omega}_m^2 \cos^2 \bar{\omega}_m \tau - 2\bar{\omega}_m \alpha \sin \bar{\omega}_m \tau \cos \bar{\omega}_m \tau + \alpha^2 \sin^2 \bar{\omega}_m \tau\right] e^{-2\alpha\tau} \quad (40)$$

In this case (damped), there is energy of another form—*energy dissipated* by the coating, L. Equation 38 accounts for the energy associated with the spring of Figure 10. The energy associated with the dashpot is

$$L = \text{Work} = \int_{x_1}^{x_2} F \, dx = \int_{x_1}^{x_2} cx' dx \quad \text{(Figure 11)}$$

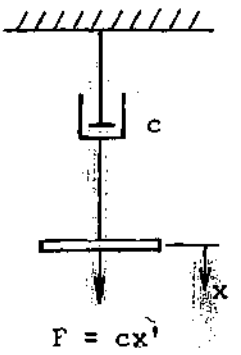

Figure 11. Force-Displacement Model of Dashpot

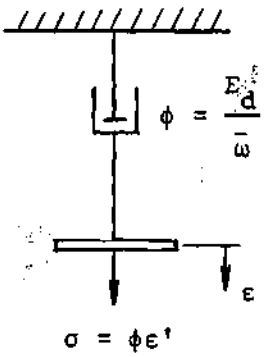

Figure 12. Stress-Strain Model of Dashpot

$$dx = \frac{dx}{d\tau} d\tau = x' d\tau$$

$$L = \int_{\tau_1}^{\tau_2} c(x')^2 d\tau$$

or for an element

$$\frac{d^3L}{dxdydz} = \int_{\varepsilon_1}^{\varepsilon_2} \sigma d\varepsilon = \int_{\varepsilon_1}^{\varepsilon_2} \phi \varepsilon' d\varepsilon \quad \text{(Figure 12)}$$

$$d\varepsilon = \frac{d\varepsilon}{d\tau} d\tau = \varepsilon' d\tau$$

$$\frac{d^3L}{dxdydz} = \int_{\tau_1}^{\tau_2} \phi(\varepsilon')^2 d\tau \tag{41}$$

For the beam of Figure 7, Equation 41 becomes

$$\frac{d^3L}{dxdydz} = \int_{\tau_1}^{\tau_2} \frac{E_d}{\bar{\omega}_m} \left(\frac{d\varepsilon_{bc}}{d\tau}\right)^2 d\tau \tag{42}$$

$$\frac{d\varepsilon_{bc}}{d\tau} = -zW_m F_m''(x)[\bar{\omega}_m \cos \bar{\omega}_m \tau - \alpha \sin \bar{\omega}_m \tau] e^{-\alpha\tau}$$

Substituting in Equation 42 and integrating with respect to time yields (with the help of tables (24))

$$\frac{d^3L}{dxdydz} = \frac{E_d z^2 W_m^2}{\bar{\omega}_m} [F_m''(x)]^2 \left\{ \bar{\omega}_m^2 \left[- \frac{e^{-2\alpha\tau} \bar{\omega}_m^{-2}}{4\alpha(\alpha^2 + \bar{\omega}_m^2)} + \right. \right. \tag{43}$$

$$+ \frac{e^{-2\alpha\tau}}{2(\alpha^2+\bar{\omega}_m^2)} (-\alpha \cos^2\bar{\omega}_m\tau + \bar{\omega}_m \sin\bar{\omega}_m\tau \cos\bar{\omega}_m\tau)\Bigg] +$$

$$+ \frac{2\bar{\omega}_m\alpha\, e^{-2\alpha\tau}}{4(\alpha^2+\bar{\omega}_m^2)} (\alpha \sin\bar{\omega}_m\tau \cos\bar{\omega}_m\tau + \bar{\omega}_m \cos 2\bar{\omega}_m\tau) +$$

$$+ \alpha^2\Bigg[- \frac{\bar{\omega}_m^2\, e^{-2\alpha\tau}}{4\alpha(\alpha^2+\bar{\omega}_m^2)} + \frac{e^{-2\alpha\tau}}{2(\alpha^2+\bar{\omega}_m^2)} (-\alpha \sin^2\bar{\omega}_m\tau +$$

$$- \bar{\omega}_m \sin \bar{\omega}_m\tau \cos \bar{\omega}_m\tau)\Bigg]\Bigg\}\Bigg|_{\tau_1}^{\tau_2}$$

Integrating over the volume,

$$L = \frac{E_d(z_2^3-z_1^3)}{6} ab\beta_m^4 W_m^2 \Bigg[\frac{\bar{\omega}_m e^{-2\alpha\tau}}{(\alpha^2+\bar{\omega}_m^2)} (-\alpha \cos^2\bar{\omega}_m\tau + \frac{\bar{\omega}_m}{2} \sin 2\bar{\omega}_m\tau) + \quad (44)$$

$$- \frac{\bar{\omega}_m^3\, e^{-2\alpha\tau}}{2\alpha(\alpha^2+\bar{\omega}_m^2)} + \frac{\alpha e^{-2\alpha\tau}}{(\alpha^2+\bar{\omega}_m^2)} (\alpha \sin 2\bar{\omega}_m\tau + \bar{\omega}_m \cos 2\bar{\omega}_m\tau) +$$

$$+ \frac{\alpha^2\, e^{-2\alpha\tau}}{\bar{\omega}_m(\alpha^2+\bar{\omega}_m^2)} (-\alpha \sin^2\bar{\omega}_m\tau - \bar{\omega}_m \sin\bar{\omega}_m\tau \cos\bar{\omega}_m\tau) +$$

$$- \frac{\bar{\omega}_m\alpha\, e^{-2\alpha\tau}}{2(\alpha^2+\bar{\omega}_m^2)}\Bigg]\Bigg|_{\tau_1}^{\tau_2}$$

As stated previously the total energy, E_1, in the system at any particular time, τ_1, is equal to the amount of energy, E_2, remaining in the system at a later time, τ_2, plus the amount of energy dissipated, L, over the interval of time τ_1 to τ_2, or

$$E_1 = E_2 + L_{1\to 2}$$

Thus

$$T_1 + V_1 = T_2 + V_2 + L_{1\to 2} \tag{45}$$

It now remains only to choose the times τ_1 and τ_2, substitute these into Equations 39, 40, and 44 to obtain T_1, T_2, V_1, V_2, and L, and in turn substitute the latter into Equation 45. An infinite number of choices of τ_1 and τ_2 may be made; however, each choice will lead to the same solution (though not the same equation). For convenience, one might choose

$$\tau_1 = 0 \qquad\qquad \tau_2 = 2\pi/\bar{\omega}_m$$

Thus, the system is considered in its initial position and again one full cycle later. (See Appendix B for other solutions.) Upon substitution, Equation 45 becomes

$$\frac{1}{2}\rho ab\bar{\omega}_m^2 W_m^2 + 0 = \frac{1}{2}\rho ab\bar{\omega}_m^2 W_m^2 e^{-4\pi\alpha/\bar{\omega}_m} + 0 + \tag{46}$$

$$+ \frac{E_d(z_2^3-z_1^3)}{6} ab\beta_m^4 W_m^2 \left[- \frac{\bar{\omega}_m \alpha \, e^{-4\pi\alpha/\bar{\omega}_m}}{\alpha^2 + \bar{\omega}_m^{-2}} + \frac{\bar{\omega}_m \alpha}{\alpha^2 + \bar{\omega}_m^{-2}} + \right.$$

$$- \frac{\bar{\omega}_m^{-3} \, e^{-4\pi\alpha/\bar{\omega}_m}}{2\alpha(\alpha^2+\bar{\omega}_m^{-2})} + \frac{\bar{\omega}_m^{-3}}{2\alpha(\alpha^2+\bar{\omega}_m^{-2})} + \frac{\bar{\omega}_m \alpha \, e^{-4\pi\alpha/\bar{\omega}_m}}{\alpha^2 + \bar{\omega}_m^{-2}} +$$

$$\left. - \frac{\bar{\omega}_m \alpha}{\alpha^2 + \bar{\omega}_m^{-2}} - \frac{\bar{\omega}_m \alpha \, e^{-4\pi\alpha/\bar{\omega}_m}}{2(\alpha^2+\bar{\omega}_m^{-2})} + \frac{\bar{\omega}_m \alpha}{2(\alpha^2+\bar{\omega}_m^{-2})} \right]$$

Dividing by $\frac{1}{2}\rho ab W_m^2$, collecting terms, and dividing by $(1-e^{-4\pi\alpha/\bar{\omega}_m})$ yields

$$\bar{\omega}_m^{-2} - \frac{E_d(z_2^3-z_1^3)\beta_m^4}{3\rho} \left[\frac{\bar{\omega}_m^{-3}}{2\alpha(\alpha^2+\bar{\omega}_m^{-2})} + \frac{\bar{\omega}_m \alpha}{2(\alpha^2+\bar{\omega}_m^{-2})} \right] = 0 \qquad (47)$$

Multiplying by $2\alpha(\alpha^2+\bar{\omega}_m^{-2})$ gives

$$2\alpha\bar{\omega}_m^{-2}(\alpha^2+\bar{\omega}_m^{-2}) - \frac{E_d(z_2^3-z_1^3)\beta_m^4}{3\rho} (\bar{\omega}_m^{-3}+\bar{\omega}_m\alpha^2) = 0$$

Dividing by $2\bar{\omega}_m^{-3}$ and rearranging terms,

$$\frac{1}{\bar{\omega}_m} \alpha^3 - \frac{E_d(z_2^3-z_1^3)\beta_m^4}{6\rho \, \bar{\omega}_m^2} \alpha^2 + \bar{\omega}_m \alpha - \frac{E_d(z_2^3-z_1^3)\beta_m^4}{6\rho} = 0 \qquad (48)$$

For the first mode (m=1), the result (damping Equation 1) is

$$\frac{1}{\bar{\omega}_1}\alpha^3 - \frac{E_d(z_2^3-z_1^3)\beta_1^4}{6\rho\,\bar{\omega}_1^2}\alpha^2 + \bar{\omega}_1\alpha - \frac{E_d(z_2^3-z_1^3)\beta_1^4}{6\rho} = 0 \qquad (49)$$

where

$$z_1 = -(h+\bar{z}) \qquad z_2 = -\bar{z} \qquad z_3 = t - \bar{z}$$

$$\bar{z} = \frac{E_b t^2 - E_c h^2}{2(E_b t + E_c h)} \quad \text{(See Appendix A)}$$

$$\rho = (\gamma_b t + \gamma_c h)/g \qquad \beta_1 = 4.730/a$$

Determination of the Damping of the System

Equation 49 is a polynomial which may be solved for α, the damping constant, if all the other variables are known. However, this is a difficult task if done by hand. Therefore, a computer program was written (see Appendix C) to calculate α from Equations 29, 34, and 49. Knowing α one may solve for the logarithmic decrement, δ, or the loss factor, η, of the composite beam since

$$\delta = \pi\eta = \frac{2\pi\alpha}{\bar{\omega}} \qquad (50)$$

(Another familiar measure of damping is damping factor, ξ, which is equivalent to c/c_c and relates the damping of a single degree of freedom system to that necessary for critical damping of the system. See

Appendix D for the derivation of Equation 50 and a relationship between ξ and δ.)

A number of other solutions are also possible. For instance, any one of the equations of Appendix B may be solved by combining it with Equations 29, 34, and 50. In addition, any two of the four *damping equations* used in conjunction with Equations 29 and 50 results in a solution. Several of these combinations of equations were solved and compared in order to verify the fact that each solution is indeed the same. A sample of these results appears in Table 1. Since Equation 49 is the simplest of the four damping equations all further calculations were performed using it in conjunction with Equations 29, 34, and 50.

Because of the complexity of calculating the log decrement for a specific case, it was thought that a series of curves might be generated from which a designer could more easily obtain the information desired. It may be shown that damping—loss factor or logarithmic decrement—is a function of only three dimensionless constants (see Appendix E and Equation 51).

$$\delta = \pi\eta = F\left(\frac{h}{t}, \frac{E_d}{E_s}, \frac{E_s}{E_b}\right) \tag{51}$$

Letting $\eta_c = \frac{E_d}{E_s}$ (see Equation 103 with $t = 0$), a series of curves, such as those of Figure 13, may be drawn giving the values of damping as a function of the properties and dimensions of the composite beams. The ratio η/η_c (or δ/δ_c) is convenient to use since η_c need not have the exact value as that for which a chart is drawn. For example, Figure 13 applies when the loss factor of the viscoelastic material is

Table 1. Comparison of Solutions

Beam constants: $E_b = 30(10)^6$ psi $E_d = 3000$ psi $E_s = 3000$ psi

$a = 50$ in. $b = 2$ in. $t = 0.050$ in. $\gamma_b = 0.284$ lb/in^3

$\gamma_c = 0.046$ lb/in^3 $\eta_c = 1.0$

$\frac{h}{t}$	VALUE OF LOGARITHMIC DECREMENT		
	Solution 1 Equations 29, 34, 49, and 50	Solution 2 Equations 29, 34, 50, and 95	Solution 3 Equations 29, 49, 50, and 95
1.00	0.0041	0.0041	0.0041
1.40	0.0084	0.0084	0.0084
2.00	0.0193	0.0193	0.0193
3.00	0.0524	0.0524	0.0524
4.00	0.1087	0.1087	0.1087
5.20	0.2105	0.2105	0.2107
7.00	0.4293	0.4293	0.4312
8.50	0.6544	0.6545	0.6482
10.00	0.8948	0.8952	0.8866
13.00	1.3493	1.3495	1.3617
16.00	1.7072	1.7080	1.6941
20.00	2.0280	2.0304	2.0482
25.00	2.2553	2.2603	2.2440
30.00	2.3766	2.3837	2.4030
40.00	2.4921	2.4933	2.5094
50.00	2.5322	2.5336	2.5485
60.00	2.5486	2.5500	2.5645
70.00	2.5553	2.5567	2.5368
85.00	2.5576	2.5591	2.5393
100.00	2.5560	2.5574	2.5376

approximately equal to unity. Curves for $\eta_c = 0.9$ would not differ greatly from those of Figure 13. (Curves for other values of η_c appear in Appendix F and may be compared to Figure 13. An example appears in Appendix G in which these curves are used to predict δ.)

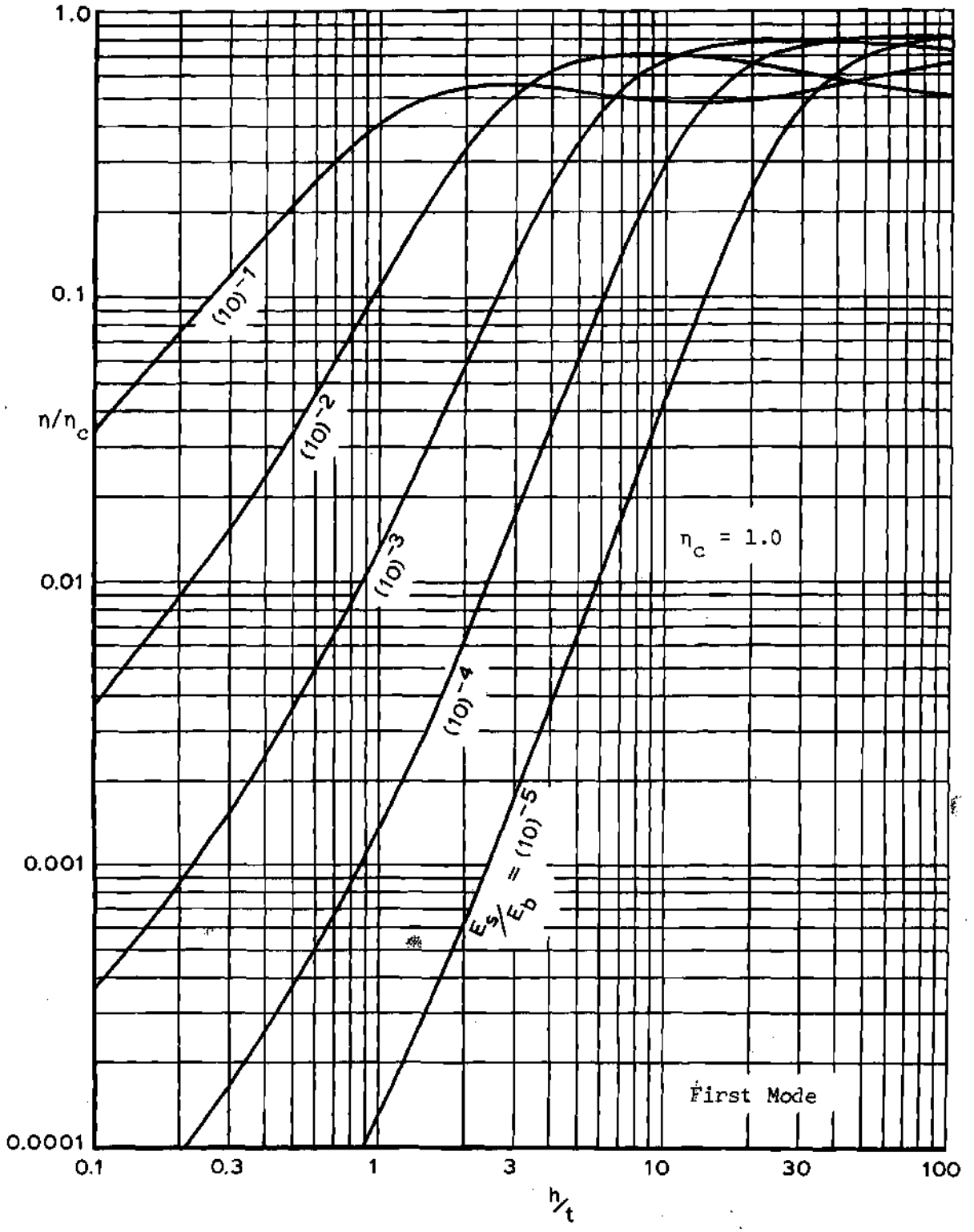

Figure 13. Damping Ratio vs. Thickness Ratio for Free-Free Beams with Coatings on One Side Only and $\eta_c = 1.0$

Approximate Solution

If it is assumed that damping is small ($\eta_c \leq 0.1$), which is the case for many materials, Equations 34 and 50 yield

$$\bar{\omega}^2 = \omega^2 - 0.0025\ \bar{\omega}^2$$

or

$$\bar{\omega} \approx \omega$$

Therefore, Equations 29, 49, and 50 yield an approximate solution for damping. It may also be shown that the higher order terms of Equation 49 are small in comparison to the others; consequently the following equation is a much simpler approximation and is valid if $\eta_c \leq 0.1$.

$$\bar{\omega}_1\alpha - \frac{E_d(z_2^3-z_1^3)\beta_1^4}{6\rho} = 0 \qquad (52)$$

where $\bar{\omega}_1$ is now given by Equation 29.

Calculations were made using these approximations for a number of cases and the results were compared to those of the original solution. A sample of these results appears in Table 2 and shows that Equation 52 may be used with confidence when damping is small. (A sample calculation employing Equation 52 appears in Appendix G.)

Beam with Two Symmetric Coatings

This case is illustrated by Figure 14 and its analysis is quite similar to that for a beam with only one side coated. The most

important difference is the fact that, in this case, the neutral axis always lies at the center of the beam.

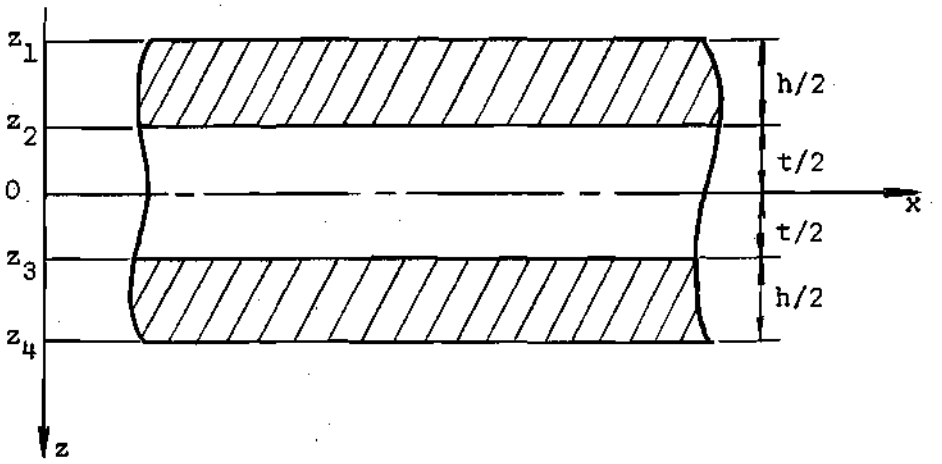

Figure 14. Beam with Two Symmetric Coatings

Derivation of Natural Frequency

Undamped Natural Frequency. Again Equations 9 and 10 are the assumed deflections. The strains are identical to Equations 11, 12, and 13; however, the strain energies of the coating are twice those given by Equations 16 and 19 since

$$z_4 - z_3 = z_2 - z_1$$

$$z_4^3 - z_3^3 = z_2^3 - z_1^3$$

$$V_{coating} = \int_{z_3}^{z_4} dV_{coating} + \int_{z_1}^{z_2} dV_{coating}$$

Table 2. Comparison of Complete and Approximate Solutions

Beam constants: $E_b = 30(10)^6$ psi $E_d = 3000$ psi $E_s = 30000$ psi

$a = 50$ in. $b = 2$ in. $t = 0.050$ in. $\gamma_b = 0.284$ lb/in^3

$\gamma_c = 0.046$ lb/in^3 $\eta_c = 0.10$

	VALUE OF LOGARITHMIC DECREMENT			
$\frac{h}{t}$	Solution 1 Equations 29, 34,49, and 50	Solution 4 Equations 29, 49, and 50	Solution 5 Equations 29, 50, and 52	Solution 6 Oberst's Solution
0.25	0.0004	0.0004	0.0004	0.0004
0.40	0.0008	0.0008	0.0008	0.0008
0.70	0.0020	0.0020	0.0020	0.0020
1.00	0.0040	0.0040	0.0040	0.0040
1.40	0.0082	0.0082	0.0082	0.0082
2.00	0.0183	0.0183	0.0183	0.0183
3.00	0.0456	0.0456	0.0456	0.0457
4.00	0.0832	0.0832	0.0832	0.0834
5.00	0.1245	0.1244	0.1244	0.1247
6.00	0.1629	0.1628	0.1628	0.1633
7.00	0.1953	0.1951	0.1951	0.1957
8.50	0.2314	0.2311	0.2311	0.2320
10.00	0.2554	0.2549	0.2549	0.2560
13.00	0.2814	0.2808	0.2808	0.2821
16.00	0.2930	0.2924	0.2924	0.2938
20.00	0.2998	0.2991	0.2991	0.3006
22.00	0.3014	0.3008	0.3008	0.3023
28.00	0.3035	0.3028	0.3028	0.3043
40.00	0.3030	0.3023	0.3023	0.3039
70.00	0.2978	0.2971	0.2971	0.2987
100.00	0.2922	0.2915	0.2915	0.2931

The kinetic energy is again given by Equation 22; therefore, the following expression results

$$\omega_1^2 = \frac{E_b(z_3^3 - z_2^3)\beta_1^4}{3\rho} + \frac{2E_c(z_2^3 - z_1^3)\beta_1^4}{3\rho} \qquad (53)$$

however,

$$z_1 = -\frac{1}{2}(t+h) \qquad z_2 = -\frac{t}{2} \qquad z_3 = \frac{t}{2}$$

Damped Natural Frequency. Again, Equation 34 applies.

Derivation of the Damping Equation

This derivation is almost identical to that of Equation 49; therefore, only the final equation is presented.

$$\frac{1}{\bar{\omega}_1}\alpha^3 - \frac{E_d(z_2^3-z_1^3)\beta_1^4}{3\rho\,\bar{\omega}_1^2}\alpha^2 + \bar{\omega}_1\alpha - \frac{E_d(z_2^3-z_1^3)\beta_1^4}{3\rho} = 0 \qquad (54)$$

Determination of the Damping of the System

A computer program (Appendix C) was again formulated to obtain numerical results, this time employing Equations 34, 50, 53, and 54. Curves similar to those for beams with a coating on only one side were generated for this case, for instance, Figure 15. Other curves will be found in Appendix F.

Approximate Solution

If small damping is again assumed ($\eta_c \leq 0.10$), Equation 54 simplifies to

$$\bar{\omega}_1\alpha - \frac{E_d(z_2^3-z_1^3)\beta_1^4}{3\rho} = 0 \qquad (55)$$

where $\bar{\omega}_1$ is now given by Equation 53.

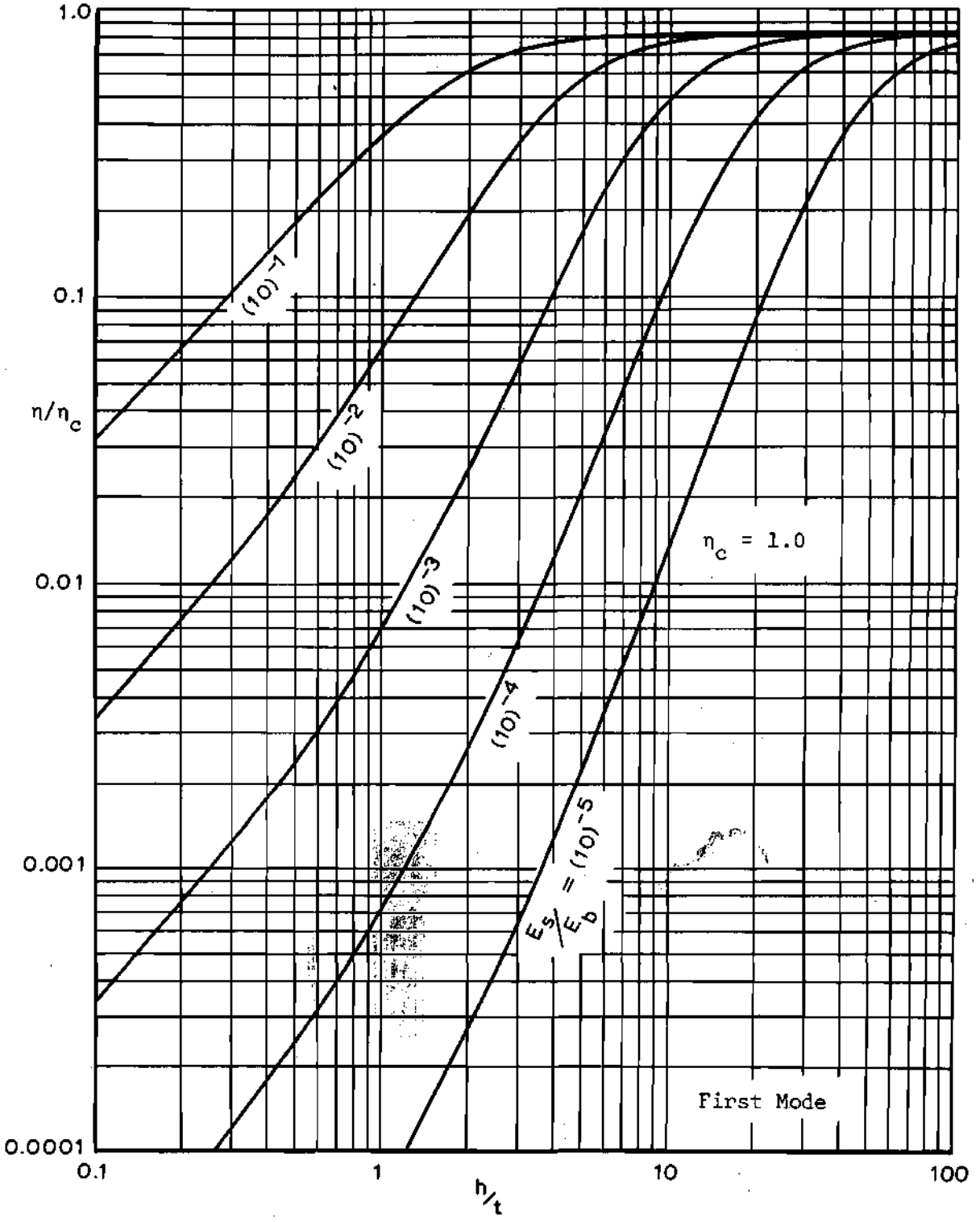

Figure 15. Damping Ratio vs. Thickness Ratio for Free-Free Beams with Two Symmetric Coatings and $\eta_c = 1.0$.

CHAPTER IV

PLATE ANALYSIS

The same energy method employed to determine the damping of beams with viscoelastic coatings can be extended to the two-dimensional case; however, the derivations for plates are somewhat more involved. In this case, the deflection of the plate is assumed to be the product of the mode shapes of two orthogonal beams. This is similar to the approach used by Warburton (25) for homogeneous, undamped plates; however, in this case, the plate is nonhomogeneous and damped. The kinetic, strain, and loss energies are derived in terms of the deflections, and the principle of conservation of energy is again applied. The assumptions made in the beam analysis (small deflection, etc.) also apply here.

Rectangular Plate with Single Unconstrained Coating

The procedure followed in the analysis of the free-free-free-free plate of Figure 16 is similar to that of a free-free beam.

Derivation of Natural Frequency

Undamped Natural Frequency. It is assumed initially that the plate of Figure 16 is undamped. The *deflections* for the mode of interest, mn, are

$$\begin{aligned} &\text{x direction} && \bar{u} = U_{mn} F_m'(x)\, G_n(y)\, \sin\omega_{mn}\tau \\ &\text{y direction} && \bar{v} = V_{mn} F_m(x)\, G_n'(y)\, \sin\omega_{mn}\tau \\ &\text{z direction} && \bar{w} = W_{mn} F_m(x)\, G_n(y)\, \sin\omega_{mn}\tau \end{aligned} \qquad (56)$$

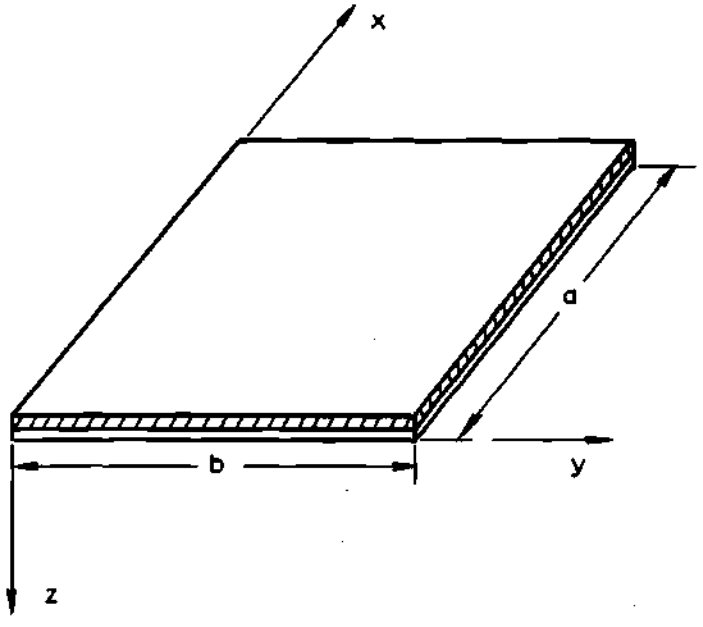

(a) Free Plate

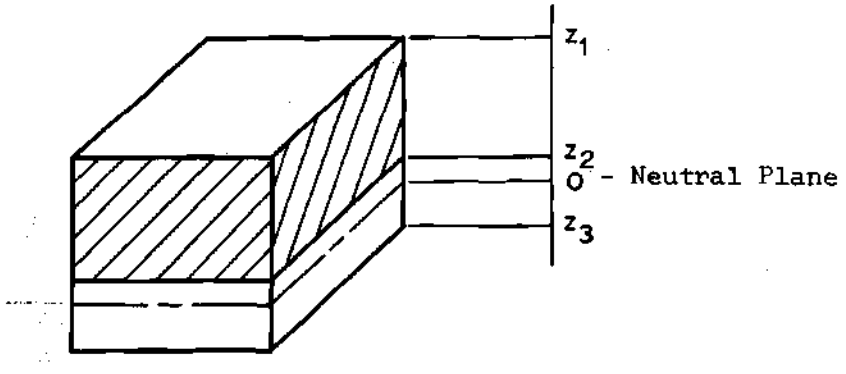

(b) Element

Figure 16. Free Plate with Single Unconstrained Coating

where (from reference 18)

$$F_m(x) = (\cosh \beta_m x - \cos \beta_m x) - \alpha_m(\sinh \beta_m x - \sin \beta_m x)$$

$$G_n(y) = (\cosh \beta_n y - \cos \beta_n y) - \alpha_n(\sinh \beta_n y - \sin \beta_n y)$$

The *strains* existing in a small element of the plate are given by Timoshenko (21) as

$$\varepsilon_x = -z \frac{\partial^2 w}{\partial x^2} \qquad \varepsilon_y = -z \frac{\partial^2 w}{\partial y^2} \qquad \gamma_{xy} = -2z \frac{\partial^2 w}{\partial x \partial y}$$

where the subscripts x, y, and z refer to directions. (The extensional strains were seen to have no effect in the derivation of natural frequency for the beam; consequently they are omitted here.) Therefore, the bending strains and shear strain of the plate and the coating are

$$\varepsilon_{xp} = \varepsilon_{xc} = -zW_{mn}F_m''(x)\, G_n(y)\, \sin\omega_{mn}\tau \tag{57}$$

$$\varepsilon_{yp} = \varepsilon_{yc} = -zW_{mn}F_m(x)\, G_n''(y)\, \sin\omega_{mn}\tau \tag{58}$$

$$\gamma_{xyp} = \gamma_{xyc} = -2z\, W_{mn}F_m'(x)\, G_n'(y)\, \sin\omega_{mn}\tau \tag{59}$$

Stresses in a plate are much more involved than those in a beam. From Timoshenko (21),

$$\sigma_x = \frac{E}{(1-\nu^2)} (\varepsilon_x+\nu\varepsilon_y) \qquad \sigma_y = \frac{E}{1-\nu^2} (\varepsilon_y+\nu\varepsilon_x) \tag{60}$$

$$\sigma_z = 0 \qquad \tau_{xy} = G\gamma_{xy} \qquad \text{where} \qquad G = \frac{E}{2(1+\nu)}$$

The *strain energy density* of the two layers, which are both assumed to be perfectly elastic (Figure 9) here, is from Timoshenko (21)

$$\frac{d^3V}{dxdydz} = \frac{\varepsilon_x\sigma_x}{2} + \frac{\varepsilon_y\sigma_y}{2} + \frac{\gamma_{xy}\tau_{xy}}{2} \tag{61}$$

or

$$\frac{d^3V}{dxdydz} = \frac{E}{2(1-\nu^2)} (\varepsilon_x^2+2\nu\varepsilon_x\varepsilon_y+\varepsilon_y^2) + \frac{1}{2} G\gamma_{xy}^2 \tag{62}$$

For the metal layer,

$$\frac{d^3V_p}{dxdydz} = \frac{E_p}{2(1-\nu_p^2)} z^2W_{mn}^2[F_m''(x)]^2 G_n^2(y) \sin^2\omega_{mn}\tau + \tag{63}$$

$$+ 2\nu_p z^2W_{mn}^2 F_m(x) F_m''(x) G_n(y) G_n''(y) \sin^2\omega_{mn}\tau +$$

$$+ z^2W_{mn}^2 F_m^2(x)[G_n''(y)]^2 \sin^2\omega_{mn}\tau +$$

$$+ \frac{E_p}{1+\nu_p} z^2W_{mn}^2[F_m'(x)]^2[G_n'(y)]^2 \sin^2\omega_{mn}\tau$$

For free-free end conditions (20),

$$\int_0^a F_m^2(x)\,dx = a \qquad \int_0^a [F_m''(x)]^2\,dx = a\beta_m^4$$

$$\int_0^a F_m(x)\,F_m''(x)\,dx = \alpha_m\beta_m(2-\alpha_m\beta_m a)$$

$$\int_0^a [F_m'(x)]^2\,dx = \alpha_m\beta_m(\alpha_m\beta_m a+6)$$

Integrating over the volume,

$$V_p = \frac{E_p G_p (z_3^3-z_2^3) W_{mn}^2}{6(1-\nu_p^2)} \sin^2\omega_{mn}\tau \tag{64}$$

where

$$G_p = ab\beta_m^4 + 2\nu_p\alpha_m\alpha_n\beta_m\beta_n(2-\alpha_m\beta_m a)(2-\alpha_n\beta_n b) + ab\beta_n^4 + \tag{65}$$

$$+ 2(1-\nu_p)\alpha_m\alpha_n\beta_m\beta_n(\alpha_m\beta_m a+6)(\alpha_n\beta_n b+6)$$

Similarly,

$$V_c = \frac{E_c G_c (z_2^3-z_1^3) W_{mn}^2}{6(1-\nu_c^2)} \sin^2\omega_{mn}\tau \tag{66}$$

$$G_c = ab\beta_m^4 + 2\nu_c\alpha_m\alpha_n\beta_m\beta_n(2-\alpha_m\beta_m a)(2-\alpha_n\beta_n b) + ab\beta_n^4 + \tag{67}$$

$$+ 2(1-\nu_c)\alpha_m\alpha_n\beta_m\beta_n(\alpha_m\beta_m a+6)(\alpha_n\beta_n b+6)$$

The total strain energy is

$$V = V_p + V_c \tag{68}$$

The *kinetic energy* is again given by Equation 21; thus,

$$T = \frac{1}{2}\rho ab\omega_{mn}^2 W_{mn}^2 \cos^2\omega_{mn}\tau \tag{69}$$

Equation 24 also applies here. Hence, $T_{max} = V_{max}$. Substituting and simplifying yields the *undamped natural frequency* of the composite plate of Figure 16.

$$\omega_{11}^2 = \frac{E_p G_p (z_3^3 - z_2^3)}{3\rho ab(1-\nu_p^2)} + \frac{E_c G_c (z_2^3 - z_1^3)}{3\rho ab(1-\nu_c^2)} \tag{70}$$

The notation used here is the same used in Equations 49, 65, and 67.

Damped Natural Frequency. Again Equation 34 applies.

Derivation of the Damping Equation

Assuming the system of Figure 16 to be linearly damped, the *deflection* for the mode at interest, mn, is

$$w = W_{mn} F_m(x)\, G_n(y) \sin \bar{\omega}_{mn}\tau\, e^{-\alpha\tau} \tag{71}$$

(Extension will again be omitted as it was shown to make no contribution.)

The bending and shear *strains* are

$$\varepsilon_{xp} = \varepsilon_{xc} = -zW_{mn}F_m''(x)\,G_n(y)\,\sin\bar{\omega}_{mn}\tau\,e^{-\alpha\tau}$$

$$\varepsilon_{yp} = \varepsilon_{yc} = -zW_{mn}F_m(x)\,G_n''(y)\,\sin\bar{\omega}_{mn}\tau\,e^{-\alpha\tau} \qquad (72)$$

$$\gamma_{xyp} = \gamma_{xyc} = -2zW_{mn}F_m'(x)\,G_n'(y)\,\sin\bar{\omega}_{mn}\tau\,e^{-\alpha\tau}$$

The *stresses* in the viscoelastic material are

$$\sigma_x = \sigma_{x1} + \sigma_{x2} = \frac{E_c}{(1-\nu_c^2)}(\varepsilon_x+\nu_c\varepsilon_y) + \frac{\phi}{(1-\nu_c^2)}\frac{\partial}{\partial\tau}(\varepsilon_x+\nu_c\varepsilon_y)$$

$$\sigma_y = \sigma_{y1} + \sigma_{y2} = \frac{E_c}{(1-\nu_c^2)}(\varepsilon_y+\nu_c\varepsilon_x) + \frac{\phi}{(1-\nu_c^2)}\frac{\partial}{\partial\tau}(\varepsilon_y+\nu_c\varepsilon_x) \qquad (73)$$

$$\sigma_z = 0 \qquad \tau_{xy} = \tau_{xy1} + \tau_{xy2} = G\gamma_{xy} + \phi\frac{\partial\gamma_{xy}}{\partial\tau}$$

Stresses in the metal are again given by Equations 60.

The *strain energy* is expressed by Equation 61. Substituting Equations 60, 72, and the elastic portions of stress from Equations 73 (σ_{x1},σ_{y1},τ_{xy1}) into Equation 61 and integrating yields

$$V_p = \frac{E_pG_p(z_3^3-z_2^3)}{6(1-\nu_p^2)}W_{mn}^2\,\sin^2\bar{\omega}_{mn}\tau\,e^{-2\alpha\tau}$$

$$V_c = \frac{E_cG_c(z_2^3-z_1^3)}{6(1-\nu_c^2)}W_{mn}^2\,\sin^2\bar{\omega}_{mn}\tau\,e^{-2\alpha\tau}$$

where G_p and G_c are defined by Equations 65 and 67.

$$V = V_p + V_c \tag{74}$$

Substituting Equation 71 into Equation 21 yields the *kinetic energy* of the system.

$$T = \frac{1}{2}\rho ab[\bar{\omega}_{mn}^2 \cos^2\bar{\omega}_{mn}\tau - 2\bar{\omega}_{mn}\alpha\sin\bar{\omega}_{mn}\tau\cos\bar{\omega}_{mn}\tau + \tag{75}$$

$$+ \alpha^2 \sin^2\bar{\omega}_{mn}\tau]W_{mn}^2 e^{-2\alpha\tau}$$

The *energy dissipated* by the coating, L, must now be determined (see Appendix H).

$$\frac{d^3L}{dxdydz} = \int_{\tau_1}^{\tau_2} (\varepsilon_x'\sigma_{x2} + \varepsilon_y'\sigma_{y2} + \gamma_{xy}'\tau_{xy2})\, d\tau \tag{76}$$

or

$$\frac{d^3L}{dxdydz} = \frac{E_d}{(1-\nu_c^2)\bar{\omega}_{mn}} \int_{\tau_1}^{\tau_2} (\varepsilon_x'^2 + 2\nu_c\varepsilon_x'\varepsilon_y' + \varepsilon_y'^2)\, d\tau \tag{77}$$

$$+ \frac{E_d}{2(1+\nu_c)\bar{\omega}_{mn}} \int_{\tau_1}^{\tau_2} \gamma_{xy}'^2\, d\tau$$

$$\frac{d^3L}{dxdydz} = \frac{E_d z^2}{(1-\nu_c^2)\bar{\omega}_{mn}} \int_{\tau_1}^{\tau_2} W_{mn}^2 e^{-2\alpha\tau}\{[F_m''(x)]^2 G_n^2(y) + \tag{78}$$

$$+ 2\nu_c F_m(x)\, F_m''(x)\, G_n(y)\, G_n''(y) + F_m^2(x)[G_n''(y)]^2 +$$

$$+ 2(1-\nu_c)[F_m'(x)]^2[G_n'(y)]^2\}\{\bar{\omega}_{mn}^2 \cos^2\bar{\omega}_{mn}\tau +$$

$$- 2\alpha\bar{\omega}_{mn}\sin\bar{\omega}_{mn}\tau\cos\bar{\omega}_{mn}\tau + \alpha^2\sin^2\bar{\omega}_{mn}\tau\}d\tau$$

Integrating with respect to time and volume,

$$L = \frac{E_d G_c (z_2^3 - z_1^3) W_{mn}^2}{6(1-\nu_c^2)} \left[\frac{\bar{\omega}_{mn}\, e^{-2\alpha\tau}}{(\alpha^2+\bar{\omega}_{mn}^2)} (-\alpha\cos^2\bar{\omega}_{mn}\tau + \right. \tag{79}$$

$$+ \bar{\omega}_{mn}\sin\bar{\omega}_{mn}\tau\cos\bar{\omega}_{mn}\tau) - \frac{\bar{\omega}_{mn}^3\, e^{-2\alpha\tau}}{2\alpha(\alpha^2+\bar{\omega}_{mn}^2)} +$$

$$+ \frac{\alpha e^{-2\alpha\tau}}{(\alpha^2+\bar{\omega}_{mn}^2)} (\alpha\sin 2\bar{\omega}_{mn}\tau + \bar{\omega}_{mn}\cos 2\bar{\omega}_{mn}\tau) +$$

$$+ \frac{\alpha^2\, e^{-2\alpha\tau}}{\bar{\omega}_{mn}(\alpha^2+\bar{\omega}_{mn}^2)} (-\bar{\omega}_{mn}\sin\bar{\omega}_{mn}\tau\cos\bar{\omega}_{mn}\tau +$$

$$\left. - \alpha\sin^2\bar{\omega}_{mn}\tau) - \frac{\bar{\omega}_{mn}\alpha\, e^{-2\alpha\tau}}{2(\alpha^2+\bar{\omega}_{mn}^2)} \right] \Bigg|_{\tau_1}^{\tau_2}$$

For convenience, the times $\tau_1 = 0$ and $\tau_2 = 2\pi/\bar{\omega}_{mn}$ are again chosen. (As in the case of a beam other times could be chosen; however, the final result is the same.) Substituting into Equation 45 and simplifying as done in the derivation for the beam yields

$$\frac{1}{\bar{\omega}_{11}}\alpha^3 - \frac{E_d G_c (z_2^3 - z_1^3)}{6\rho ab(1-\nu_c^2)\bar{\omega}_{11}^2}\alpha^2 + \bar{\omega}_{11}\alpha - \frac{E_d G_c (z_2^3 - z_1^3)}{6\rho ab(1-\nu_c^2)} = 0 \qquad (80)$$

Determination of the Damping of the System

The complete solution, for which a computer program was written (Appendix C), results from Equations 34, 50, 70, and 80. Again several series of curves were plotted for a number of different cases and appear in Figure 17 and Appendix F.

Approximate Solution

If it is assumed that damping is small ($\eta_c \leq 0.1$), then $\bar{\omega} \doteq \omega$ as in the case of a beam, and an accurate approximation results from a solution combining Equations 50, 70, and 82.

$$\bar{\omega}_{11}\alpha - \frac{E_d G_c (z_2^3 - z_1^3)}{6\rho(1-\nu_c^2)ab} = 0 \qquad (82)$$

Rectangular Plate with Two Symmetric Coatings

The following equations apply in this case:

$$\omega_{11}^2 = \frac{E_p G_p (z_3^3 - z_2^3)}{3\rho ab(1-\nu_p^2)} + \frac{2E_c G_c (z_2^3 - z_1^3)}{3\rho ab(1-\nu_c^2)} = 0 \qquad (83)$$

where

$$z_1 = -\frac{1}{2}(t+h) \qquad z_2 = -\frac{t}{2} \qquad z_3 = \frac{t}{2}$$

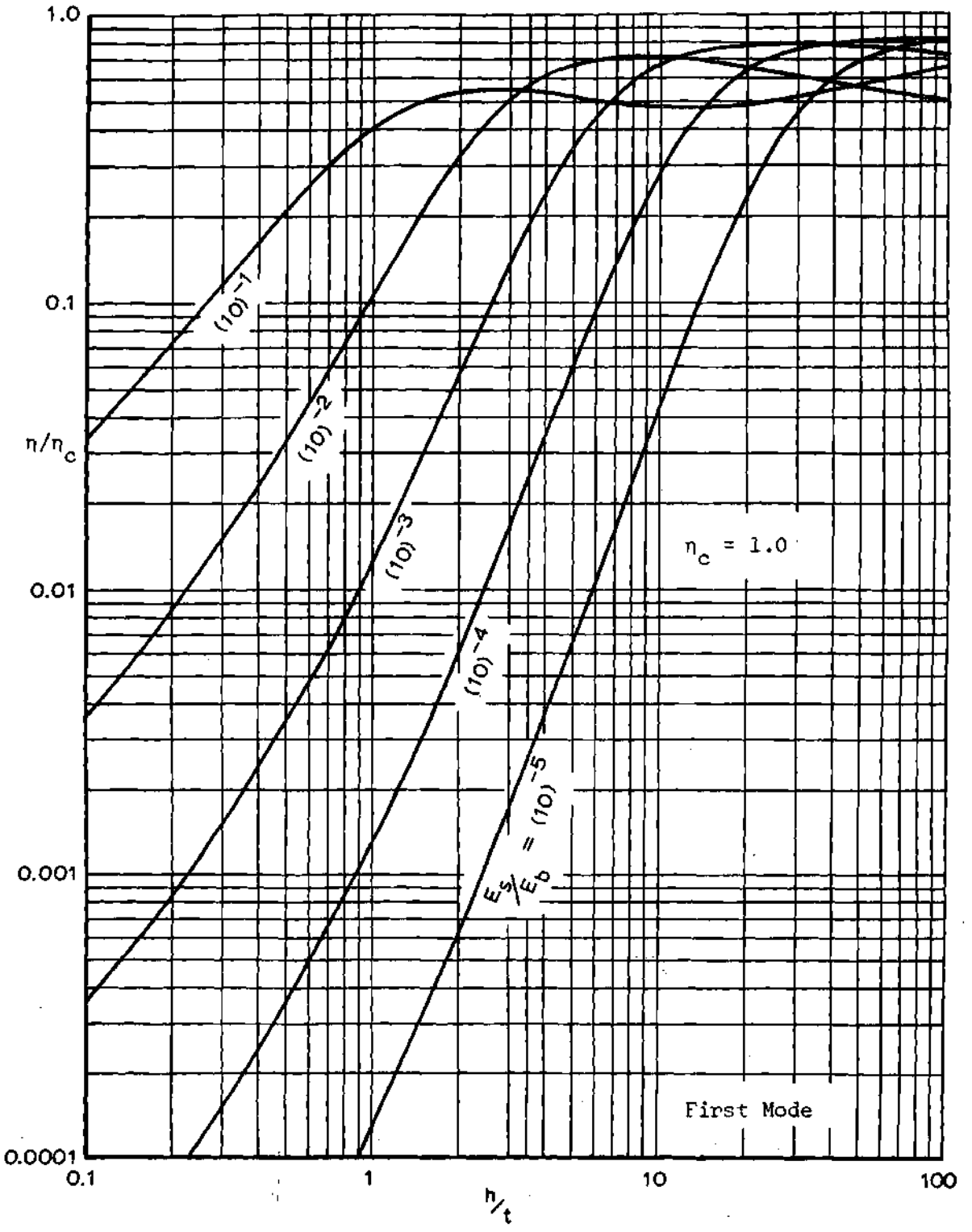

Figure 17. Damping Ratio vs. Thickness Ratio for Free Plates with Coatings on One Side Only and $\eta_c = 1.0$

$$\bar{\omega}_{11}^2 = \omega_{11}^2 - \alpha^2 \tag{84}$$

$$\frac{1}{\bar{\omega}_{11}}\alpha^3 - \frac{E_d G_c (z_2^3 - z_1^3)}{3\rho ab(1-\nu_c^2)\bar{\omega}_{11}^2}\alpha^2 + \bar{\omega}_{11}\alpha - \frac{E_d G_c (z_2^3 - z_1^3)}{3\rho ab(1-\nu_c^2)} = 0 \tag{85}$$

where G_c and G_p are given by Equations 65 and 67, and

$$\rho = \frac{\gamma_b t + \gamma_c h}{g} \qquad \alpha_1 = 0.998 \qquad \beta_1 = 4.730/a$$

Curves for this case appear in Appendix F.

An approximate solution valid when $\eta_c \leq 0.1$ is

$$\bar{\omega}_{11}\alpha - \frac{E_d G_c (z_2^3 - z_1^3)}{3\rho ab(1-\nu_c^2)} = 0 \tag{86}$$

where $\bar{\omega}_{11}$ is given by Equation 83.

CHAPTER V

EXPERIMENTAL INVESTIGATION

In order to verify the authenticity of the analytical solutions of Chapters III and IV, a number of beam and plate models with viscoelastic coatings were constructed and tested. (All tests were conducted at room temperature.)

Construction of Models

The models used in these tests were composed of aluminum and steel bases coated with various thicknesses of buna-N rubber (butadiene-acrylonitrile copolymer), plexiglas (acrylic plastic), and styrofoam (see Table 3). Bonding materials used were: (a) Plastic rubber cement (Sears, Roebuck and Co.); (b) Epoxy cement (Sears, Roebuck and Co.). The surfaces of both the base and coating were cleaned thoroughly before being glued together insuring proper adhesion. In addition, adequate time was allowed for thorough drying of the adhesive prior to actual testing. Adhesive (a) was used with the buna-N coatings since the two materials have similar properties. A stronger adhesive was needed for the stiffer coatings, however. There was little doubt that an adequate bond was achieved with the epoxy. As a check for the efficacy of the plastic rubber, several tests were repeated using epoxy in its place; the results were the same. It should also be mentioned that the thickness of the bonding material was small in comparison to that of the coating.

Table 3. Dimensions of Experimental Models

Base Material	a(in.)	b(in.)	t(in.)	Thickness of Coating (in.)		
				Buna-N	Plexiglas	Styrofoam
Steel	8-1/16	2	0.030	0.073,0.114,0.264	0.129,0.227	17/32,15/16
Steel	8-1/16	2	0.047	0.073,0.114,0.264	0.132,0.222	1/2,15/16
Aluminum	8-1/16	2	0.032	0.073,0.114,0.264	0.126,0.226	1/2,15/16
Aluminum	7-7/8	2	0.054	0.073,0.114,0.264	0.130,0.247	17/32,15/16
Aluminum	8-1/16	2	0.062	0.073,0.114,0.264	0.135,0.222	17/32,15/16
Aluminum	12	12	0.032	0.073,0.114,0.264	0.130,0.235	9/32,17/32
Aluminum	12	12	0.047	0.073,0.114,0.264	0.130,0.235	1/2,15/16
Aluminum	12	12	0.062	0.073,0.114,0.264	0.130,0.235	17/32,15/16
Aluminum	8-1/16	2	0.062	Two 0.264 layers		
Aluminum	7-7/8	2	0.054	Two 0.114 layers		
Aluminum	8-1/16	2	0.047	Two 0.073 layers		
Aluminum	8-1/16	2	0.032	Two 0.114 layers, Two 0.264 layers		

Instrumentation and Equipment

The equipment used to conduct the testing of the above models consisted of that listed in Table 4, chemical stands, and thin string. A schematic diagram of the experimental setups used is shown in Figure 18. Strain gages were used almost exclusively with the beam models, although several models were also tested using the accelerometer. (The same output was obtained from each transducer.) However, in many cases, the magnitude of the plate deflections was not large enough to measure

Table 4. Equipment for Testing

Item	Manufacturer	Specifications
Strain gages	Baldwin-Lima-Hamilton	SR-4 Type A-1 120ohm. Gage factor - 2.05
Bridge-amplifier-meter	Ellis Associates	Model BAM-1
Oscilloscope	Tektronix	Dual Beam Type 502A
Oscilloscope camera	Tektronix	Polaroid Type C-12
Accelerometer	Bruel and Kjaer	Type 4336
Power amplifier	MB Electronics	Model 2125MB
Electromagnetic shaker	MB Electronics	Model PM25
Frequency oscillator	Hewlett-Packard	Model 200CD

the decay accurately (using strain gages). It was found that the type 4336 accelerometer was much more sensitive than the strain gages on hand and was light enough that it did not add significant weight to the system (2 grams); therefore, it was used with the plate models. (Strain gage and accelerometer outputs also proved to be the same for several plates which were tested using both transducers.)

Beam models were excited by impact with a small hammer and allowed to vibrate freely. Upon impact a beam begins vibrating in its fundamental mode with various higher modes superimposed. The higher modes die out very quickly, however, and the decay and frequency of the fundamental mode may be measured from the trace of the motion on the oscilloscope. Photographs of the traces for each model were taken in

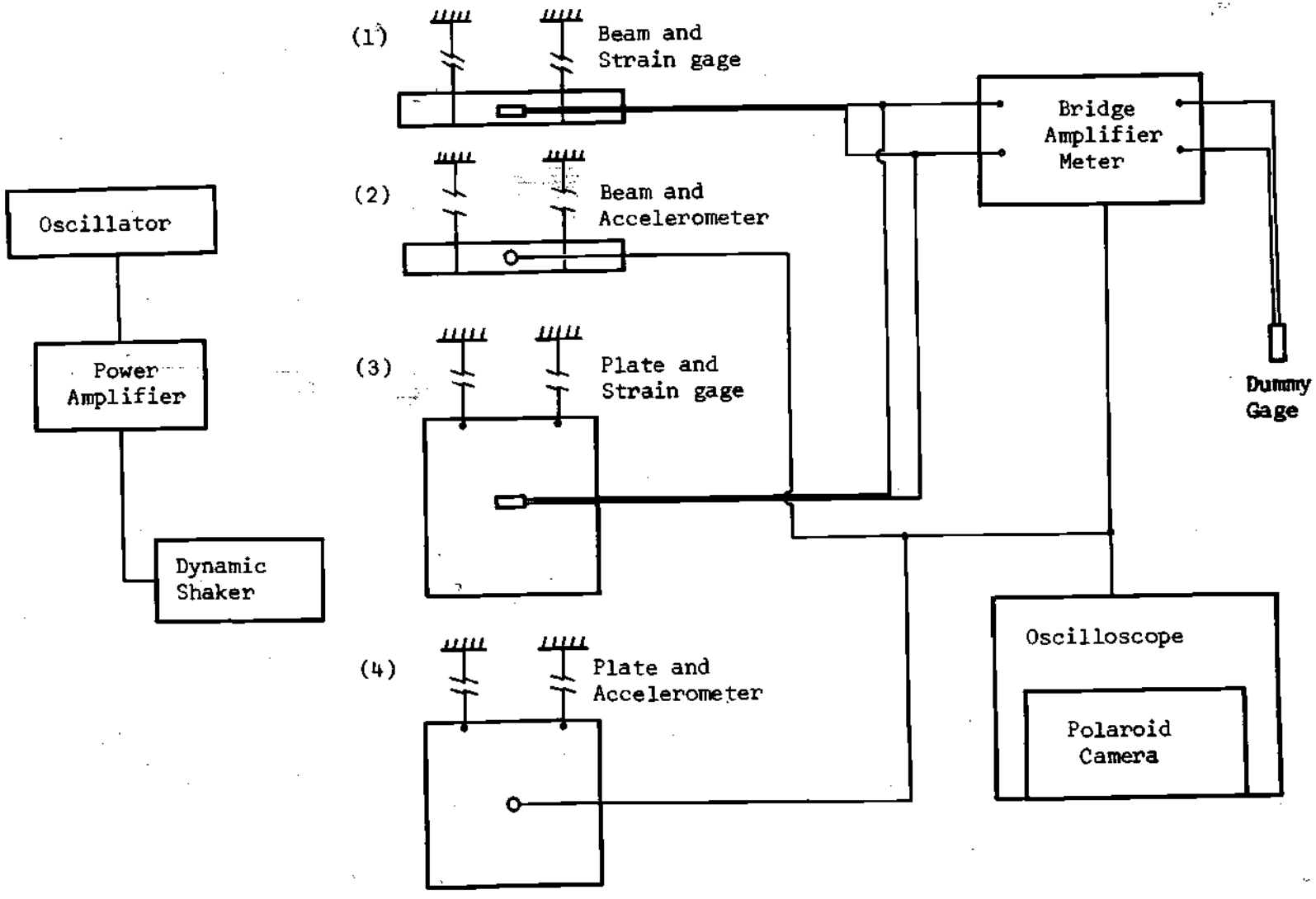

Figure 18. Schematic Diagram of the Experimental Apparatus

order to make accurate measurements. Figure 19 is an example of such a photograph. (The ordinate is displacement; the abscissa is time.) This particular photograph shows the decay of a 5"x2"x0.062" aluminum beam with a 0.264" thick buna-N coating. Each division represents one centimeter and the time scale is 5 milisec/cm. It should be noted that frequency does not vary with time, indicating that damping is linear (proportional to velocity).

It was discovered that the fundamental plate mode can not be excited by impact. Instead, the phenomenon of beats is produced as two beam frequencies (corresponding to beams having lengths equal to the length and width of the plate) are excited. In order to produce the first *plate* mode, a dynamic shaker must be employed. Each plate model was placed in its fundamental resonant mode, then the shaker was disengaged, and finally a photograph was taken of the decaying free vibration. (This same procedure was employed with several beams which had already been tested by the impact technique, and the results of the two methods were found to be the same.) By using the dynamic shaker, higher modes of both beams and plates could be studied; however, this investigation is limited to the fundamental mode as mentioned previously.

Measurement of Damping and Frequency

Several methods of measuring damping are widely used as described by Van Santen (26). The most convenient and thorough method, considering available equipment, was the decaying vibration method which is described in subsequent paragraphs.

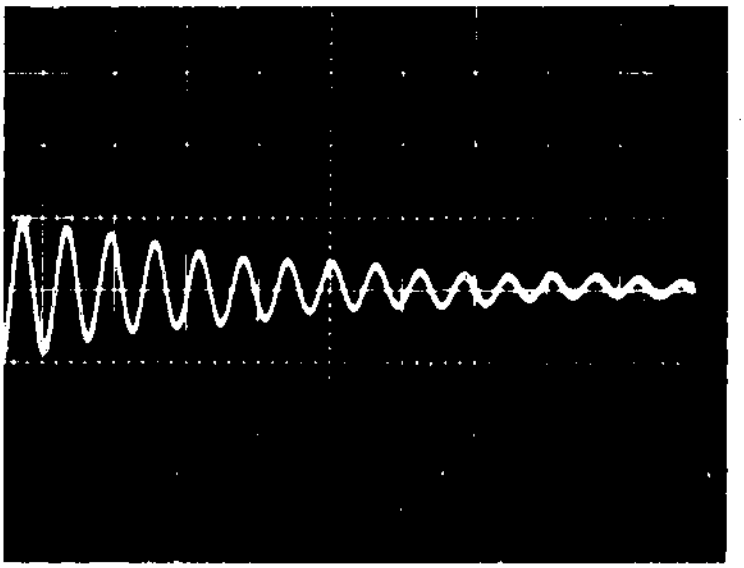

Figure 19. Photograph of Decaying Vibration

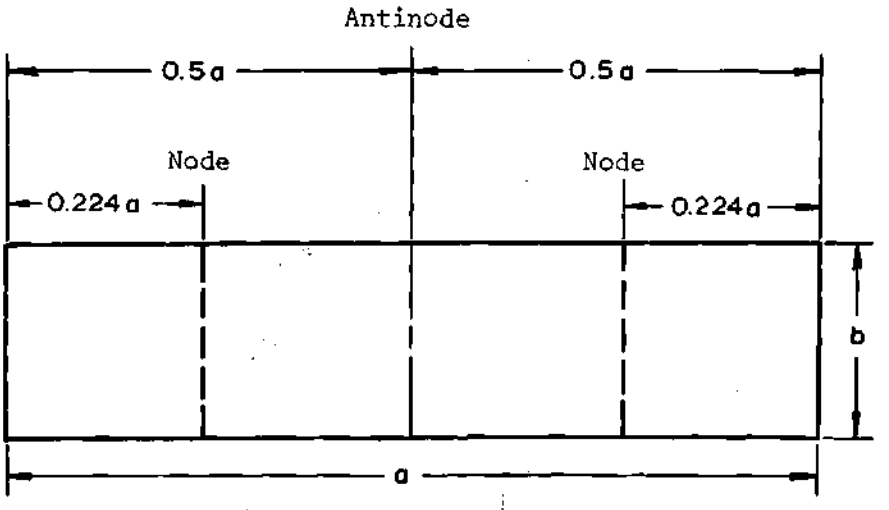

Figure 20. Position of Nodes for Free-Free Beam in First Mode

Beams

The beam of Figure 20 (free-free) has nodes and an antinode at the positions shown according to Oberst (8) and others. The beam models were supported by thin string at the nodes to insure freedom of damping from the supports and were suspended vertically so that the force of gravity had no influence on the motion. The strain gages (and accelerometer) were positioned at the center of the beams in order to obtain the largest readings possible. Motion was induced as described in the previous section and a photographic record made, such as Figure 19, for each of the beams of Table 3.

Figure 19 will be used to illustrate how the desired measurements—damped natural frequency and logarithmic decrement—were obtained. It is seen that approximately 6-1/2 cycles occur in 4 centimeters (time scale—5milisec/cm).

Thus

$$\bar{\omega}_1 = \frac{6.5 \text{ cycles}}{(4.0 \text{ cm.})(0.005 \text{ sec.})} = 325 \text{ c.p.s.}$$

Logarithmic decrement is

$$\delta = \frac{1}{n} \ln(X/X_n) \qquad (87)$$

where X is the amplitude at any time,

X_n is the amplitude n cycles later.

The amplitude of Figure 19 decays from 1.0 cm. to 0.5 cm. in 5-3/4 cycles; therefore,

$$\delta = \frac{1}{5.75} \ln(1.0/0.5) = 0.1205$$

Readings of log decrement were standardized by using the above procedure, i.e., determining the number of cycles required to decay half an amplitude (1.0 cm. to 0.5 cm.). The results of these tests are discussed in Chapter VI and compared to theoretical predictions.

Plates

The plate models were suspended vertically just as the beams were; however, they could not be supported at the node (see Figure 21).

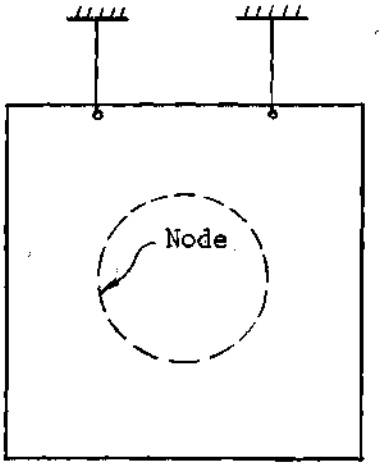

Figure 21. Fundamental Plate Mode

(It was expected that the supports would have a slight effect on the damping of the plates, but the effect was found to be negligible. Frequency was affected slightly, however.) The fundamental plate mode was obtained by varying the frequency of the oscillator until the plate

went into resonance. The existence of resonance was easily recognizable as the output of the accelerometer (which was placed at the center of the plate to obtain maximum output) increases greatly compared to its magnitude when the plate is not in resonance. Then a check was made to see that the mode shape of Figure 21 was present. When this was obtained, the dynamic shaker was disengaged, and a photograph (similar to Figure 19) was taken of the decaying vibration. Damped natural frequency and logarithmic decrement were then measured as explained in the case of beams. The results of these tests are also discussed in Chapter VI.

Determination of Material Properties

In order to calculate the natural frequency and log decrement for a particular beam or plate (using the equations of Chapters III and IV), a number of material properties must be known in addition to the dimensions of the model.

Metal Properties

Since the metals used were common alloys, their properties were taken from handbooks, but were checked by calculating the natural frequencies of metal beams and comparing these values to the measured values for several cases. The properties pertinent to this problem are shown in Table 5. After preliminary tests it was assumed, as done by Oberst (8), that the internal damping of the metals is small in comparison to that of the viscoelastic materials and can be neglected.

Table 5. Metal Properties

Metal	Young's Modulus E (psi)	Density γ(lb/in^3)	Poisson's Ratio ν(dimensionless)
Steel	$30(10)^6$	0.284	0.292
Aluminum	$10.6(10)^6$	0.098	0.334

Viscoelastic Properties

The values of most of the properties of the viscoelastic materials used were not available from reference literature. Even though the damping characteristics of buna-N rubber were available from Nolle's work (16), it was found (as stated by Preiss and Skinner (27)) that they were of no real value unless the composition of the compound and the curing conditions of the rubber are known. Therefore, the properties were determined experimentally.

Density. This was obtained by simply weighing a sample of each material. The values appear in Table 6.

Table 6. Viscoelastic Properties

Material	Density γ(lb./in.^{3})	Poisson's Ratio ν(dimensionless)
Buna-N Rubber (1/16")	0.046	0.50
Buna-N Rubber (1/8")	0.052	0.50
Buna-N Rubber (1/4")	0.046	0.50
Plexiglas (1/8")	0.043	0.247
Plexiglas (1/4")	0.043	0.247
Styrofoam	0.00098	0.155

Poisson's Ratio. Values of this quantity were not available from reference literature for plexiglas and styrofoam. The value for rubber is given by the *Shock and Vibration Handbook* (28) as 0.50. It was found that the exact value has no significant effect upon calculated values of ω and δ (see Appendix E). An approximation of the values for plexiglas and styrofoam was obtained by employing Equations 34 and 70. Experiments were run to determine the frequencies of several models, leaving ν as the only unknown quantity in the above equations. The values of ν determined from these tests appear in Table 6.

Young's Modulus, E_s, and Dynamic Modulus, E_d. These properties were measured for the three viscoelastic coatings used by a method similar to that of Preiss and Skinner (27). A beam model consisting of a metal base with a viscoelastic coating was constructed and tested as described in the previous section to determine its damped natural frequency and logarithmic decrement. This same model was then reduced in length and retested to determine these same quantities. (The lengths were varied so as to cover a frequency range of 50-500 cycles per second.) The relations developed in Chapter III then yield the two moduli according to the following procedure:

(a) Calculate the undamped natural frequency. From Equation 50,

$$\alpha = \frac{\bar{\omega}_1 \delta}{2\pi} \tag{88}$$

Substituting in Equation 34,

$$\omega_1^2 = \bar{\omega}_1^2 + \alpha^2 \tag{89}$$

(b) Determine E_c from Equation 29 (assuming $\bar{z} = t/2$).

$$E_c = \frac{3\rho}{(z_2^3 - z_1^3)\beta_1^4}\left[\omega_1^2 - \frac{E_b(z_3^3 - z_2^3)\beta_1^4}{3\rho}\right] \tag{90}$$

Now calculate $\bar{z}$ from Equation 93. If it differs significantly from t/2 recalculate E_c using the new value of $\bar{z}$. Repeat until E_c is determined to the desired accuracy.

(c) Determine E_d. From Equations 49 and 88,

$$E_d = \frac{3\rho}{(z_2^3 - z_1^3)\beta_1^4}\left[\frac{\frac{1}{\bar{\omega}_1}\alpha^3 + \bar{\omega}_1\alpha}{\frac{1}{2\bar{\omega}_1^2}\alpha^2 + \frac{1}{2}}\right] \tag{91}$$

(d) Calculate E_s. From Equation 17,

$$E_s^2 = E_c^2 - E_d^2 \tag{92}$$

As an illustration of the results of the previous procedure, the measured values of natural frequency and log decrement and the corresponding calculated moduli of a specimen of buna-N rubber are presented in Table 7 and Figure 22. The dynamic properties of the other viscoelastic materials used appear in Appendix I. It will be noted that

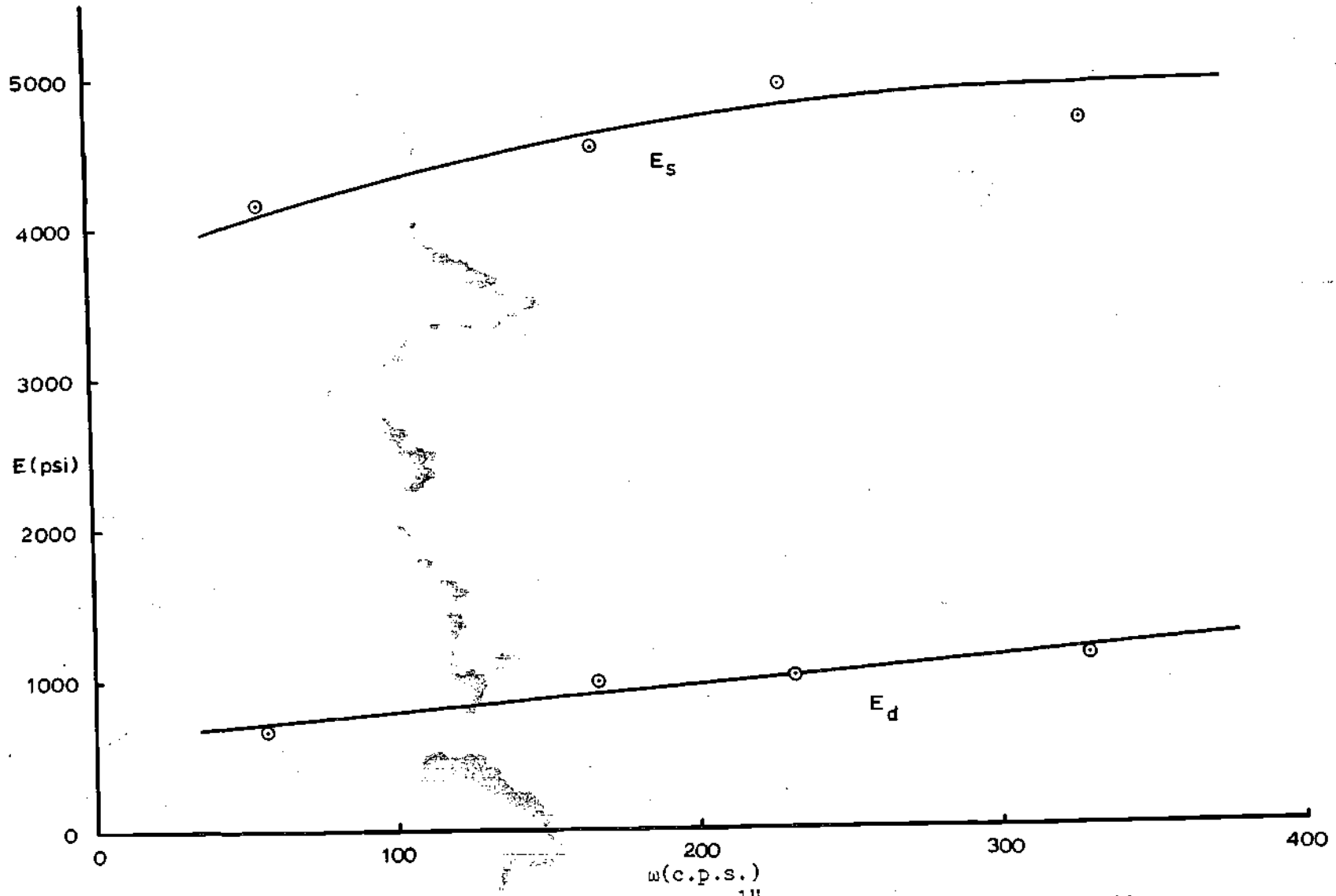

Figure 22. Static and Dynamic Moduli of $\frac{1}{4}$" Thick Specimen of Buna-N Rubber

there are three sets of curves for buna-N rubber. Initially, only one thickness was tested and the others were assumed to have the same properties. However, poor results were obtained in calculations for models made from the other two thicknesses. When actually tested, specimens from the other thicknesses were found to have much different properties. Therefore, it must be concluded that unless the exact composition and method of fabrication are known, each material must be tested firsthand in order to obtain an accurate measure of its dynamic properties.

Table 7. Measurement of Buna-N Properties

Base	Coating	a(in.)	b	t	h	$\bar{\omega}_1$(cps)	δ
Aluminum	Buna-N	12	2	0.062	0.264	56.6	0.0715
Aluminum	Buna-N	7	2	0.062	0.264	167	0.1050
Aluminum	Buna-N	6	2	0.062	0.264	229	0.1067
Aluminum	Buna-N	5	2	0.062	0.264	329	0.1205

CHAPTER VI

DISCUSSION OF THE RESULTS

The numerical results of the theoretical analyses of Chapters III and IV and the experimental results of Chapter V will now be evaluated and compared.

Comparison of the Theoretical and Experimental Values of Frequency and Logarithmic Decrement

Of course, the main objective of the investigation is to relate damping to the amount of coating used (and the properties and dimensions of the structure). It was found that damping also depends (indirectly) upon natural frequency which is itself a function of these same properties and dimensions, and whose value is always of concern in a vibratory problem. Consequently, values of both damped natural frequency and log decrement were measured experimentally and calculated using the theory of Chapters III and IV. The values obtained for each of the models of Table 3 appear in Tables 8, 9, and 10. Experimental and theoretical values of both frequency and log decrement may be seen to be in fairly good agreement.

Further comparison of experimental and theoretical values of damping is presented in Figures 23-32. It will be noted that log decrement itself is not plotted as a function of thickness ratio, but instead η/η_c (or δ/δ_c) is plotted. The loss factor of the coating, η_c ($=E_d/E_s$), is a function of frequency (reference 16); therefore, η

Table 8. Calculated and Experimental Values of Damped Natural Frequency and Logarithmic Decrement for Beams with Coatings on One Side Only

Metal	Coating	$\frac{h}{t}$	Frequency		Log Decrement	
			Cal.	Exp.	Cal.	Exp.
Steel	Buna-N	1.55	134	135	0.00781	0.0069
Steel	Buna-N	2.43	128	125	0.01797	0.0174
Steel	Buna-N	2.43	81.8	80.0	0.02173	0.0192
Steel	Buna-N	3.80	77.1	72.5	0.05296	0.0390
Steel	Buna-N	5.62	116	116	0.06825	0.0703
Steel	Buna-N	8.80	74.1	72.5	0.17357	0.1440
Aluminum	Buna-N	1.18	161	155	0.01208	0.0110
Aluminum	Buna-N	1.35	144	140	0.01610	0.0182
Aluminum	Buna-N	1.84	148	140	0.02594	0.0231
Aluminum	Buna-N	2.11	132	120	0.03529	0.0240
Aluminum	Buna-N	2.28	73.2	73.0	0.05075	0.0256
Aluminum	Buna-N	3.56	66.7	61.5	0.11750	0.0895
Aluminum	Buna-N	4.26	126	122	0.08822	0.0913
Aluminum	Buna-N	4.89	113	112	0.11713	0.133
Aluminum	Buna-N	8.25	67.1	64.5	0.28086	0.261
Steel	Plexiglas	2.87	262	275	0.12457	0.133
Steel	Plexiglas	4.57	257	267	0.14508	0.142
Steel	Plexiglas	4.83	431	440	0.13519	0.118
Steel	Plexiglas	7.73	450	465	0.13475	0.118
Aluminum	Plexiglas	2.27	347	356	0.12125	0.118
Aluminum	Plexiglas	2.52	342	355	0.12458	0.118
Aluminum	Plexiglas	3.71	522	525	0.12015	0.145
Aluminum	Plexiglas	4.25	301	306	0.13320	0.138
Aluminum	Plexiglas	4.70	588	595	0.11491	0.111
Aluminum	Plexiglas	7.34	497	500	0.11560	0.099
Steel	Styrofoam	10.64	176	180	0.01269	0.0139
Steel	Styrofoam	17.70	158	165	0.02744	0.0302
Steel	Styrofoam	19.96	274	275	0.03149	0.0356
Steel	Styrofoam	31.27	295	300	0.04000	0.0407
Aluminum	Styrofoam	8.56	246	250	0.01686	0.0231
Aluminum	Styrofoam	9.83	244	244	0.02102	0.0375
Aluminum	Styrofoam	15.13	376	384	0.03458	0.0322
Aluminum	Styrofoam	15.63	207	220	0.03350	0.0554
Aluminum	Styrofoam	17.37	398	400	0.03809	0.0386
Aluminum	Styrofoam	29.31	424	433	0.04432	0.0566

Table 9. Calculated and Experimental Values of Damped Natural Frequency and Logarithmic Decrement for Plates with Coatings on One Side Only

Metal	Coating	$\frac{h}{t}$	Frequency		Log Decrement	
			Cal.	Exp.	Cal.	Exp.
Aluminum	Buna-N	1.18	228	205	0.01234	0.00601
Aluminum	Buna-N	1.55	165	159	0.02186	0.01185
Aluminum	Buna-N	1.84	204	186	0.02621	0.0250
Aluminum	Buna-N	2.28	104	98	0.05078	0.0233
Aluminum	Buna-N	2.43	145	141	0.04884	0.0356
Aluminum	Buna-N	3.56	94.0	83.4	0.11689	0.0925
Aluminum	Buna-N	4.26	178	165	0.09336	0.0816
Aluminum	Buna-N	5.62	132	123	0.15717	0.1260
Aluminum	Buna-N	8.25	95.0	90.0	0.28831	0.2770
Aluminum	Plexiglas	2.23	488	460	0.11614	0.111
Aluminum	Plexiglas	2.91	457	439	0.12420	0.124
Aluminum	Plexiglas	3.92	785	733	0.10948	0.111
Aluminum	Plexiglas	4.31	436	408	0.12758	0.129
Aluminum	Plexiglas	5.17	761	720	0.10873	0.109
Aluminum	Plexiglas	7.59	732	684	0.10548	0.111
Aluminum	Styrofoam	8.56	350	318	0.01800	0.0170
Aluminum	Styrofoam	8.78	186	160	0.01814	0.0272
Aluminum	Styrofoam	10.64	306	289	0.02464	0.0240
Aluminum	Styrofoam	15.13	535	472	0.03592	0.0250
Aluminum	Styrofoam	16.59	319	258	0.03589	0.0325
Aluminum	Styrofoam	19.96	553	478	0.04151	0.0304

Table 10. Calculated and Experimental Values of Damped Natural Frequency and Logarithmic Decrement for Beams with Two Symmetric Coatings

Metal	Coating	$\frac{h}{t}$	Frequency		Log Decrement	
			Cal.	Exp.	Cal.	Exp.
Aluminum	Buna-N	3.11	98.3	91.6	0.04141	0.0207
Aluminum	Buna-N	4.22	104	92.5	0.06713	0.0603
Aluminum	Buna-N	7.13	54.7	48.5	0.21366	0.1387
Aluminum	Buna-N	8.52	104	100	0.14677	0.1682
Aluminum	Buna-N	16.50	61.4	58.0	0.37079	0.420

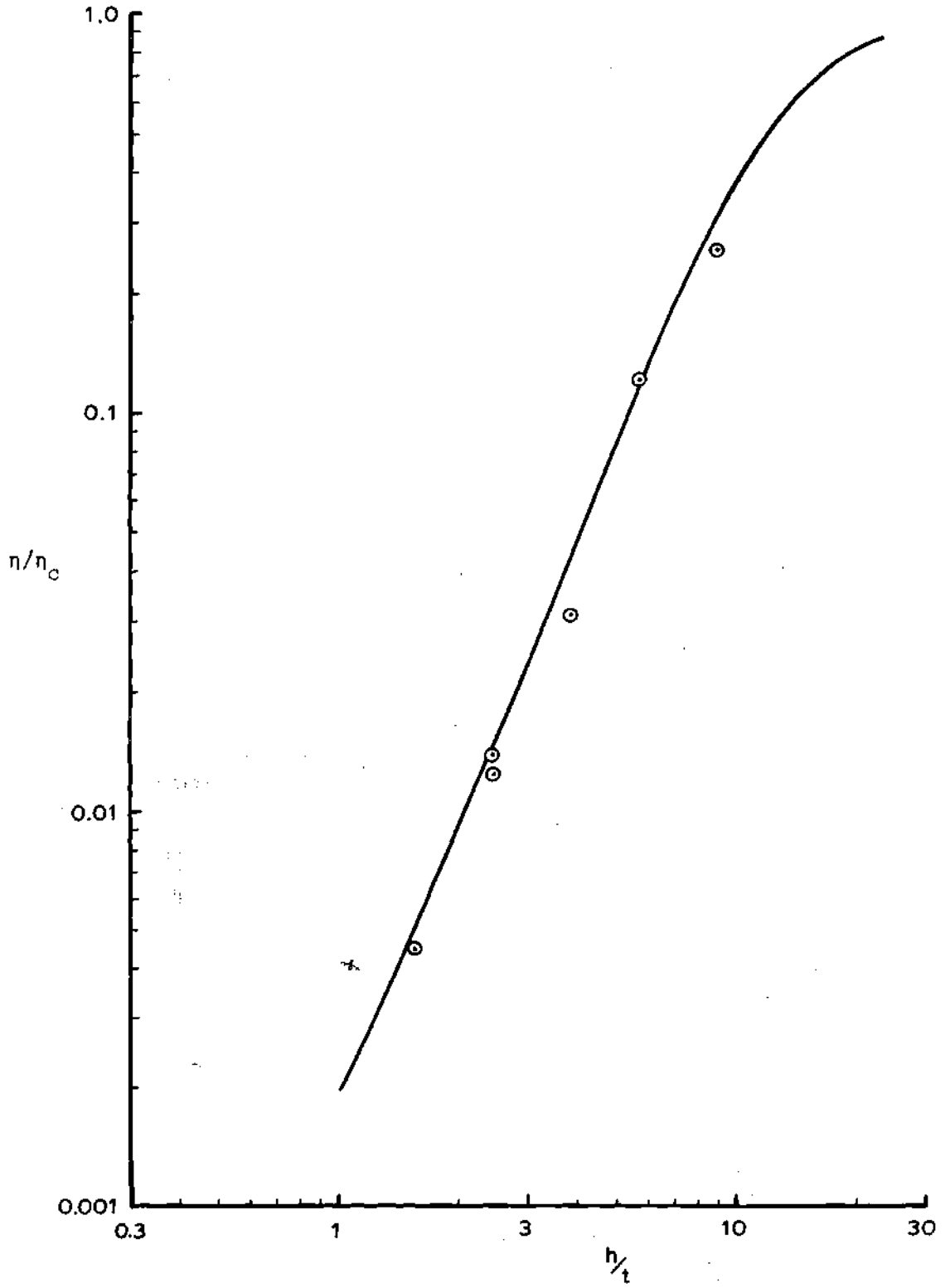

Figure 23. Experimental vs. Theoretical Values of Damping for Free-Free Steel Beams with Buna-N Coatings on One Side Only

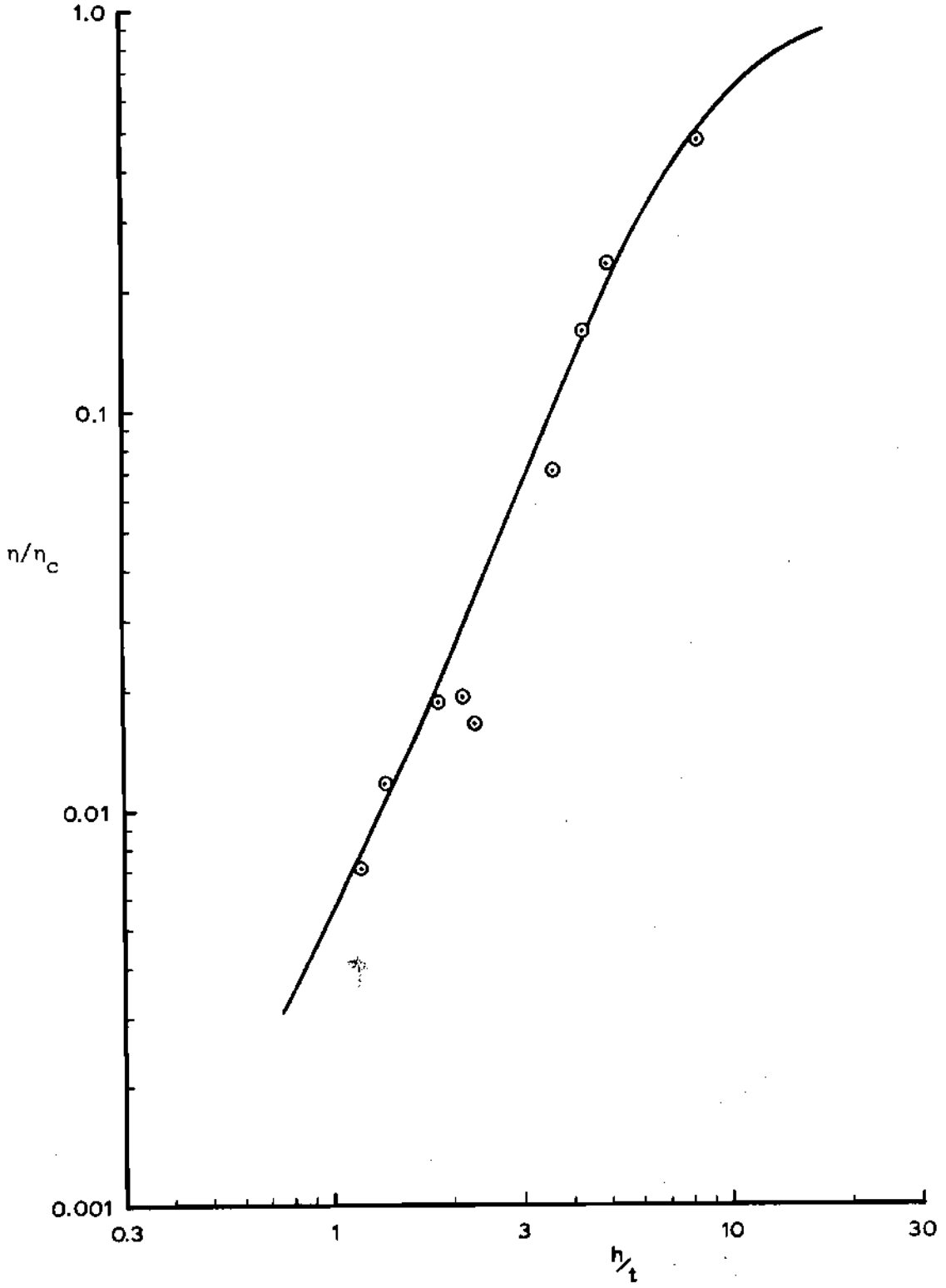

Figure 24. Experimental vs. Theoretical Values of Damping for Free-Free Aluminum Beams with Buna-N Coatings on One Side Only

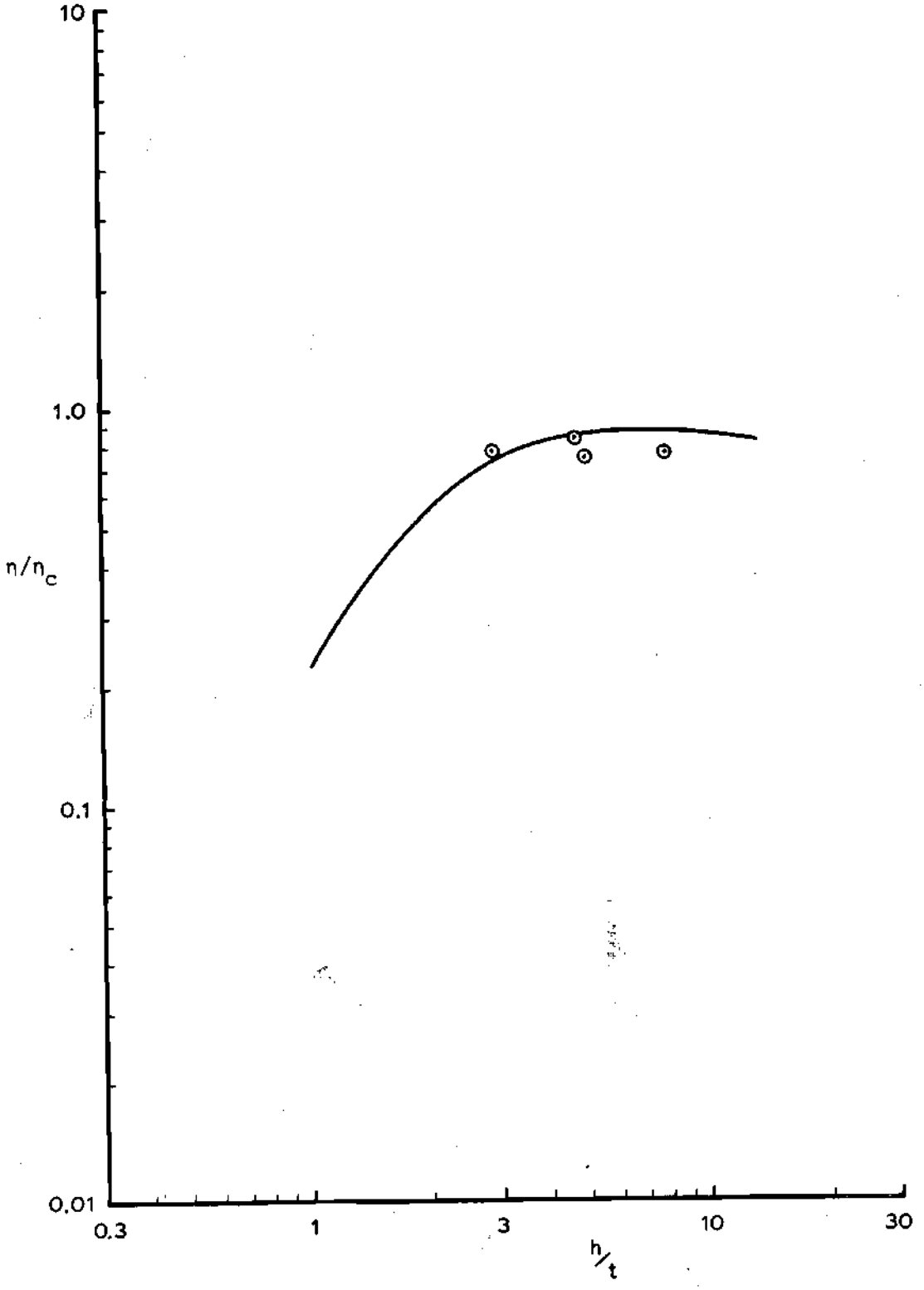

Figure 25. Experimental vs. Theoretical Values of Damping for Free-Free Steel Beams with Plexiglas Coatings on One Side Only

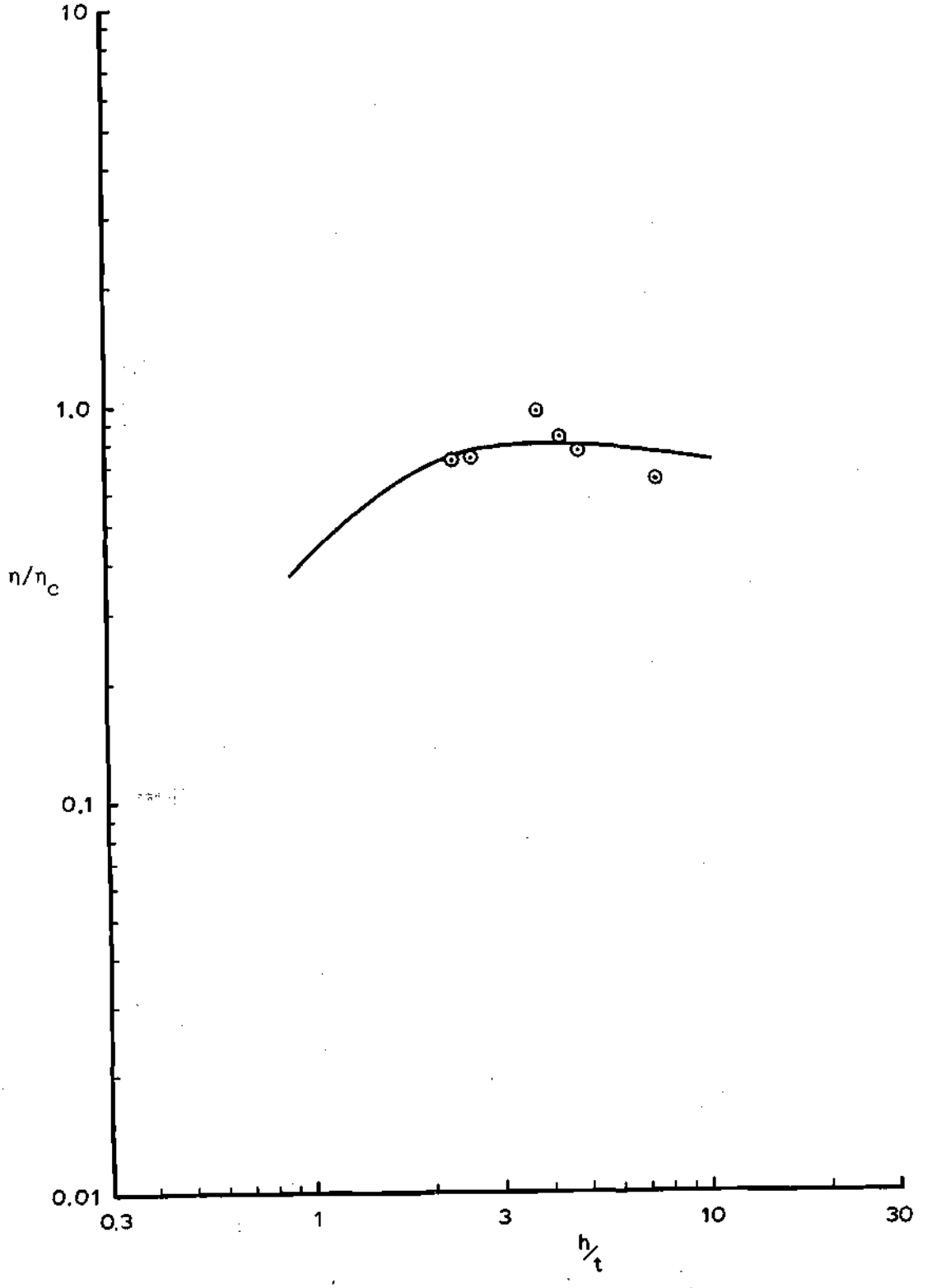

Figure 26. Experimental vs. Theoretical Values of Damping for Free-Free Aluminum Beams with Plexiglas Coatings on One Side Only

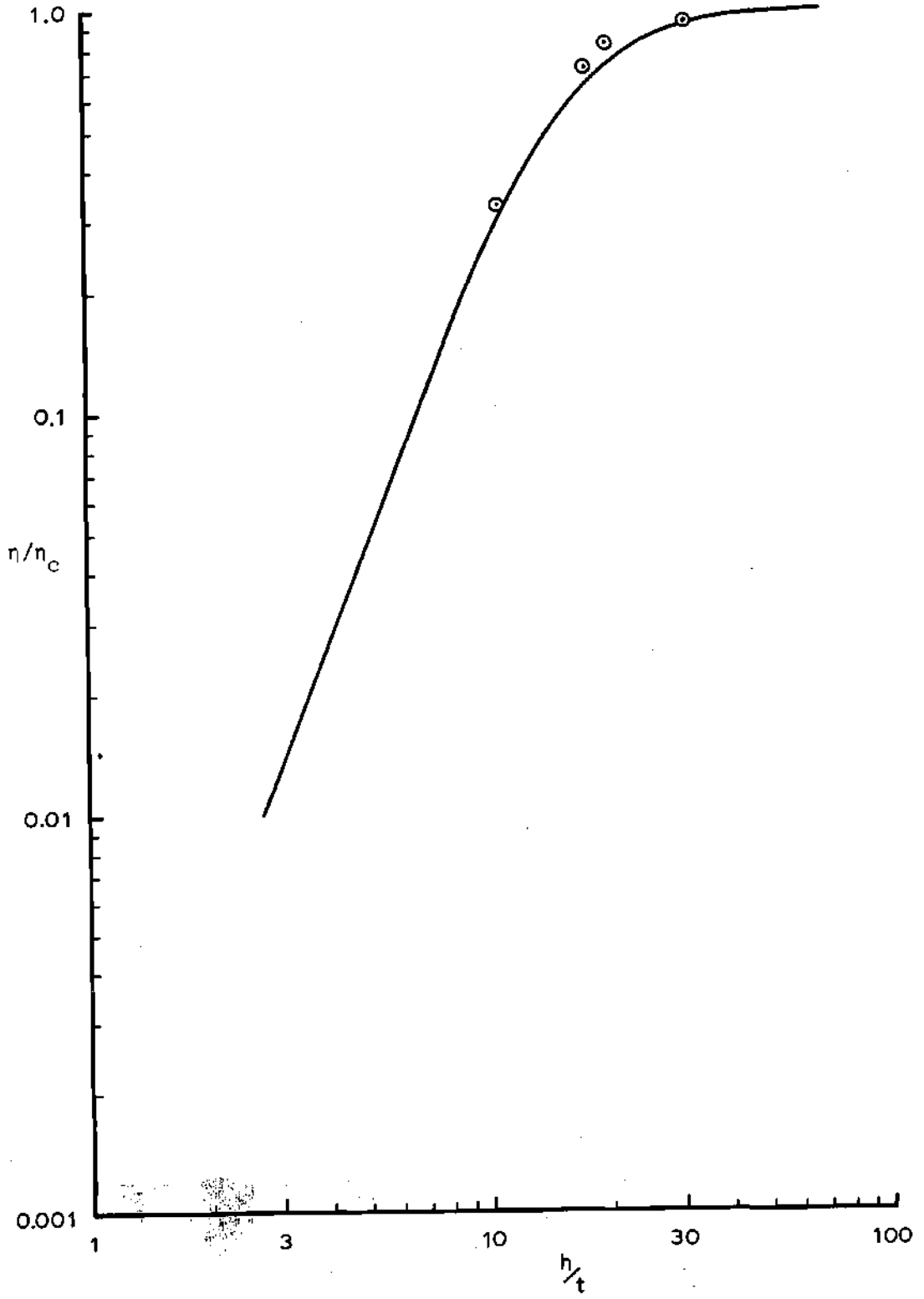

Figure 27. Experimental vs. Theoretical Values of Damping for Free-Free Steel Beams with Styrofoam Coatings on One Side Only

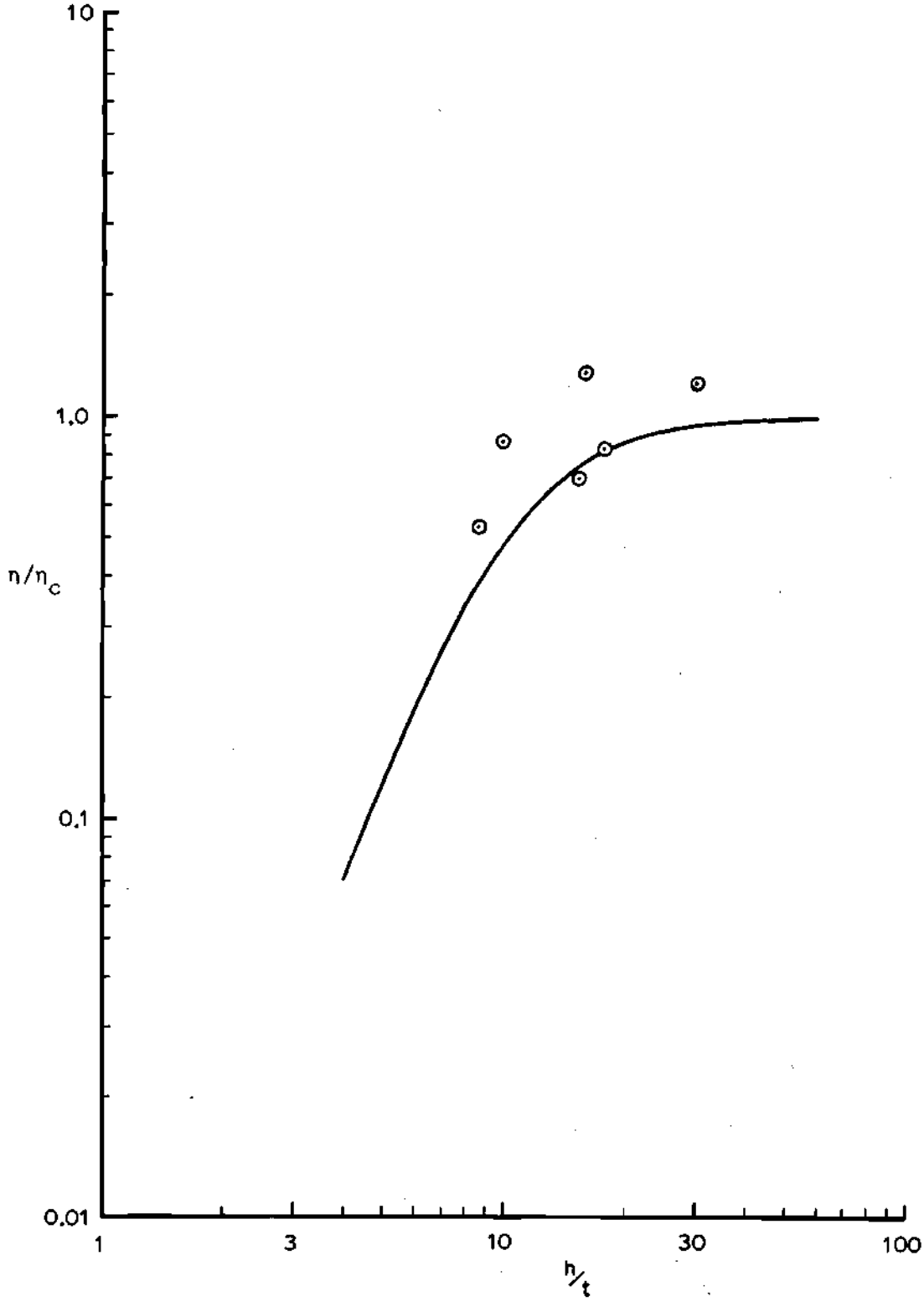

Figure 28. Experimental vs. Theoretical Values of Damping for Free-Free Aluminum Beams with Styrofoam Coatings on One Side Only

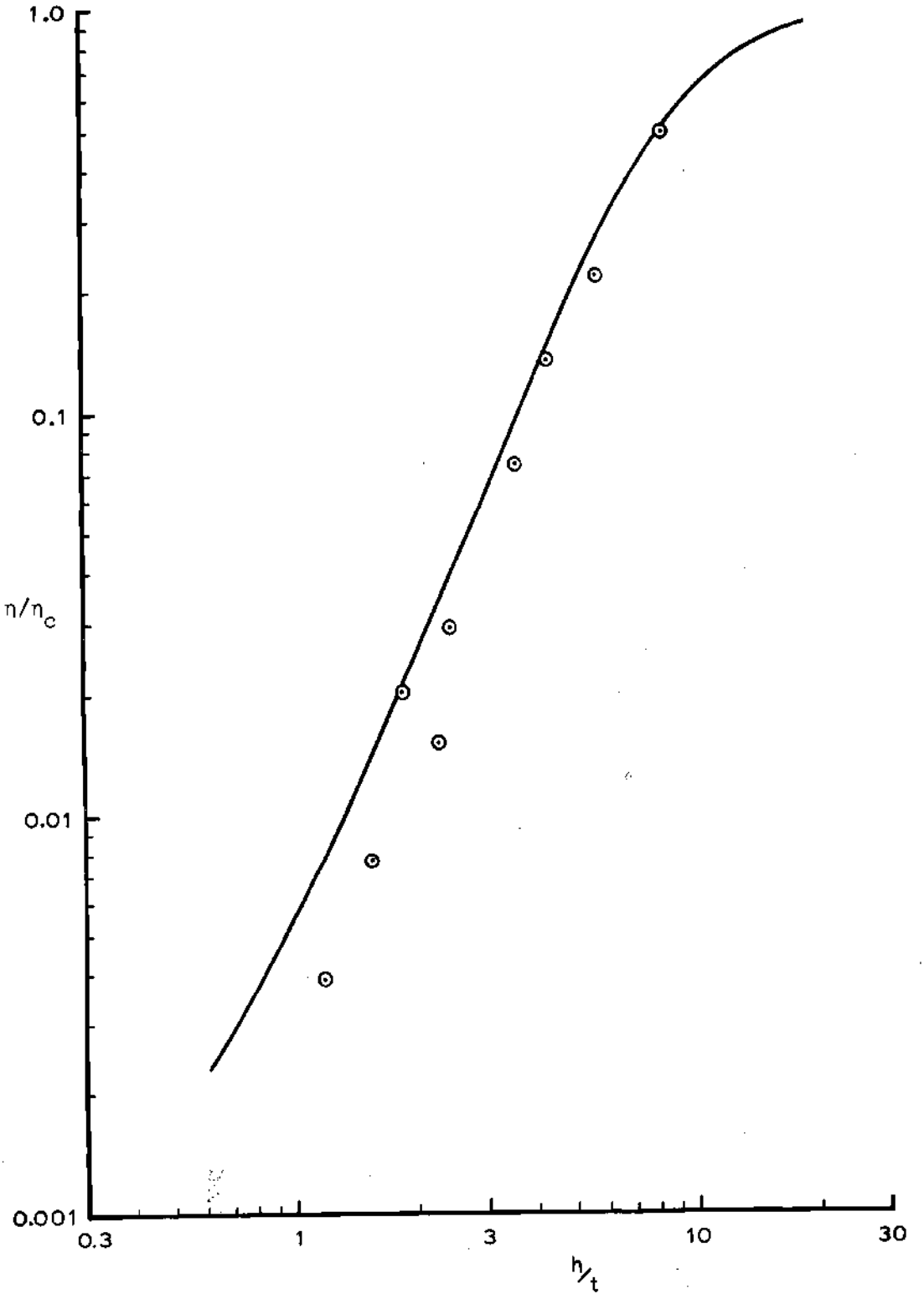

Figure 29. Experimental vs. Theoretical Values of Damping for Free Plates (Aluminum) with Buna-N Coatings on One Side Only

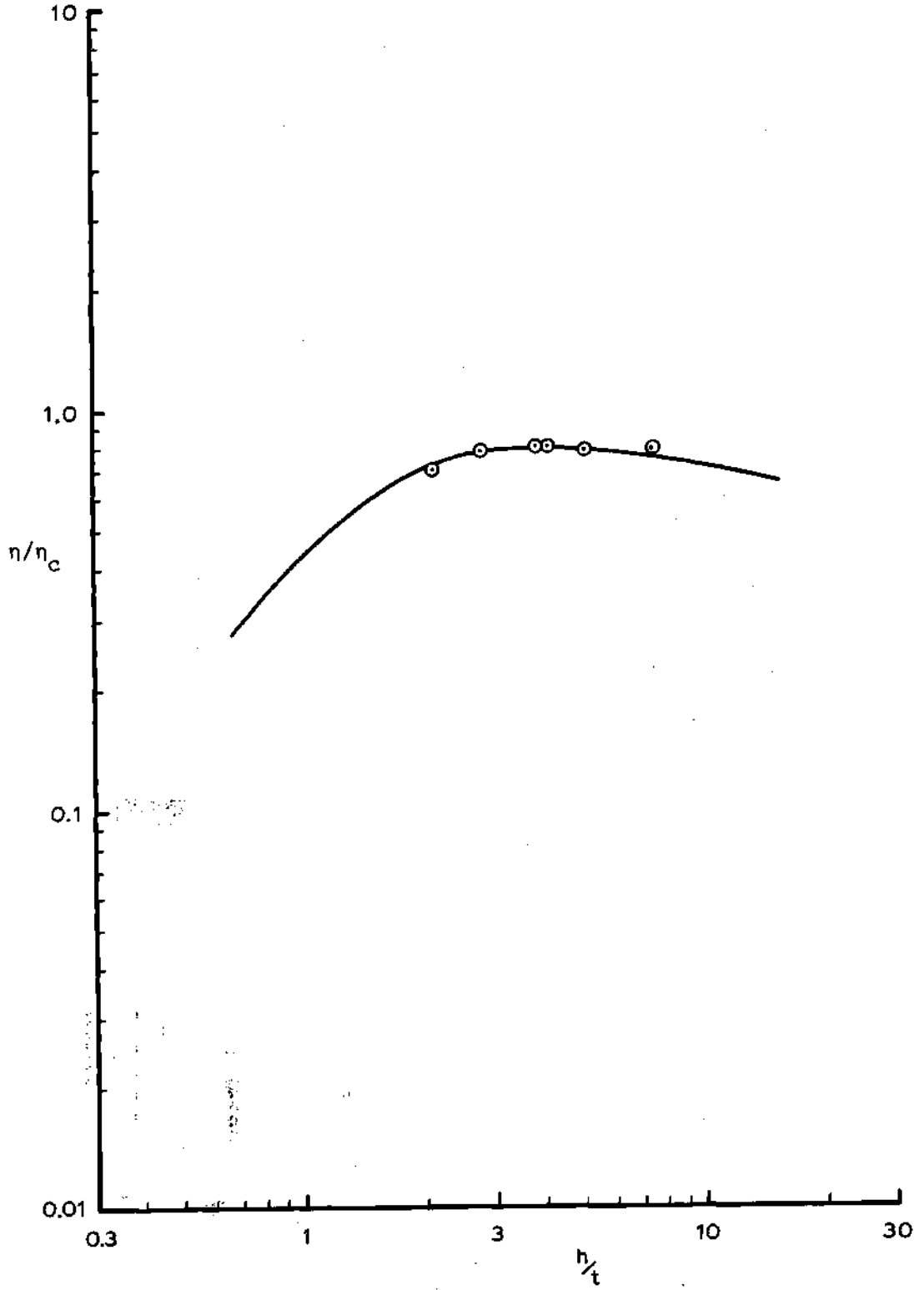

Figure 30. Experimental vs. Theoretical Values of Damping for Free Aluminum Plates with Plexiglas Coatings on One Side Only

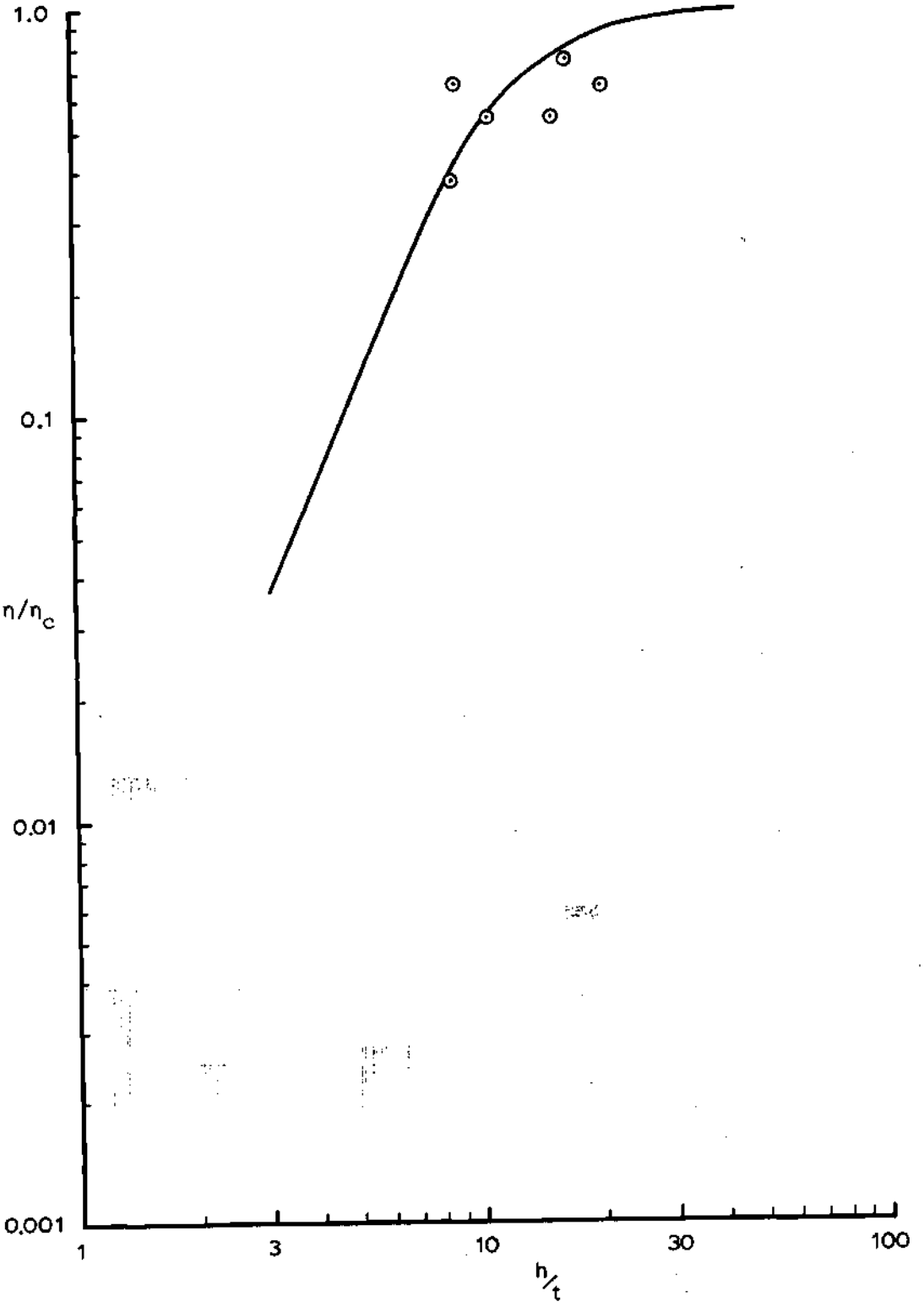

Figure 31. Experimental vs. Theoretical Values of Damping for Free Aluminum Plates with Styrofoam Coatings on One Side Only

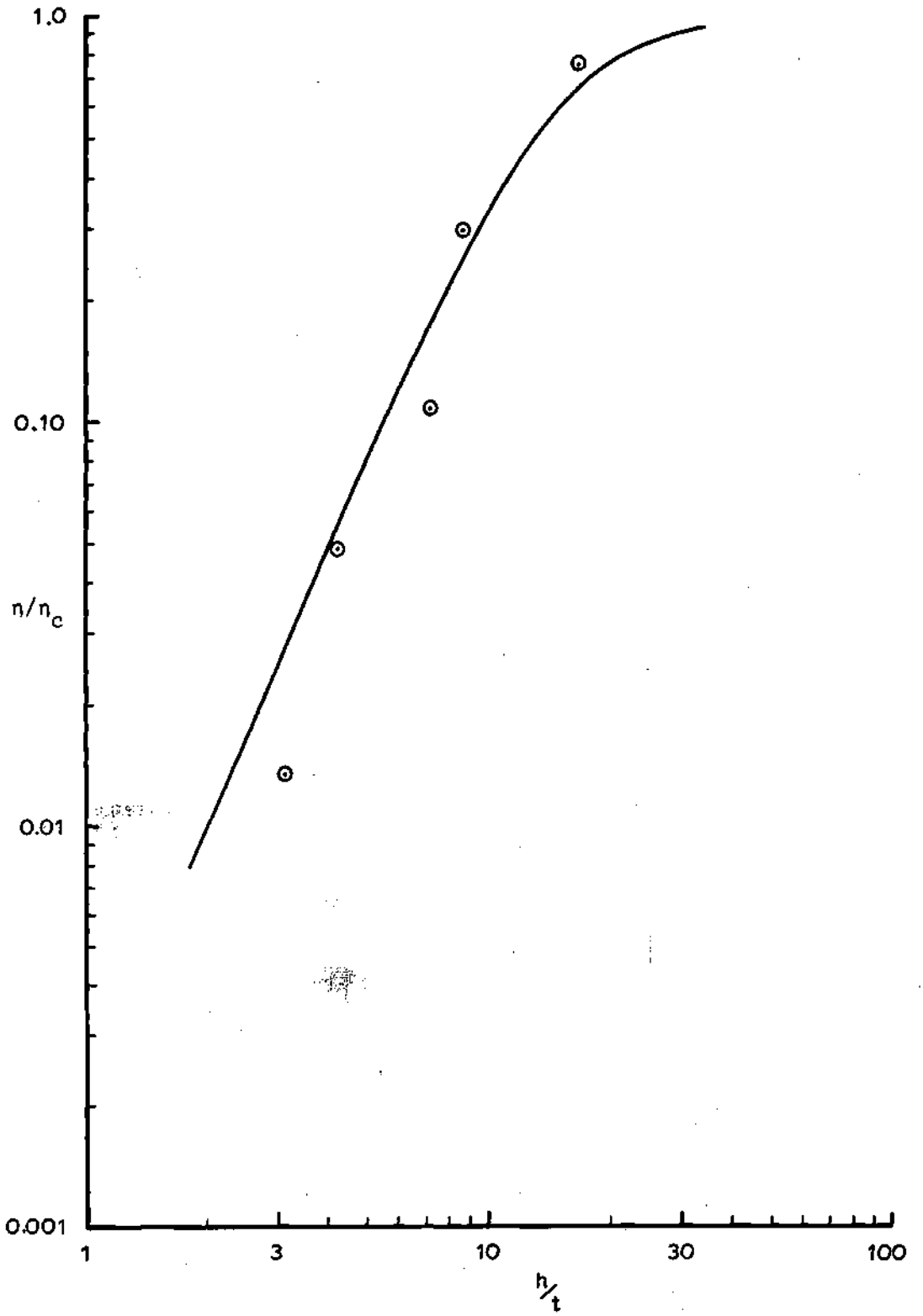

Figure 32. Experimental vs. Theoretical Values of Damping for Free-Free Aluminum Beams with Two Symmetric Buna-N Coatings

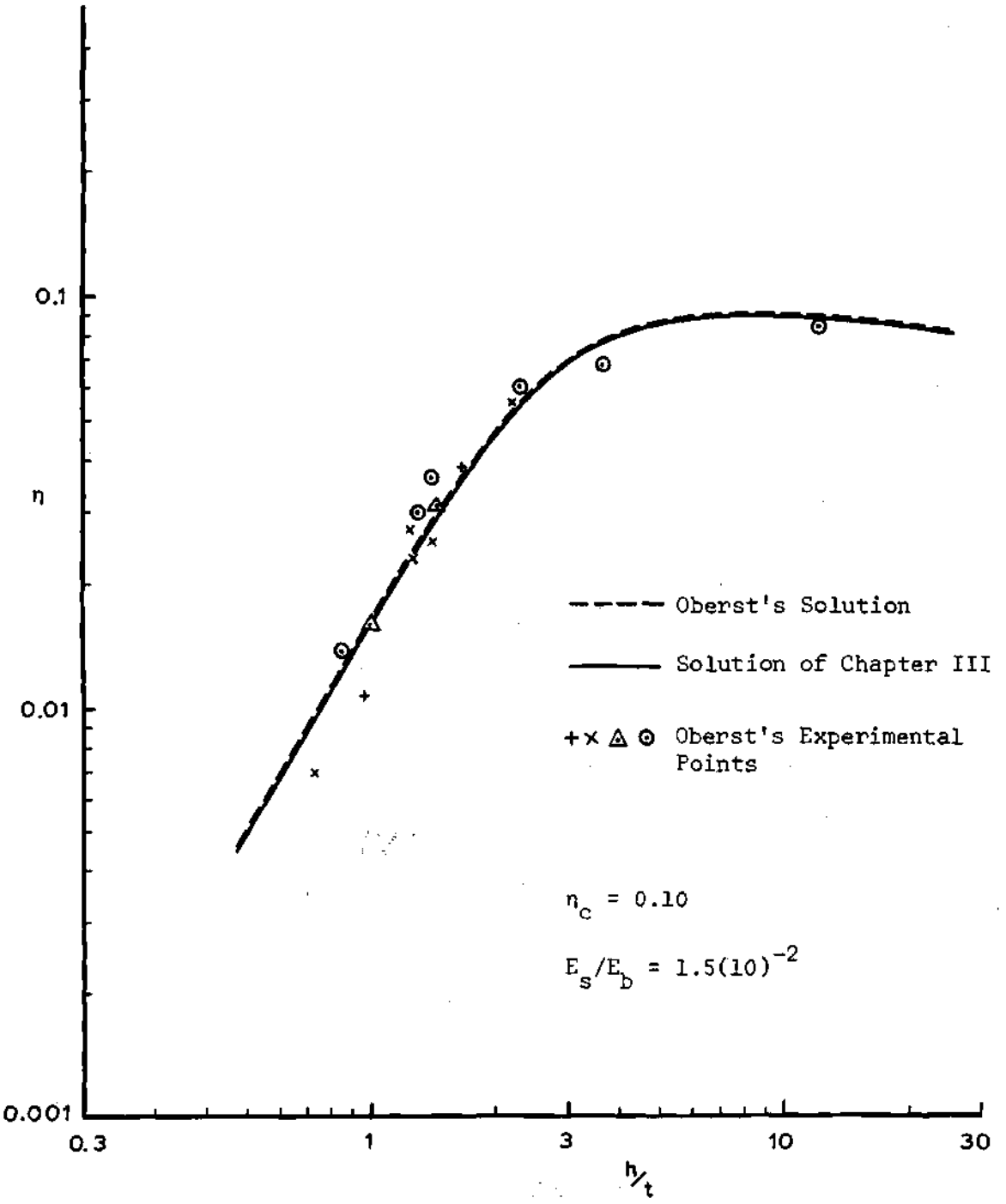

Figure 33. Experimental (Oberst's) vs. Theoretical Values of Damping for Free-Free Beams with Coatings on One Side Only

(hence δ) is a function of frequency. However, the ratio η/η_c is independent of frequency and plots nicely.

Comparison is also made with the theoretical and experimental results of another investigator. Figure 33 shows values of damping calculated from the solution of Chapter III and from Oberst's solution (8) as compared to Oberst's experimental values for a number of cases. Agreement with Oberst's values was quite good. Table 11 gives a more accurate comparison of the two solutions.

Comparison of Beam and Plate Damping

Comparison of Figures 13 and 17 shows that the damping ratio for a beam composed of a particular metal and coating and having a particular thickness ratio is approximately the same as that for a plate composed of the same materials and having the same thickness ratio. (A better comparison may be made by comparing the numerical results of Table 12.) Naturally, plate frequencies differ considerably from beam frequencies, and since η_c is a function of frequency the loss factor, η (hence δ), is not necessarily the same for beams and plates with the same coating to metal thickness ratio and composed of the same materials. (η is the same if the beam and plate happen to have the same natural frequency or if the loss factor of the coating does not change with frequency.) However, the magnitudes of the two values will be comparable.

Table 11. Comparison of Beam Solution and Oberst's Solution for Beams with Coatings on One Side Only, $\eta_c = 0.10$ and $E_s/E_b = 1.5(10)^{-2}$

$\frac{h}{t}$	LOGARITHMIC DECREMENT	
	Solution 1 Equations 29, 34, 49, and 50	Oberst's Solution
0.50	0.0154	0.0155
0.62	0.0220	0.0220
0.74	0.0297	0.0297
0.88	0.0401	0.0401
1.00	0.0499	0.0500
1.24	0.0718	0.0719
1.50	0.0974	0.0975
1.76	0.1229	0.1231
2.00	0.1453	0.1456
2.50	0.1852	0.1857
3.00	0.2150	0.2156
4.00	0.2506	0.2514
5.00	0.2673	0.2681
6.00	0.2749	0.2758
8.00	0.2789	0.2799
10.00	0.2776	0.2786
15.00	0.2693	0.2703
20.00	0.2605	0.2615

Comparison of the Effectiveness of Symmetric Coatings and Coatings Applied to One Side Only

It may be seen from Figures 13 and 15 and from Table 13 that for small (and moderate) thickness ratios it is much more efficient to employ all of the viscoelastic coating on one side rather than divide it between the two sides. However, when the thickness ratio becomes relatively large (depending upon the relative strengths of the metal and coating) the neutral axis is shifted significantly when the coating is applied to only one side and a point is reached (for instance, $h/t = 7.0$ in Table 13) beyond which it is more efficient to use two

Table 12. Comparison of Damping Ratios of Beams and Plates with Coatings on One Side Only for $\eta_c = 1.0$ and $E_s/E_b = E_s/E_p = (10)^{-4}$

$\frac{h}{t}$	η/η_c	
	Beam	Plate
0.10	0.00004	0.00004
0.20	0.00009	0.00009
0.30	0.00015	0.00015
0.40	0.00024	0.00024
0.70	0.00064	0.00064
1.00	0.00130	0.00129
1.40	0.00268	0.00267
2.00	0.00614	0.00610
2.50	0.01058	0.01052
3.00	0.01669	0.01658
4.00	0.03460	0.03439
5.00	0.06077	0.06042
6.00	0.09513	0.09460
7.00	0.13664	0.13593
8.00	0.18351	0.18263
9.00	0.23362	0.23259
10.00	0.28482	0.28367
13.00	0.42951	0.42825
16.00	0.54343	0.54229
20.00	0.64552	0.64465
22.00	0.68012	0.67938
25.00	0.71788	0.71730
28.00	0.74377	0.74331
30.00	0.75649	0.75609
40.00	0.79326	0.79305
50.00	0.80603	0.80589
60.00	0.81127	0.81114
70.00	0.81339	0.81328
85.00	0.81413	0.81403
100.00	0.81360	0.81350
200.00	0.80387	0.80372
300.00	0.79311	0.79290
500.00	0.77047	0.77015

Table 13. Comparison of the Effectiveness of Symmetric Coatings and Coatings on One Side Only for Beams with $\eta_c = 1.0$ and $E_s/E_b = (10)^{-2}$

$\frac{h}{t}$	η/η_c	
	Two Symmetric Coatings	Coating on One Side
0.10	0.00329	0.00361
0.20	0.00721	0.00857
0.30	0.01177	0.01502
0.40	0.01702	0.02311
0.70	0.03709	0.05779
1.00	0.06376	0.10752
1.40	0.10887	0.19093
2.00	0.19182	0.32678
2.50	0.26760	0.42796
3.00	0.34294	0.50908
4.00	0.47569	0.61457
5.00	0.57589	0.66846
6.00	0.64650	0.69457
7.00	0.69512	0.70622
8.00	0.72862	0.71021
9.00	0.75200	0.70999
10.00	0.76860	0.70741
13.00	0.79895	0.69365
16.00	0.81135	0.67743
20.00	0.81892	0.65648
25.00	0.82304	0.63313
30.00	0.82493	0.61306
40.00	0.82649	0.58114
50.00	0.82706	0.55764
60.00	0.82732	0.54022
70.00	0.82745	0.52728
85.00	0.82755	0.51397
100.00	0.82760	0.50581
200.00	0.82767	0.50673
300.00	0.82767	0.53313
500.00	0.82768	0.58438
1000.00	0.82768	0.66251

symmetric coatings rather than employ all of the material on one side. For most practical cases, however, the use of coatings on one side only is more efficient.

Optimum Thickness Ratio

Another interesting observation from Figure 13 and 17 is that the theory predicts that beyond a certain thickness ratio, damping *decreases* with an increase in the amount of coating applied. This fact is substantiated by experiment as shown in Figures 25, 26, and 30 for both beams and plates coated on one side only. It will be noted in Figure 15 (beams coated with two symmetric layers), however, that no optimum thickness ratio exists. Instead, damping values level off beyond a certain value of thickness ratio. The difference in the two cases is the fact that the neutral axis is shifted in the unsymmetric case while it remains at the center of the composite symmetric structure. (The shift of this axis decreases the extension of the fibers of the coating.)

In the design of a system, one would not want to use material and receive no damping in return; thus, the value of the optimum thickness ratio is of concern. An approximation of this value may be obtained by examination of Figures 13 and 17 (and those of Appendix F). (Also to be considered is the leveling off which occurs just prior to the optimum value of damping. Even for the symmetric case of Figure 15 there is a leveling off point beyond which very little profit is received from investment of material.) To obtain the value of optimum thickness ratio accurately, one must apply an optimization technique to

the theoretical relationship. This is done in Appendix J for the case of small damping, i.e., $\eta_c \leq 0.10$. (The general case is so involved that nothing can be gleaned from it.) It is first shown that no optimum thickness ratio exists for the symmetric case. Then an eighth order polynomial in h/t is derived for the unsymmetrical case which depends only upon the ratio E_s/E_b. A graphical solution appears in Figure 34 which is valid for both beams and plates with $\eta_c \leq 0.10$. (The optimum thickness ratios of Figures 25, 26, and 30 substantiate these values.)

Higher Modes

As stated previously, this investigation is limited to a study of the fundamental mode only. However, higher modes may be considered with little additional effort. For instance, in the solution for beams with coatings on one side (Equations 29, 34, 49, and 50), only β changes from mode to mode: $\beta_1 = 4.730/a$, $\beta_2 = 7.8532/a$, ..., $\beta_m = (2m+1)/2a$. (See reference 18.) It is shown in Appendix E that damping depends upon only three dimensionless ratios, none of which involves length, hence β. Therefore, damping in higher modes is only affected by material properties as they change with frequency. (If the loss factor of a material increases with frequency, damping is greater as the mode number increases or vice versa.) It should be noted that the effects of rotary inertia become increasingly significant at higher frequencies, however, and the assumptions upon which the theory is based will at some point lose their validity as this effect becomes more dominant.

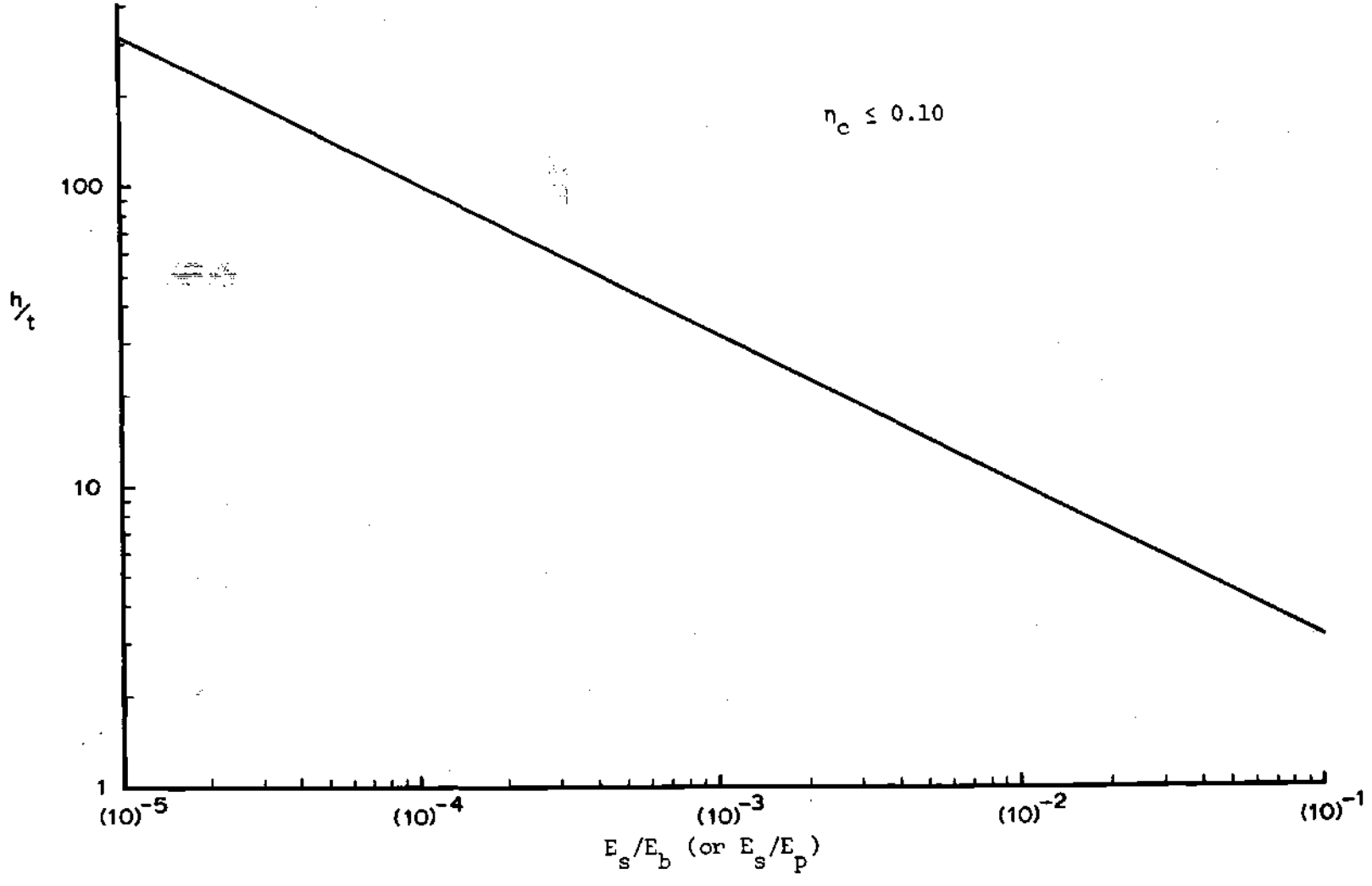

Figure 34. Optimum Thickness Ratios

Other End Conditions

This investigation is also limited to the case of free-free beams and plates; however, a number of other end conditions may easily be considered with the help of Felgar (20). The derivations are identical to those of Chapters III and IV except for the fact that under other constraints the values of α_m and β_m as well as the integrals of the characteristic mode functions, $F_m(x)$ and $G_n(y)$, differ from those for the free-free case.

CHAPTER VII

CONCLUSIONS

As a result of the investigation to determine the damping effects of unconstrained viscoelastic coatings on the transverse vibrations of beams and plates, the following conclusions may be drawn:

The dynamic behavior of a viscoelastic material may be accurately described by a Voigt (Kelvin) model (spring and dashpot in parallel) used in conjunction with curves of the static and dynamic moduli of the material as they vary with frequency. Actually, using a Voigt model in conjunction with modulus vs. frequency curves is equivalent to using a more complex model.

Curves describing the static and dynamic moduli of a viscoelastic material as they vary with frequency are of little value to the user unless the exact composition and method of fabrication of the material are also known.

Incorporation of a viscoelastic material with an elastic structure not only adds damping to the system, but also alters the natural frequency of the system. The amount of damping produced by a given thickness of viscoelastic material and the natural frequency of the new composite structure can be predicted accurately for both beams and plates with coatings on one or both sides using the theory of Chapters III and IV. In general, the thicker the coating applied to a beam or plate, the greater the amount of damping produced; however, for the case

of coatings on one side only, there is an optimum thickness ratio beyond which addition of viscoelastic coating *decreases* the amount of damping because of the shift of the neutral axis. (This was verified experimentally in the plexiglas beam and plate tests.) Also, the higher the dynamic (loss) modulus, E_d, of the viscoelastic material the greater the amount of damping for a given thickness ratio.

The theoretical results for a beam coated on one side and restricted to light damping ($\eta_c \leq 0.10$) are almost identical to those of Oberst (8). In addition, the natural frequency of the structure is known and the solution is not restricted to light damping, neither of which is the case with Oberst's solution.

Damping depends directly upon only three dimensionless ratios, h/t, E_d/E_s, E_s/E_b; however, indirectly it also depends upon length and density (and Poisson's ratio in the case of plates) since E_d and E_s vary with frequency. If the static and dynamic moduli of a viscoelastic material do *not* vary with frequency, then damping is independent of length, density, Poisson's ratio, and frequency.

For small and moderate thickness ratios, it is more effective to employ a given amount of viscoelastic material on one side of the metal rather than divide it equally between the two sides; however, there is a thickness ratio beyond which it is more efficient to use two symmetric coatings rather than one.

If a beam and plate are composed of the same materials and have the same coating to base thickness ratio, the damping of each will be of the same order of magnitude; it will be the same if the beam and

plate have the same natural frequency or if the moduli of the visco-elastic material do not vary with frequency.

CHAPTER VIII

RECOMMENDATIONS

The following recommendations are made concerning possible areas of future investigation:

The case of a viscoelastic material constrained by an outer stiff layer ("sandwich"), which was mentioned in Chapter I, might also be attacked using this method in order to provide some more easily accessible design data concerning damping than that of Kerwin (1) and others.

Kimel, Kirmser, Patel, and Raville (18) found the *frequencies* of undamped, "sandwich" *beams* as mentioned earlier. Their work might be extended to determining the natural frequencies of "sandwich" *plates* using the method of Chapter IV.

In addition, it would be worthwhile to survey a broad range of materials comparing their relative advantages and disadvantages as damping materials. This has been done within the family of rubber-like materials, but not for other categories of materials.

Damping in higher modes might also be studied to determine the validity of the assumptions in this region since the effects of rotary inertia become increasingly significant at higher frequencies.

APPENDIX

APPENDIX A

DETERMINATION OF THE POSITION OF THE NEUTRAL AXIS

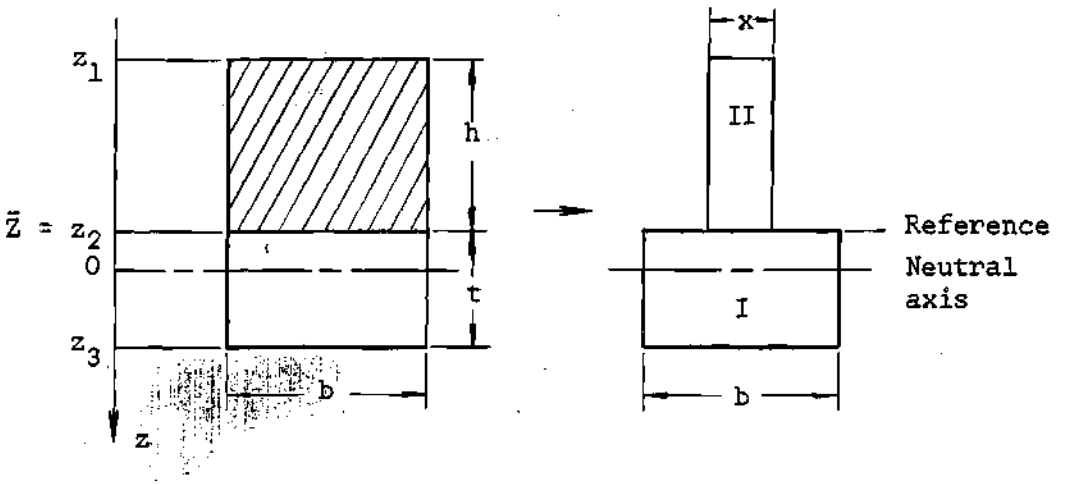

(a) Two layer beam (b) Equivalent metal beam

Figure 35. Beam Cross Sections

The two layer beam of Figure 35(a) is first transformed to an equivalent beam of only one material, but having the same bending stiffness, B.

$$B = EI = \frac{E}{12} bz^3$$

$$\frac{E_b}{12} xh^3 = \frac{E_c}{12} bh^3$$

$$x = \frac{E_c}{E_b} b$$

Now the position of the neutral axis of the T-shaped cross section of Figure 35(b) may be easily determined. From elementary mechanics of materials,

$$\bar{z}\Sigma A = \Sigma z_c A$$

Section	z_c	A	$z_c A$
I	$t/2$	bt	$(1/2)bt^2$
II	$-h/2$	$hx = hb(E_c/E_b)$ $\Sigma A = b(t+h\frac{E_c}{E_b})$	$-(1/2)bh^2(E_c/E_b)$ $\Sigma z_c A = \frac{b}{2}(t^2-h^2\frac{E_c}{E_b})$

Thus,

$$\bar{z} = \frac{1}{2}\,\frac{E_b t^2 - E_c h^2}{E_b t + E_c h} \tag{93}$$

This is the same relation as that derived by Oberst (8).

APPENDIX B

OTHER DAMPING EQUATIONS

Damping Equation 2

Choosing the times $\tau_1 = 0$ and $\tau_2 = \pi/2\bar{\omega}_m$ yields

$$2\bar{\omega}_m\alpha^5 - \frac{2E_d(z_2^3-z_1^3)\beta_m^4}{3\rho}\alpha^4 + 2\left[\bar{\omega}_m(\bar{\omega}_m^2+\omega_m^2) - \bar{\omega}_m^3 e^{\pi\alpha/\bar{\omega}_m}\right]\alpha^3 + \qquad (94)$$

$$+ \frac{E_d(z_2^3-z_1^3)\beta_m^4\bar{\omega}_m^2}{3\rho}\left(3e^{\pi\alpha/\bar{\omega}_m}-1\right)\alpha^2 + 2\left[\bar{\omega}_m^3\omega_m^2 - \bar{\omega}_m^5 e^{\pi\alpha/\bar{\omega}_m}\right]\alpha +$$

$$+ \frac{E_d(z_2^3-z_1^3)\beta_m^4}{3\rho}\bar{\omega}_m^4\left(e^{\pi\alpha/\bar{\omega}_m}-1\right) = 0$$

The exponential terms cannot be eliminated in this case. A series expansion of the form shown below may be substituted in Equation 94 to yield a polynomial in α which is soluble.

$$e^{\pi\alpha/\bar{\omega}_m} = 1 + \frac{\pi\alpha}{\bar{\omega}_m} + \frac{\pi^2\alpha^2}{2\bar{\omega}_m^2} + \frac{\pi^3\alpha^3}{6\bar{\omega}_m^3} + \cdots$$

Damping Equation 3

Letting $\tau_1 = \pi/2\bar{\omega}_m$ and $\tau_2 = 5\pi/2\bar{\omega}_m$ yields

$$\frac{1}{\bar{\omega}_m^3}\alpha^5 - \frac{E_d(z_2^3-z_1^3)\beta_m^4}{3\rho\bar{\omega}_m^4}\alpha^4 + \frac{\omega_m^2 - \bar{\omega}_m^2}{\bar{\omega}_m^3}\alpha^3 - \frac{E_d(z_2^3-z_1^3)\beta_m^4}{2\rho\bar{\omega}_m^2}\alpha^2 + \tag{95}$$

$$+ \frac{\omega_m^2}{\bar{\omega}_m}\alpha - \frac{E_d(z_2^3-z_1^3)\beta_m^4}{6\rho} = 0$$

Damping Equation 4

In the first three damping equations, one or several of the terms of Equations 39, 40, and 44 vanish for the values of time chosen. If $\tau_1 = \pi/8\bar{\omega}_m$ and $\tau_2 = 17\pi/8\bar{\omega}_m$, however, none of the terms vanish. Thus, the influence of each is involved in the final expression which is

$$\frac{0.146}{\bar{\omega}_m^3}\alpha^5 - \left[\frac{0.707}{\bar{\omega}_m^2} + \frac{0.146\ E_d(z_2^3-z_1^3)\beta_m^4}{3\rho\bar{\omega}_m^4}\right]\alpha^4 + \tag{96}$$

$$+ \left[\frac{1}{\bar{\omega}_m} + \frac{0.146\ \omega_m^2}{\bar{\omega}_m^3} + \frac{0.354\ E_d(z_2^3-z_1^3)\beta_m^4}{3\rho\bar{\omega}_m^3}\right]\alpha^3 +$$

$$- \left[0.707 + \frac{0.646\ E_d(z_2^3-z_1^3)\beta_m^4}{3\rho\bar{\omega}_m^2}\right]\alpha^2 + \left[0.854\ \bar{\omega}_m + \frac{0.146\ \omega^2}{\bar{\omega}_m} + \right.$$

$$\left. + \frac{0.354\ E_d(z_2^3-z_1^3)\beta_m^4}{3\rho\bar{\omega}_m}\right]\alpha - \frac{E_d(z_2^3-z_1^3)\beta_m^4}{6\rho} = 0$$

APPENDIX C

COMPUTER PROGRAMS
(Burroughs B-5500 Computer)

Beam with Single Unconstrained Coating

```
?COMPILE   XXXX/BEAM 1   ALGOL   .03S800015   PEARCE B K
?DATA.
           BEGIN
INTEGER    I,J,K,N                                                    ;
REAL       AL,AL1,BETA,C,C0,C1,C2,C3,OMB,OM1,CPS,D,DEL,E,F,
            F1,OM,Q,R,R0,ZB,Z1,Z2,Z3,EC,G,G1,NU,CPSB,NUC,S            ;
ARRAY      A[0:100],B[0:100],EB[0:100],ES[0:100],ED[0:100],
            GAB[0:100],GAC[0:100],H[0:100],
            T[0:100]                                                  ;
FILE IN    FI(2,10)                                                   ;
FILE OUT   BKP 16(2,15)                                               ;
FORMAT OUT FMT1(X4,"A",X7,"B",X7,"H",X6,"T",X6,"H/T",X6,"EB
                ",X9,"ES",X9,"ED",X8,"ES/EB",X5,"J",X6,
                "ALPHA",X5,"OMEGA",X4,"DELTA"/)                       ;
FORMAT OUT FMT2(X1,F6.3,X2,F6.3,X2,F6.4,X2,F5.3,X2,F6.2,X1,
                F10.1,X1,F10.1,X1,F10.1,X2,F9.7,X1,I3,X2,
                F8.2,X2,F8.2,X2,F8.5/)                                ;
FORMAT OUT FMT3(X3,"K=",I2,X3,"CPSB=",F8.2,X3,"NU=",F8.5,
                X3,"NU/NUC=",F8.5/)                                   ;
LABEL      L1,L2,L3,L4,L5,L6,L7,L8,L9,L10,L11,L12,L13,
            METAL,COMB                                                ;
LIST       LT1(I)                                                     ;
LIST       LT2(FOR N←1 STEP 1 UNTIL I DO [A[N],B[N],EB[N],
               GAB[N],GAC[N],T[N],H[N],ES[N],ED[N]])                  ;
LIST       LT3(A[N],B[N],H[N],T[N],R,EB[N],ES[N],ED[N],Q,
               J,AL,CPS,DEL)                                          ;
LIST       LT4(K,CPSB,NU,S)                                           ;
           WRITE (BKP,FMT1)                                           ;
           READ(FI,/,LT1)                                             ;
           READ(FI,/,LT2)                                             ;
           N ← 1                                                      ;
L1:        IF N←I THEN GO TO L6 ELSE GO TO L2                         ;
L2:        R←H[N]/T[N]                                                ;
           BETA←4.730/A[N]                                            ;
           RO←((GAB[N]xT[N])+(GAC[N]xH[N]))/386.0                     ;
           IF H[N]=0.0 THEN GO TO METAL ELSE GO TO COMB               ;
```

```
METAL:    Z2← -T[N]/2                                                    ;
          Z3←  T[N]/2                                                    ;
          C ← (EB[N]x(Z3*3-Z2*3)x(BETA*4))/(3xR0)                        ;
          OM ← SQRT(C)                                                   ;
          CPS ← OM/6.283                                                 ;
          DEL ← 0.0                                                      ;
          Q ← 0.0                                                        ;
          J ← 0.0                                                        ;
          AL ← 0.0                                                       ;
          WRITE(BKP,FMT2,LT3)                                            ;
          N ← N + 1                                                      ;
          GO TO L1                                                       ;
COMB:     EC ← SQRT(ES[N]*2 + ED[N]*2)                                   ;
          ZB ← ((EB[N]x(T[N]*2))-(ECx(H[N]*2)))/(2x((
                 EB[N]xT[N]) + (ECxH[N])))                               ;
          Z1 ← -(H[N] + ZB)                                              ;
          Z2 ← -ZB                                                       ;
          Z3 ← T[N] - ZB                                                 ;
          C ← ((EB[N])x(Z3*3-Z2*3)x(BETA*4))/(3xR0)                      ;
          D ← (ECx(Z2*3-Z1*3)x(BETA*4))/(3xR0)                           ;
          OMB ← SQRT(C + D)                                              ;
          CPSB ← OMB/6.283                                               ;
          Q ← ES[N]/EB[N]                                                ;
          E ← (ED[N]x(Z2*3-Z1*3)x(BETA*4))/(3xR0)                        ;
          OM1 ← OMB                                                      ;
          K ← 1                                                          ;
          C0 ← -0.50xE                                                   ;
L7:       C1 ← OM1                                                       ;
          C2 ← (-0.50xE)/(OM1*2)                                         ;
          C3 ← 1.0/OM1                                                   ;
          AL1 ← 1.0                                                      ;
          J ← 1                                                          ;
L3:       F ← (C3x(AL1*3)) + (C2x(AL1*2)) + (C1xAL1) + C0                ;
          F1 ← (3xC3x(AL1*2)) + (2xC2xAL1) + C1                          ;
          AL ← AL1 - (F/F1)                                              ;
          IF ABS(AL-AL1) ≤ 0.010 THEN GO TO L5 ELSE GO TO L4             ;
L4:       AL1 ← AL                                                       ;
          J ← J + 1                                                      ;
          GO TO L3                                                       ;
L5:       G ← (OM1*2) + (AL*2)-(OMB*2)                                   ;
          G1 ← 2xOM1                                                     ;
          OM ← OM1 - (G/G1)                                              ;
          IF ABS(OM/OM1)<0.990 THEN GO TO L9 ELSE GO TO L10              ;
L9:       OM1 ← OM                                                       ;
          K ← K + 1                                                      ;
          GO TO L7                                                       ;
L10:      C1 ← OM                                                        ;
          C2 ← (-0.50xE)/(OM*2)                                          ;
```

```
            C2 ← (-0.50xE)/(OM*2)                                          ;
            C3 ← 1.0/OM                                                    ;
            AL1 ← 1.0                                                      ;
            J ← 1                                                          ;
L11:        F ← (C3x(AL1*3)) + (C2x(AL1*2)) + (C1xAL1) + C0                ;
            F1 ← (3xC3x(AL1*2)) + (2xC2xAL1) + C1                          ;
            AL ← AL1 - (F/F1)                                              ;
            IF ABS(AL-AL1)≤0.01 THEN GO TO L13 ELSE GO TO L12              ;
L12:        AL1 ← AL                                                       ;
            J ← J + 1                                                      ;
            GO TO L11                                                      ;
L13:        CPS ← OM/6.283                                                 ;
            DEL ← ABS((6.283xAL)/OM)                                       ;
            NU ← DEL/3.1416                                                ;
            NUC ← ED[N]/ES[N]                                              ;
            S ← NU/NUC                                                     ;
            WRITE(BKP,FMT2,LT3)                                            ;
            WRITE(BKP,FMT3,LT4)                                            ;
            N ← N + 1                                                      ;
            GO TO L1                                                       ;
L6:         N ← N                                                          ;
            END.
```

Data for this program must be fed in on cards, the first card bearing the number of beams for which calculations will be made, and the following cards carrying the data pertinent to each beam in the order given by LIST LT2. For example, to run the program for only the beam of Appendix G, the following data is needed:

```
?DATA FI
1,
8.0625,2.0,30000000.0,0.284,0.046,0.047,0.264,4380.0,810.0,
```

Beam with Two Symmetric Coatings

The program for this case is identical to the previous one but for the following exceptions:

```
            Calculation of ZB is omitted.
            Z1 ← -0.50x(T[N] + H[N])                                       ;
            Z2 ← -T[N]/2                                                   ;
            Z3 ← T[N]/2                                                    ;
```

```
OMB ← SQRT(C + 2xD)                                    ;
CO ← -E                                                ;
C2 ← -E/(OM1*2)                                        ;
C2 ← -E/(OM*2)                                         ;
```

Plate Programs

These programs are quite similar to those for the beams. There are additional variables in this case; however, the procedure is identical to that in the previous cases and consequently will not be repeated.

APPENDIX D

DAMPING RELATIONS

Relation Between α and δ

By definition,

$$\delta = \ln\left(\frac{X_n}{X_{n+1}}\right) = \ln\left(\frac{X_o\, e^{-\alpha\tau_n}}{X_o\, e^{-\alpha(\tau_n+T)}}\right)$$

where X_o - initial amplitude.

X_n - amplitude at any time, τ_n.

X_{n+1} - amplitude one cycle later.

T(period) $= 2\pi/\bar{\omega}$.

Therefore,

$$\delta = \ln(e^{\alpha T}) = \alpha T$$

$$\delta = \frac{2\pi}{\bar{\omega}}\alpha \tag{97}$$

Relation Between δ and ξ

From Tse, Morse, and Hinkle (29),

$$\bar{\omega}^2 = \omega^2(1-\xi^2) \tag{98}$$

where $\xi = c/c_c$.

Substituting Equation 34 into Equation 98 yields

$$\xi = \alpha/\omega$$

Obtaining α from Equation 97 and making use of Equation 98, Equation 99 becomes

$$\xi = \frac{\delta}{2\pi} \cdot \frac{\bar{\omega}}{\omega} = \frac{\delta}{2\pi} (1-\xi^2)^{1/2}$$

or

$$\xi^2 = \frac{\delta^2}{\delta^2 + 4\pi^2} \qquad (100)$$

APPENDIX E

DIMENSIONAL ANALYSIS

In order to simplify this analysis, it is assumed that damping is small ($\eta_c \leq 0.1$); then undamped and damped natural frequency are approximately equal, and the approximate solution (Equation 52) applies. From Equations 50 and 52,

$$\alpha = \frac{\eta\omega_1}{2} = \frac{\delta\omega_1}{2\pi} \tag{101}$$

$$\alpha = \frac{E_d(z_2^3 - z_1^3)\beta_1^4}{6\rho\omega_1} \tag{102}$$

Equating Equations 101 and 102 and substituting from Equation 29 yields

$$\eta = \frac{\frac{E_d(z_2^3 - z_1^3)\beta_1^4}{3\rho}}{\frac{E_b(z_3^3 - z_2^3)\beta_1^4}{3\rho} + \frac{E_s(z_2^3 - z_1^3)\beta_1^4}{3\rho}} \tag{103}$$

where

$$z_1 = -(h+\bar{z}) \qquad z_2 = -\bar{z} \qquad z_3 = t - \bar{z}$$

$$\bar{z} = \frac{E_b t^2 - E_c h^2}{2(E_b t + E_c h)} \quad \text{and} \quad E_c \simeq E_s$$

Since β_1 and ρ cancel out,

$$\eta = F(h, t, E_d, E_s, E_b)$$

Employing the techniques of dimensional analysis,

$$\eta = K\, h^a t^b E_d^c E_s^d E_b^e \tag{104}$$

where K is a dimensionless constant.

	h	t	E_d	E_s	E_b
M	0	0	1	1	1
L	1	1	-1	-1	-1
T	0	0	-2	-2	-2

(M - mass, L - length, T - time)

Thus,

$$c + d + e = 0 \tag{105}$$

$$a + b - c - d - e = 0 \tag{106}$$

$$-2c - 2d - 2e = 0 \tag{107}$$

Equations 105 and 107 are dependent; therefore,

$$N(\text{No. of dimensionless constants}) = 5 - 2 = 3$$

Substituting Equation 105 into 106 yields b = -a. From Equation 105, d = -c - e. Hence, Equation 104 becomes

$$\eta = K\, h^{a} t^{-a} E_d^{c} E_s^{-c-e} E_b^{e}$$

oe

$$\eta = K\left(\frac{h}{t}\right)^{a} \left(\frac{E_d}{E_s}\right)^{c} \left(\frac{E_b}{E_s}\right)^{e} \tag{108}$$

Calculations for a number of cases show that variation of length and density do not affect the value of damping for the *complete* beam solution (Equations 29, 34, 49, and 50) even when damping is large. The plate solution also depends only upon the three dimensionless ratios of Equation 108 as may be shown by an analysis similar to that for the beam. In the case of large damping, log decrement is again independent of length and density (and Poisson's ratio) as illustrated by Tables 14, 15, and 16.

Table 14. Variation of Log Decrement with Length for Large Damping of Plates with Coatings on One Side, $\eta_c = 1.0$, and $E_s/E_b = (10)^{-4}$

$\frac{h}{t}$	LOGARITHMIC DECREMENT		
	a = 24 in. b = 24 in.	a = 24 in. b = 12 in.	a = 12 in. b = 12 in.
1.00	0.00406	0.00407	0.00406
1.40	0.00840	0.00842	0.00840
2.00	0.01924	0.01927	0.01924
3.00	0.05227	0.05235	0.05227
4.00	0.10839	0.10855	0.10839
5.20	0.20996	0.21027	0.20996
7.00	0.42824	0.42881	0.42824
8.50	0.65302	0.65378	0.65302
10.00	0.89315	0.89405	0.89315
13.00	1.34754	1.34854	1.34754
16.00	1.70562	1.70652	1.70562
20.00	2.02672	2.02741	2.02672
25.00	2.25446	2.25493	2.25446
30.00	2.37601	2.37632	2.37601
40.00	2.49181	2.49198	2.49181
50.00	2.53203	2.53214	2.53203
60.00	2.54845	2.54853	2.54845
70.00	2.55515	2.55522	2.55515
85.00	2.55750	2.55757	2.55750
100.00	2.55585	2.55592	2.55585

Table 15. Variation of Log Decrement with Density for Large Damping of Plates with Coatings on One Side, $\eta_c = 1.0$, and $E_s/E_b = (10)^{-4}$

$\frac{h}{t}$	LOGARITHMIC DECREMENT	
	γ_c=0.046	γ_c=0.150 lb/in^3
1.00	0.00406	0.00406
1.40	0.00840	0.00840
2.00	0.01924	0.01924
3.00	0.05227	0.05227
4.00	0.10839	0.10839
5.20	0.20996	0.20996
7.00	0.42824	0.42824
8.50	0.65302	0.65302
10.00	0.89315	0.89315
13.00	1.34754	1.34754
16.00	1.70562	1.70562
20.00	2.02672	2.02672
25.00	2.25446	2.25446
30.00	2.37601	2.37601
40.00	2.49181	2.49181
50.00	2.53203	2.53203
60.00	2.54845	2.54845
70.00	2.55515	2.55515
85.00	2.55750	2.55750
100.00	2.55585	2.55585

Table 16. Variation of Log Decrement with Poisson's Ratio for Large Damping of Plates with Coatings on One Side, $\eta_c = 1.0$, and $E_s/E_b = (10)^{-4}$

$\frac{h}{t}$	LOGARITHMIC DECREMENT		
	ν_c=0.20	ν_c=0.30	ν_c=0.40
1.00	0.00424	0.00406	0.00395
1.40	0.00877	0.00840	0.00818
2.00	0.02009	0.01924	0.01873
3.00	0.05453	0.05227	0.05090
4.00	0.11294	0.10839	0.10562
5.20	0.21836	0.20996	0.20484
7.00	0.44358	0.42824	0.41884
8.50	0.67371	0.65302	0.64026
10.00	0.91814	0.89315	0.87794
13.00	1.37438	1.34754	1.33070
16.00	1.72977	1.70562	1.69032
20.00	2.04507	2.02672	2.01500
25.00	2.26668	2.25446	2.24661
30.00	2.38425	2.37601	2.37070
40.00	2.49619	2.49181	2.48898
50.00	2.53484	2.53203	2.53021
60.00	2.55059	2.54845	2.54706
70.00	2.55703	2.55515	2.55394
85.00	2.55928	2.55750	2.55635
100.00	2.55769	2.55585	2.55465

APPENDIX F

DESIGN CURVES

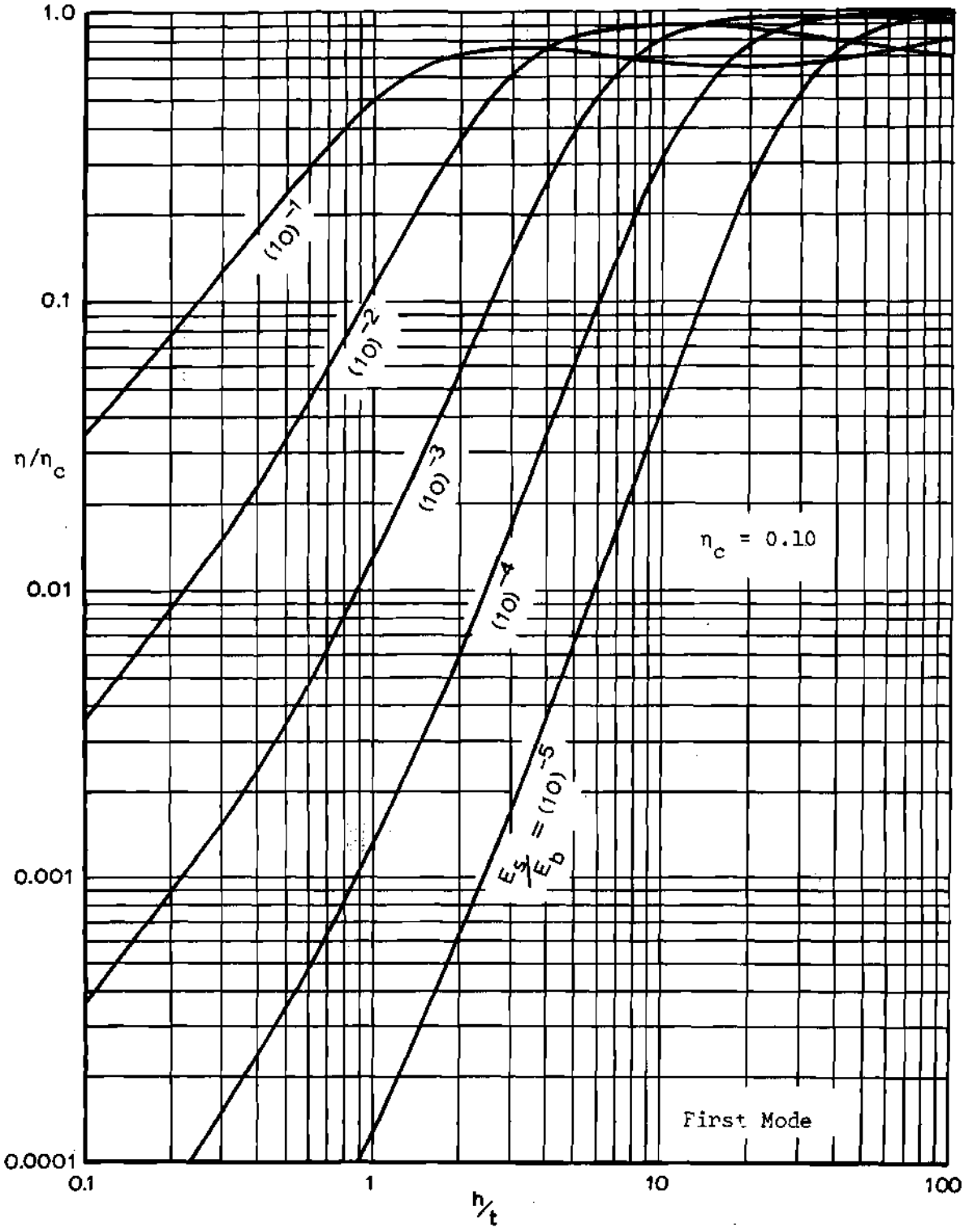

Figure 36. Damping Ratio vs. Thickness Ratio for Free-Free Beams and Plates with Coatings on One Side Only and $\eta_c = 0.10$

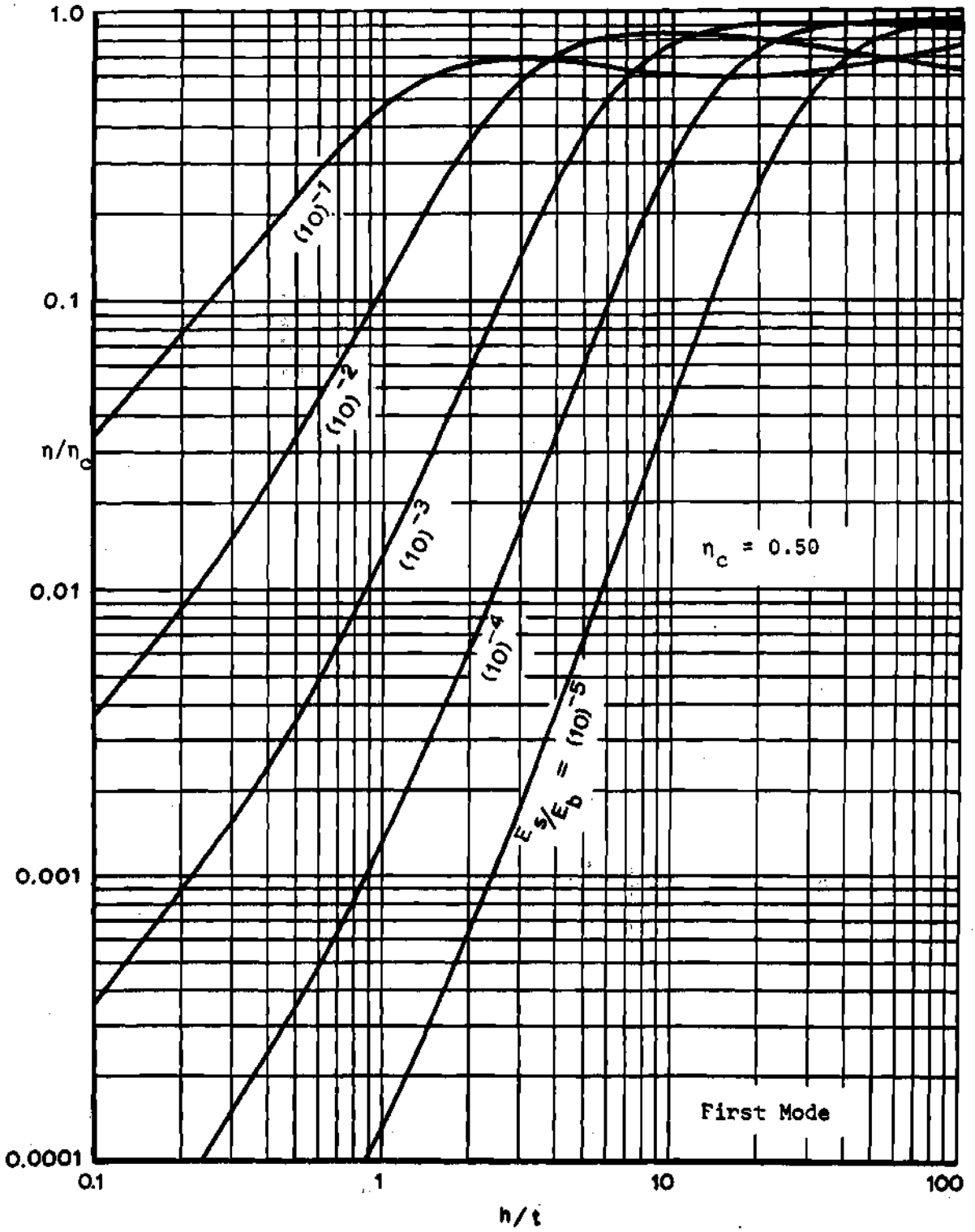

Figure 37. Damping Ratio vs. Thickness Ratio for Free-Free Beams and Plates with Coatings on One Side Only and $\eta_c = 0.50$

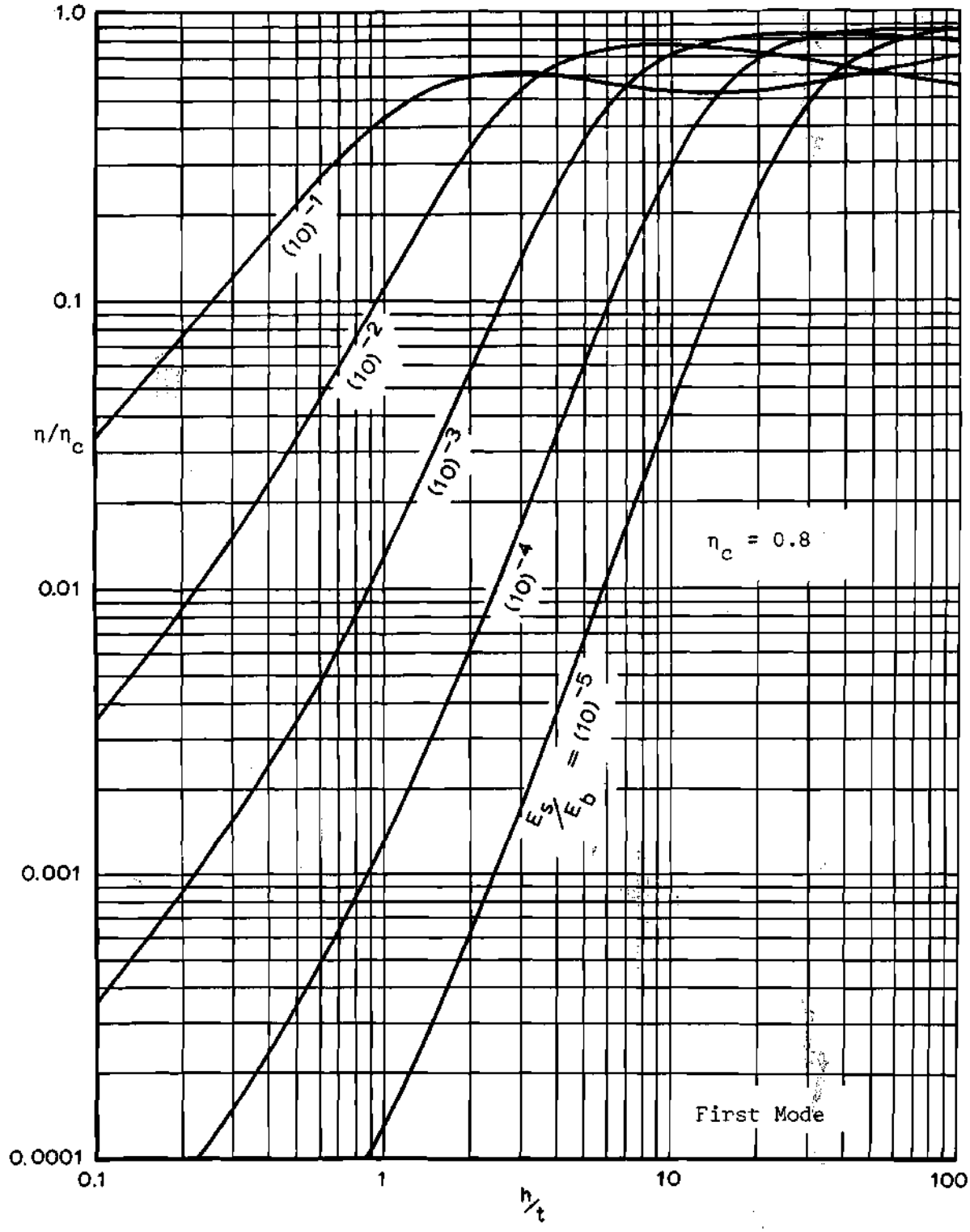

Figure 38. Damping Ratio vs. Thickness Ratio for Free-Free Beams and Plates with Coatings on One Side Only and η_c = 0.80

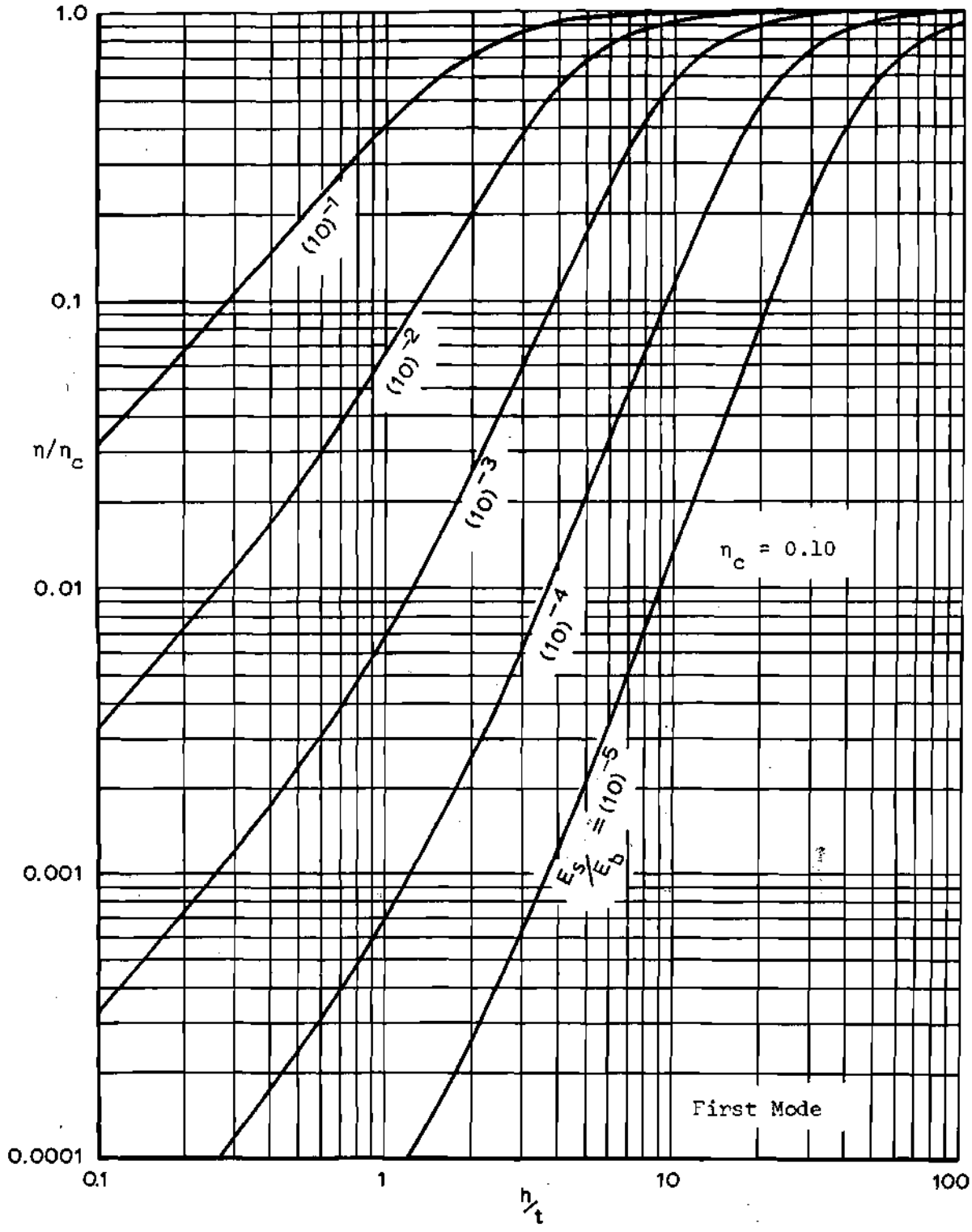

Figure 39. Damping Ratio vs. Thickness Ratio for Free-Free Beams and Plates with Two Symmetric Coatings and $\eta_c = 0.10$

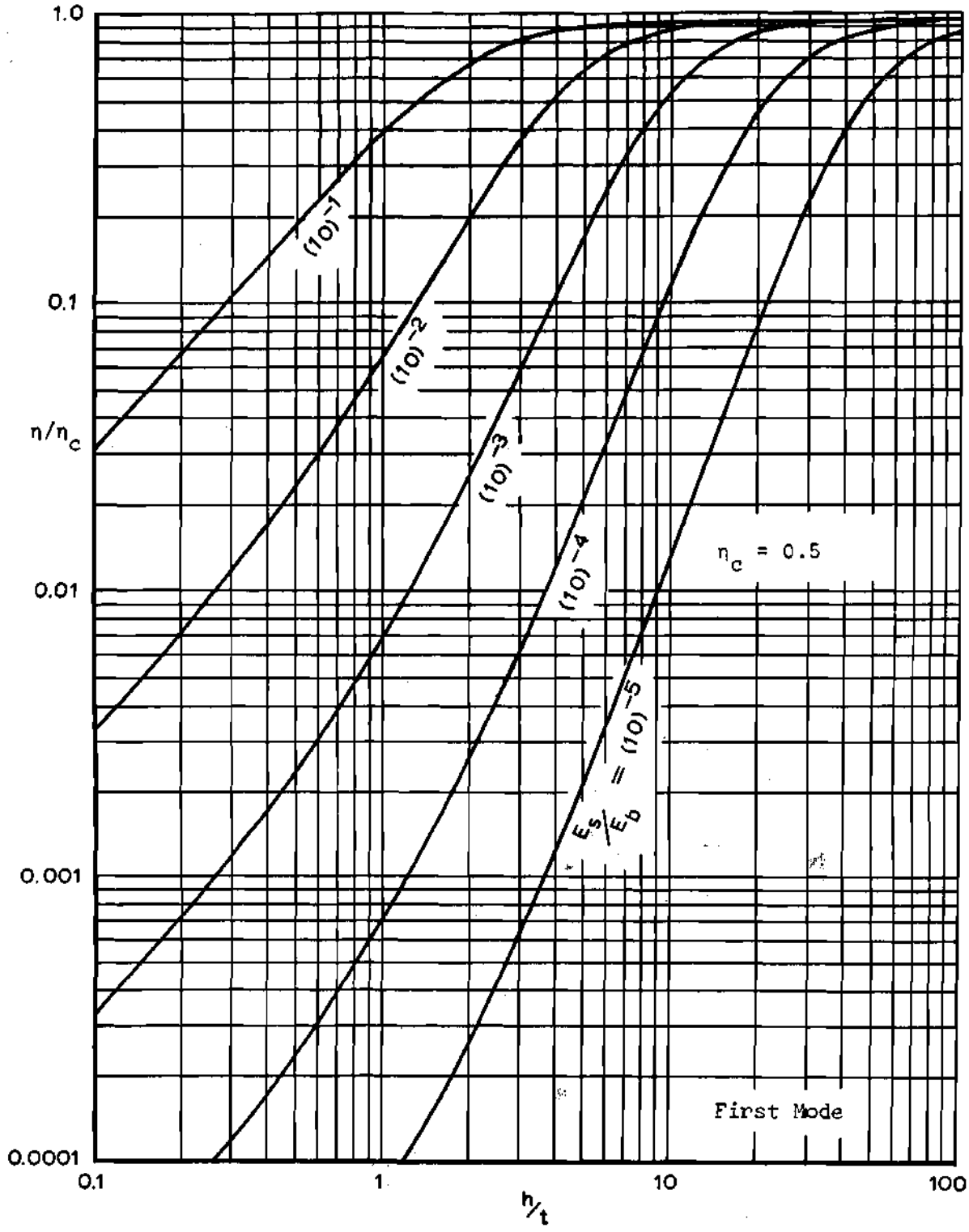

Figure 40. Damping Ratio vs. Thickness Ratio for Free-Free Beams and Plates with Two Symmetric Coatings and $\eta_c = 0.50$

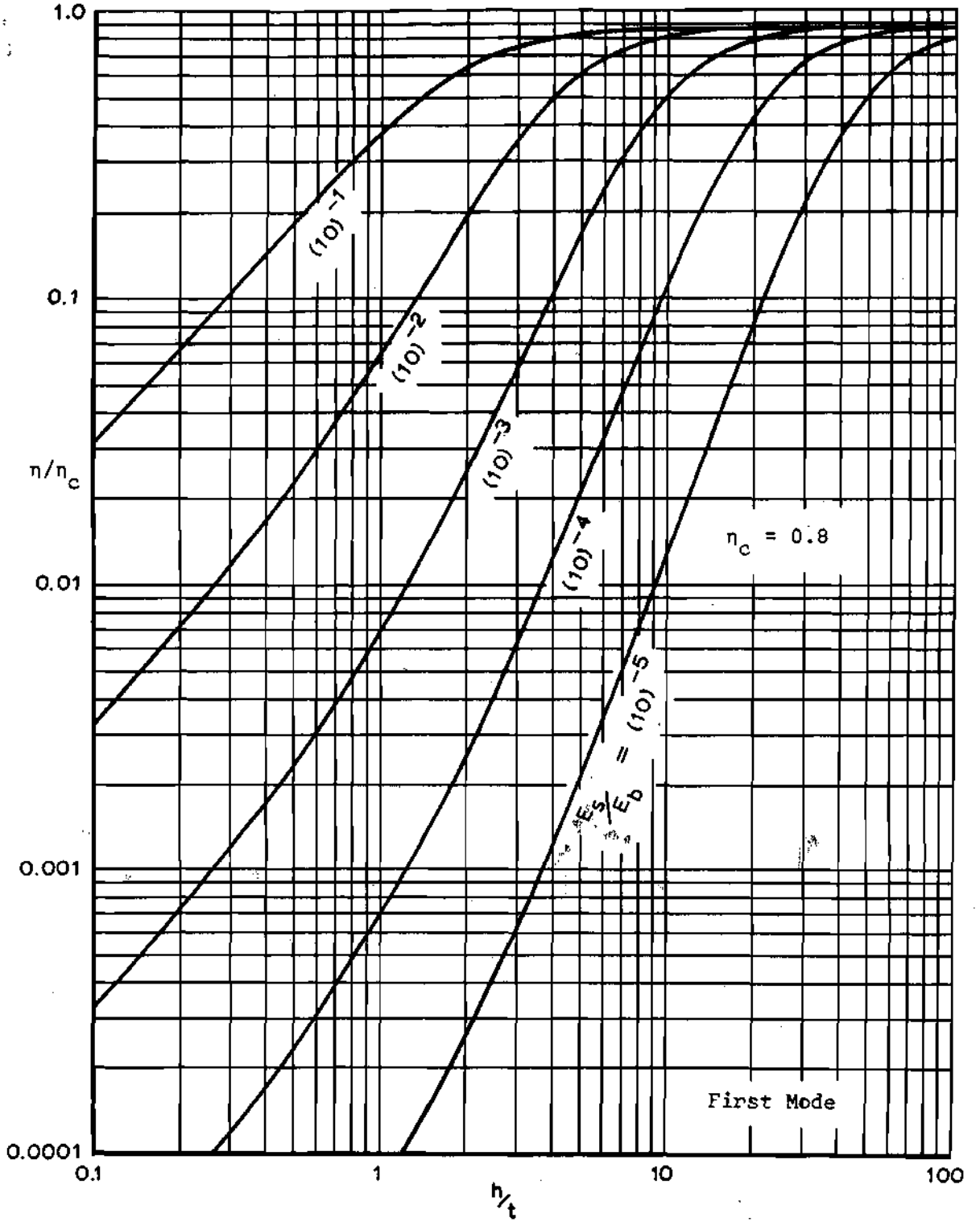

Figure 41. Damping Ratio vs. Thickness Ratio for Free-Free Beams and Plates with Two Symmetric Coatings and $\eta_c = 0.80$

APPENDIX G

SAMPLE CALCULATIONS

Given: 8-1/16" x 2" x 0.047" steel beam with a 0.264" thick buna-N coating on one side.

Problem: Determine the natural frequency and logarithmic decrement for the composite structure in the fundamental mode of vibration.

Note: Measured values for a model of the above dimensions are

$$\bar{\omega}_1 = 116 \text{ c.p.s.}$$

$$\delta = 0.0703$$

The properties which apply in this case are taken from Tables 5 and 6 and from Figure 22. (Normally, frequency will not be known; therefore, a frequency value must be assumed, then the values of E_d and E_s taken from Figure 22, and a calculation made to determine whether or not the assumption was correct. This should be repeated until the two values correspond. Here it is assumed that $\bar{\omega}_1 = 116$ c.p.s. since the value is known.)

$$E_b = 30(10)^6 \text{psi} \qquad \gamma_b = 0.284 \text{ lb/in}^3$$

$E_s = 4380$ psi $\qquad E_d = 810$ psi $\qquad \gamma_c = 0.046$ lb/in^3

Also

$h = 0.264$ in. $\qquad t = 0.047$ in. $\qquad a = 8\text{-}1/16$ in.

Natural Frequency

From Equation 17, $E_c = 4450$ psi. Using Equation 93,

$$\bar{z} = \frac{1}{2}\,\frac{30(10)^6(0.047)^2 - 4450(0.264)^2}{30(10)^6(0.047) + 4450(0.264)} = 0.0234 \text{ in.}$$

Then

$$z_1 = -(h+\bar{z}) = -0.2874 \text{ in.}$$

$$z_2 = -\bar{z} = -0.0234 \text{ in.}$$

and

$$z_3 = t - \bar{z} = 0.0236 \text{ in.}$$

$$\beta_1 = 4.730/a = 0.585$$

$$\rho = \frac{0.284(0.047) - 0.046(0.264)}{386} = 0.661(10)^{-4}$$

Substituting the above into Equation 29 yields

$$\omega_1^2 = \frac{30(10)^6[(0.0236)^3-(-0.0234)^3](0.585)^4}{3(0.661)(10)^{-4}} +$$

$$+ \frac{4450[(-0.0234)^3-(-0.2874)^3](0.585)^4}{3(0.661)(10)^{-4}}$$

$$\omega_1^2 = 52.92(10)^4$$

$$\omega_1 = 728 \text{ rad/sec} = 116 \text{ c.p.s.}$$

Since η_c is rather small, damped and undamped values of frequency are probably about the same. However, this is checked below.

Equation 50 gives

$$\alpha = \frac{\delta\bar{\omega}_1}{2\pi} = \frac{\eta\bar{\omega}_1}{2}$$

$$\alpha_{max.} = \frac{\eta_{max.}\bar{\omega}_1}{2} \qquad (\eta_{max.} = \eta_c)$$

From Equation 34,

$$\bar{\omega}_1^2 = \omega_1^2 - \alpha^2 = \omega_1^2 - 0.00860\ \bar{\omega}_1^2$$

$$1.003\ \bar{\omega}_1 = \omega_1$$

$$\bar{\omega}_1 = 115.5 \text{ c.p.s.}$$

Therefore, the value of *damped* natural frequency is essentially the same as *undamped* and agrees very well with the experimental value.

Logarithmic Decrement

From Design Curves

$$\eta_c = \frac{E_d}{E_s} = 0.1850 \qquad \frac{h}{t} = 5.62 \qquad \frac{E_s}{E_b} = 1.459(10)^{-4}$$

The value of η/η_c from Figure 13 at a thickness ratio of 5.62 and a E_s/E_b ratio of $1.0(10)^{-4}$ is 0.083. This value is a little lower than that for $E_s/E_b = 1.459(10)^{-4}$, but should give a good estimate of the actual value. Thus,

$$\eta = 0.083(0.1850) = 0.001537$$

or

$$\delta = \pi\eta = 0.0483$$

This value is, as expected, somewhat smaller than that actually measured ($\delta = 0.0703$), but is a fair approximation.

By Calculation

As η_c is relatively small, Equation 52 should be fairly accurate.

$$\alpha = \frac{810[(-0.0234)^3-(-0.2874)^3](0.585)^4}{6(0.661)(10)^{-4}(728)} = 7.90$$

From Equation 50,

$$\delta = \frac{2\pi(7.90)}{728} = 0.0681$$

This value is in good agreement with that actually measured ($\delta = 0.0703$) and also with the value calculated from the complete solution by computer ($\delta = 0.06825$).

APPENDIX H

ENERGY DISSIPATION EXPRESSION FOR TWO DIMENSIONS

An isotropic, Hookean material is defined by Langhaar (30) in the following manner: the strain energy density of such a material may be represented by (neglecting thermal effects)

$$U_o\left(= \frac{d^3V}{dxdydz}\right) = \frac{1}{2} \sum_{i=1}^{3} \sum_{j=1}^{3} b_{ij}\, \varepsilon_i \varepsilon_j \tag{109}$$

In a viscoelastic material, stresses (hence energy) depend not only upon strain but also strain rate (see Equations 2 and 41). Therefore the loss energy density of an isotropic viscoelastic material may be defined by the following expression.

$$L\left(= \frac{d^3L}{dxdydz}\right) = \int \sum_{i=1}^{3} \sum_{j=1}^{3} c_{ij}\, \varepsilon_i' \varepsilon_j'\, d\tau \tag{110}$$

As shown in Langhaar (30), determination of the constants b_{ij} in Equation 109 and simplification to the state of plane stress yields Equation 61. Similarly, Equation 110 leads to the expression for energy dissipated given by Equation 76.

APPENDIX I

DYNAMIC PROPERTIES OF VISCOELASTIC MATERIALS

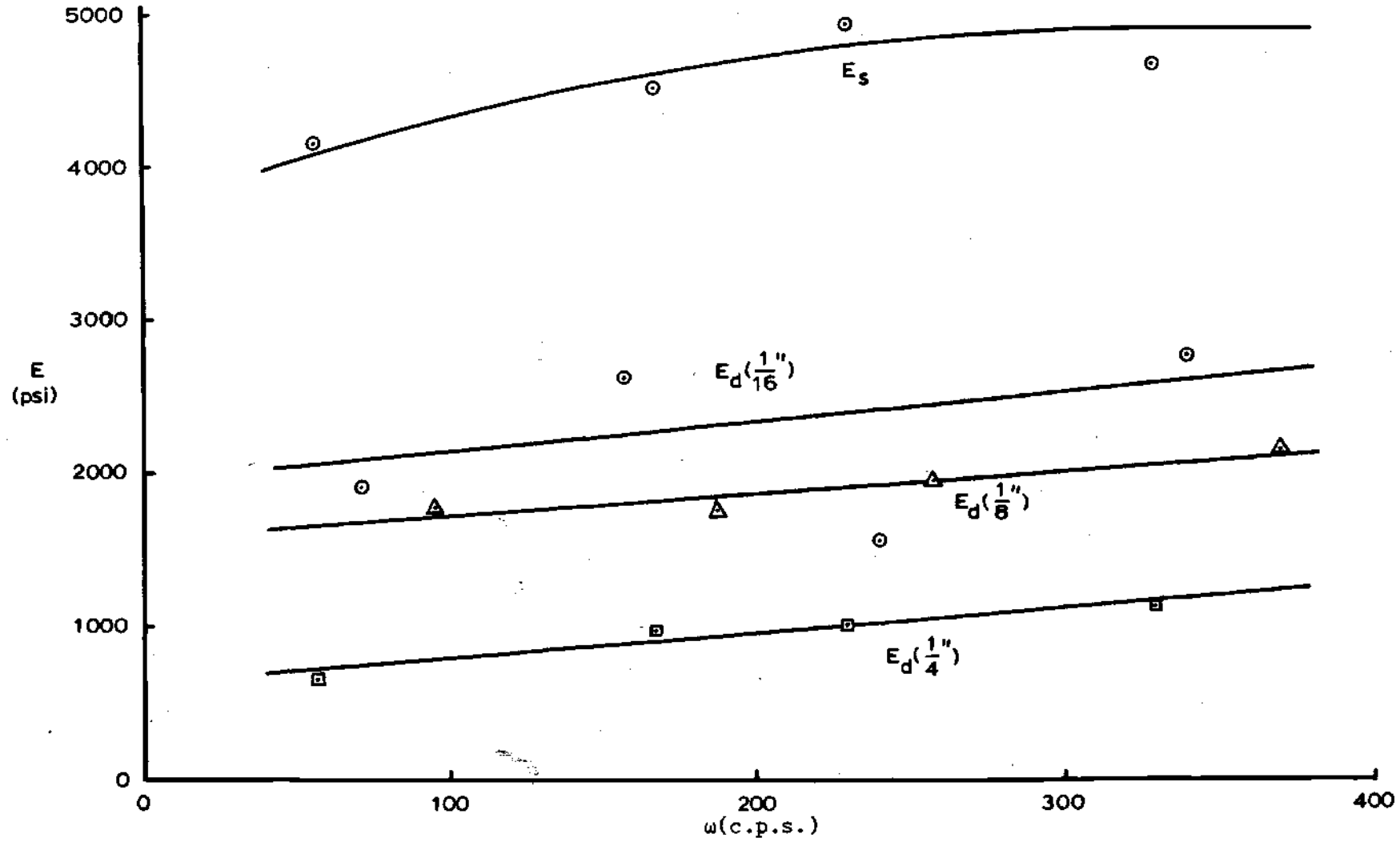

Figure 42. Static and Dynamic Moduli of Buna-N Rubber Specimens

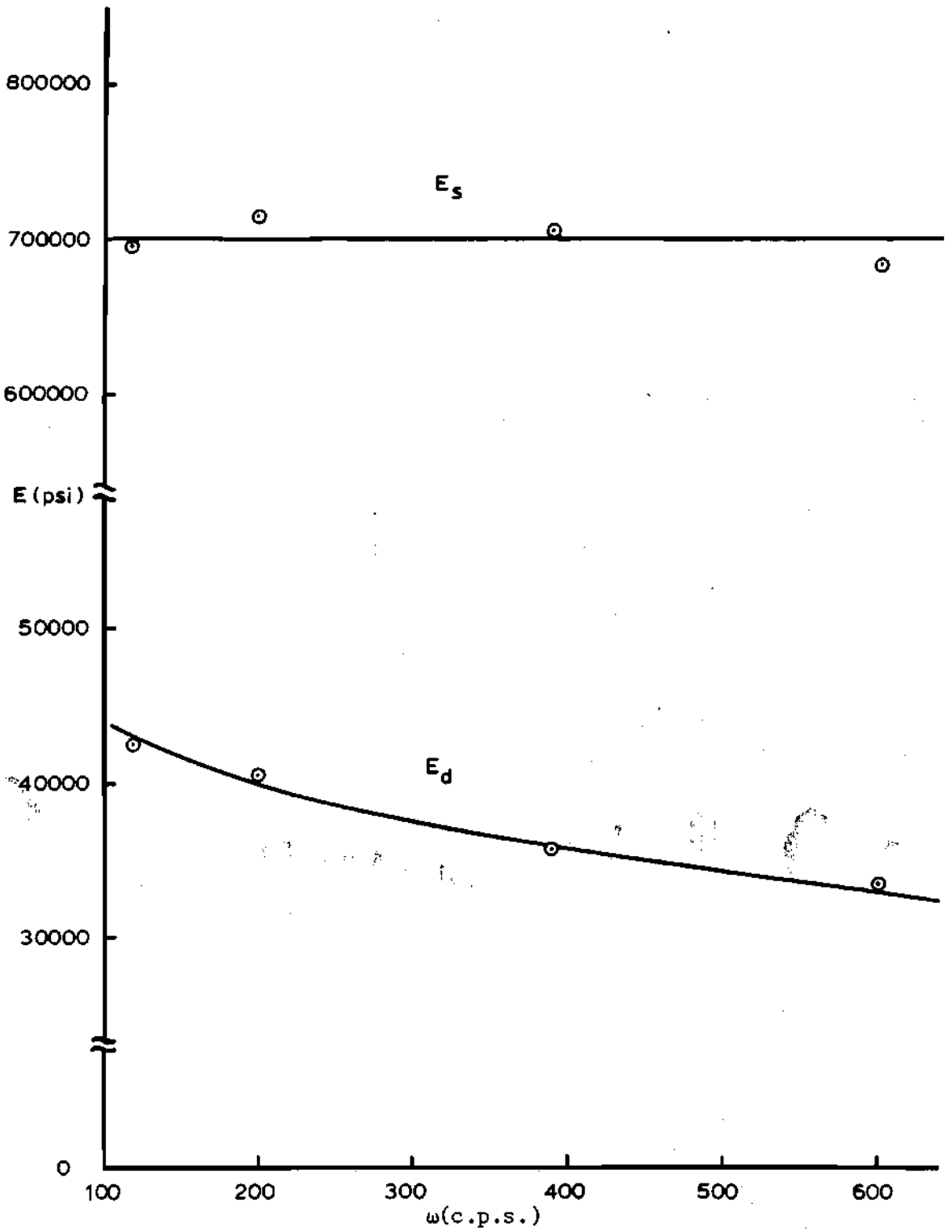

Figure 43. Static and Dynamic Moduli of 1/8" Thick Specimen of Plexiglas

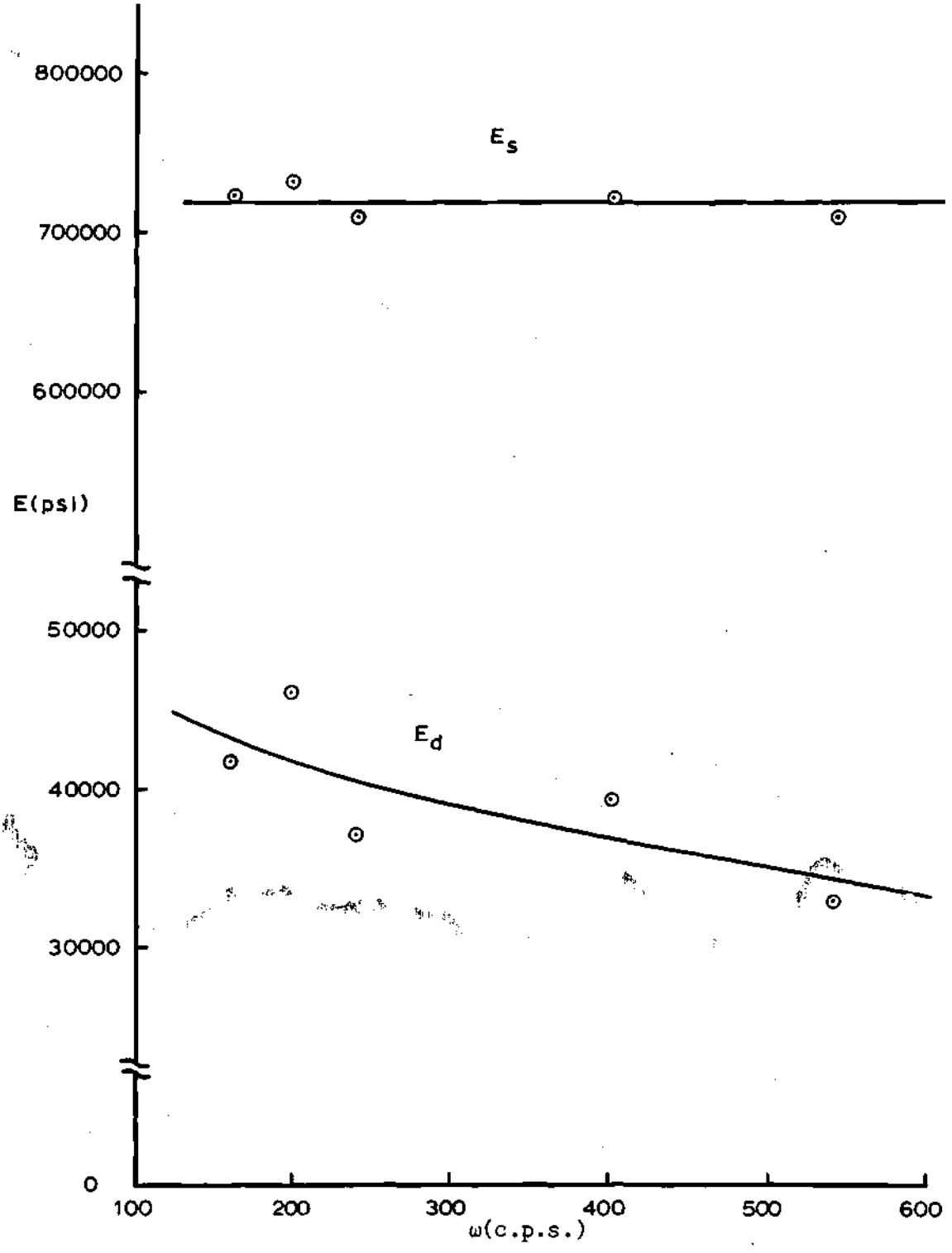

Figure 44. Static and Dynamic Moduli of 1/4" Thick Specimen of Plexiglas

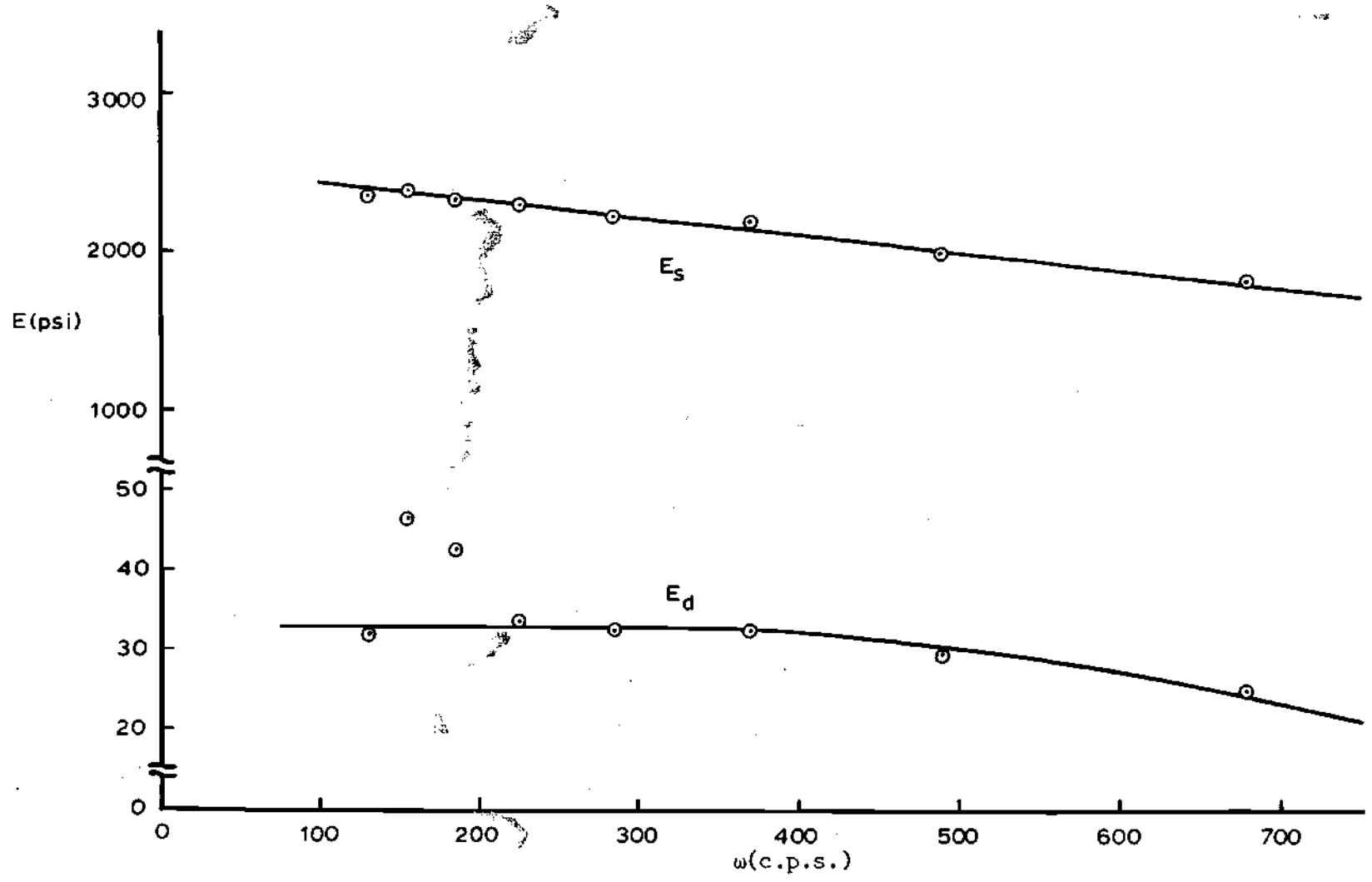

Figure 45. Static and Dynamic Moduli of Styrofoam

APPENDIX J

DETERMINATION OF OPTIMUM THICKNESS RATIO

In order to obtain usable results, it is necessary to restrict this analysis to the case of small damping, i.e., $\eta_c \leq 0.10$ and $\bar{\omega} = \omega$.

Beam with Two Symmetric Coatings

For this case, Equations 50, 53, and 55 apply; therefore,

$$\delta = \frac{2\pi E_d (z_2^3 - z_1^3)\beta_1^4}{3\rho\omega_1^2} \tag{111}$$

where

$$z_1 = -\frac{1}{2}(t+h) \qquad z_2 = -t/2 \qquad z_3 = t/2$$

and ω_1 is given by Equation 53. δ is either a maximum or a minimum when

$$\frac{d\delta}{d(\frac{h}{t})} = 0 \tag{112}$$

Let

$$f(\frac{h}{t}) = z_3^3 - z_2^3 = t^4/4 \tag{113a}$$

$$g(\frac{h}{t}) = z_2^3 - z_1^3 = \frac{t^3}{8}\left[3(\frac{h}{t}) + 3(\frac{h}{t})^2 + (\frac{h}{t})^3\right] \qquad (113b)$$

$$e(\frac{h}{t}) = \rho = \frac{t}{g}\left[\gamma_b + \gamma_c(\frac{h}{t})\right] \qquad (113c)$$

Then

$$f'(\frac{h}{t}) = \frac{df(\frac{h}{t})}{d(\frac{h}{t})} = 0$$

$$g'(\frac{h}{t}) = \frac{t^3}{8}\left[3 + 6(\frac{h}{t}) + 3(\frac{h}{t})^2\right] \qquad (114)$$

$$e'(\frac{h}{t}) = \frac{\gamma_c t}{g}$$

Upon substitution, Equation 112 becomes

$$e\,\omega_1^2\,g' - ge'\omega_1^2 - eg(\omega_1^2)' = 0 \qquad (115)$$

Letting

$$A = \frac{1}{3}E_b\beta_1^4 \qquad \text{and} \qquad B = \frac{2}{3}E_c\beta_1^4, \quad \text{Equation 113}$$

becomes

$$eg'\left[A\frac{f}{e} + B\frac{g}{e}\right] - ge\left[A\frac{f}{e} + B\frac{g}{e}\right] - eg\left[A\frac{ef'-fe'}{e^2} + B\frac{eg'-ge'}{e^2}\right] = 0 \qquad (116)$$

Multiplying Equation 116 out and collecting terms yields

$$Afg' = 0$$

or

$$A \frac{t^6}{32} \left[3 + 6\left(\frac{h}{t}\right) + 3\left(\frac{h}{t}\right)^2\right] = 0 \qquad (117)$$

The term in brackets cannot be zero for any real positive value of h/t; nor can A be zero; therefore, t must be zero. Thus $h/t \to \infty$ or there is no value of h/t for which δ is a maximum (as suggested by Figure 15). The same is true in the case of a plate with two symmetric coatings.

Beam with Single Unconstrained Coating

This case is much more involved than the previous one. Equations 29, 50, and 52 apply in this instance. Thus,

$$\delta = \frac{\pi E_d (z_2^3 - z_1^3) \beta_1^4}{3\rho\omega_1^2} \qquad (118)$$

where

$$z_1 = -(h+\bar{z}) \qquad z_2 = -\bar{z} \qquad z_3 = t - \bar{z}$$

$$\bar{z} = \frac{E_b t^2 - E_c h^2}{2(E_b t + E_c h)}$$

and ω_1 is given by Equation 29. Equation 112 is again the criterion used to find the value of h/t for which δ is an extremum.

Let

$$f(\frac{h}{t}) = z_3^3 - z_2^3 = t^3 - 3t^2\left[\frac{E_b - E_c(\frac{h}{t})^2}{\frac{2}{t}(E_b + E_c\frac{h}{t})}\right] + 3t\left[\frac{E_b - E_c(\frac{h}{t})^2}{\frac{2}{t}(E_b + E_c\frac{h}{t})}\right]^2 \quad (119a)$$

$$g(\frac{h}{t}) = z_2^3 - z_1^3 = t^3(\frac{h}{t})^3 + 3t^2(\frac{h}{t})^2\left[\frac{E_b - E_c(\frac{h}{t})^2}{\frac{2}{t}(E_b + E_c\frac{h}{t})}\right] + \quad (119b)$$

$$+ 3t(\frac{h}{t})\left[\frac{E_b - E_c(\frac{h}{t})^2}{\frac{2}{t}(E_b + E_c\frac{h}{t})}\right]^2$$

$$e(\frac{h}{t}) = \rho = \frac{t}{g}\left[\gamma_b + \gamma_c\frac{h}{t}\right] \quad (119c)$$

Equation 112 again yields Equation 115, however, e, f, g and their derivatives now come from Equations 119 and are much more complex. Substituting in Equation 115 and simplifying yields

$$fg' - f'g = 0 \quad (120)$$

As seen from Equation 119, f and g are rather complicated functions of h/t as are the derivatives f' and g'. However, substitution of these functions into Equation 120 and much algebraic manipulation finally yields

$$\frac{3}{2}\left(\frac{E_c}{E_b}\right)^4\left(\frac{h}{t}\right)^8 + 6\left(\frac{E_c}{E_b}\right)^4\left(\frac{h}{t}\right)^7 + \left[-6\left(\frac{E_c}{E_b}\right)^2 + 6\left(\frac{E_c}{E_b}\right)^3 + 6\left(\frac{E_c}{E_b}\right)^4\right]\left(\frac{h}{t}\right)^6 + \quad (121)$$

$$+ \left[-18\left(\frac{E_c}{E_b}\right)^2 + 12\left(\frac{E_c}{E_b}\right)^3\right]\left(\frac{h}{t}\right)^5 - 15\left(\frac{E_c}{E_b}\right)^2\left(\frac{h}{t}\right)^4 +$$

$$+ \left[12\left(\frac{E_c}{E_b}\right) - 18\left(\frac{E_c}{E_b}\right)^2\right]\left(\frac{h}{t}\right)^3 + \left[6 + 6\left(\frac{E_c}{E_b}\right) - 6\left(\frac{E_c}{E_b}\right)^2\right]\left(\frac{h}{t}\right)^2 +$$

$$+ 6\left(\frac{h}{t}\right) + \frac{3}{2} = 0$$

Since η_c is small, $E_c \approx E_s$ and $\frac{E_c}{E_b} = \frac{E_s}{E_b}$ for this case.

For a given coating and metal, the smallest positive real root of Equation 121 is the thickness ratio for which an optimum amount of damping occurs. By use of a computer solution, results were obtained for a wide range of strength ratios and appear in Figure 34. These results apply only when damping is small. (It will be noted that the values of h/t from Figure 34 are a little larger than those read from the charts for large damping.) These results are applicable in the case of both beams and plates with single unconstrained coatings.

LITERATURE CITED

1. Kervin, E. M., "Damping of Flexural Waves by a Constrained Visco-Elastic Layer," *Journal of the Acoustical Society of America*, Vol. 31, No. 7, July, 1959, pp. 952-962.

2. Ungar, E. E., and Ross, D., "Damping of Flexural Vibrations by Alternate Visco-Elastic and Elastic Layers," *4th Midwestern Conference on Solid Mechanics*, 1959, p. 441.

3. Whittier, J. S., "The Effect of Configurational Additions Using Viscoelastic Interfaces on the Damping of a Cantilever Beam," *WADC Technical Report 58-568*, 1958.

4. Mead, D. J. and Froud, G. R., "The Damping of Aluminum Honeycomb Sandwich Beams," *U.S.A.A. Report No. 144*, University of South-Hampton, 1960.

5. Thorn, R. P., "Built-in Damping," *Machine Design*, November 25, 1965, p. 174.

6. Jones, I. W., and Blasingame, W., "An Analytical and Experimental Evaluation of the Damping Capacity of Sandwich Beams with Visco-elastic Cores," *ASME Paper No. 66-WA/UnT-3*, 1966.

7. DiTaranto, R. A., and Blasingame, W., "Composite Damping of Vibrating Sandwich Beams," *ASME Paper No. 67-Vibr-6*, 1966.

8. Oberst, von Hermann, "Uber die Dampfung der Biegeschwingungen Dunner Bleche Durch Feste Haftende Belage," *Acustica*, Vol. 2, 1952, pp. AB 181-194.

9. Lienard, P., "Les Mesures d'Amortissement dan les Materiaux Plastiques ou Fibreux," *Annales des Telecommunicatione*, Vol. 12, No. 10, 1957, pp. 359-366.

10. Plass, H. J., "Damping of Vibration in Elastic Rods and Sandwich Structures by Incorporation of Additional Viscoelastic Material," *Third Midwestern Conference on Solid Mechanics at University of Texas*, 1957.

11. Lal, J. S., *Damping of Flexural Vibrations in Beams by Viscoelastic Materials*, Master's Thesis, Georgia Institute of Technology, Atlanta, Georgia, 1966.

12. Myncke, H. and van Itterbeek, A., "Vibrations of Plates Covered with a Damping Layer," *Acustica*, Vol. 3, 1958, pp. 207-212.

13. Giddens, D. P., "Investigation of the Effect of Various Damping Materials on Dynamic Stresses in Flat Panels," *Lockheed-Georgia Co. Report No. SRD 72-21-419*, 1963.

14. Hertelendy, P. and Goldsmith, W., "Flexural Vibrations of an Elastic Plate with Two Symmetric Viscoelastic Coatings," *Journal of Applied Mechanics Paper No. 66-WA/APM-20*, 1965.

15. Alfrey, T. and Dory, P., "The Methods of Specifying the Properties of Viscoelastic Materials," *Journal of Applied Physics*, Vol. 16, 1945, pp. 700-713.

16. Nolle, A. W., "Dynamic Mechanical Properties of Rubberlike Materials," *Journal of Polymer Science*, Vol. 5, 1950, pp. 1-54.

17. Kimel, Kirmser, Patel, and Raville, "Natural Frequencies of Vibration of Simply-Supported Sandwich," *Fourth Midwestern Conference on Solid Mechanics*, 1959, pp. 441-449.

18. Young, D. and Felgar, R. P., "Tables of Characteristic Functions Representing Normal Modes of Vibration of a Beam," *The University of Texas Circular No. 44*, 1949.

19. Boresi, A. P., *Elasticity in Engineering Mechanics*, Prentice-Hall, Inc., 1965.

20. Felgar, R. P., "Formulas for Integrals Containing Characteristic Functions of a Vibrating Beam," *The University of Texas Circular No. 14*, 1950.

21. Timoshenko, S., *Vibration Problems in Engineering*, Nostrand Co., 1937.

22. Hurty, W. C. and Rubenstein, M. F., *Dynamics of Structures*, Prentice-Hall, Inc., 1964.

23. Hansen, H. M. and Chenea, P. F., *Mechanics of Vibration*, Wiley and Sons, New York, 1952.

24. Burington, R. S., *Handbook of Mathematical Tables and Formulas*, Handbook Publishers, Inc., Sandusky, Ohio, 1958.

25. Warburton, G. B., "The Vibration of Rectangular Plates," *Proceedings of the Institution of Mechanical Engineers*, Vol. 168, pp. 371-384.

26. Van Santen, G. W., *Introduction to a Study of Mechanical Vibration*, Elsevier Press Inc., Houston, Texas, 1953, pp. 186-188.

27. Preiss, G. M. and Skinner, D. W., "Damping Characteristics of Elastomers," *Rubber Age*, August, 1965.

28. Harris, C. M., *Shock and Vibration Handbook*, McGraw-Hill, New York, 1961, Vol. III, p. 36-19.

29. Tse, Morse, and Hinkle, *Mechanical Vibrations*, Allyn and Bacon Co., Boston, Mass., 1963, pp. 34-39.

30. Langhaar, Henry L., *Energy Methods in Applied Mechanics*, Wiley and Sons Inc., New York, 1962, pp. 121-125, 161.

OTHER REFERENCES

1. Bergen, J. T., *Viscoelasticity, Phenomenological Aspects*, Academic Press, New York, 1960.

2. Ferry, J. D., *Viscoelastic Properties of Polymers*, Wiley and Sons, New York, 1961.

3. Jones, D. I. G., "Some Aspects of the Analysis of Damping and Vibration in Simple Structures," *AFML TR-65-151*, 1965.

4. Kolsky, H., *Stress Waves in Solids*, Oxford, Clarendon Press, 1953.

5. Langhaar, H. L., *Dimensional Analysis and Theory of Models*, John Wiley and Sons, New York, 1951.

6. Mead, D. J. and Pearce, T. G., "The Optimum Use of Unconstrained Layer Damping Treatments," *ML-TDR-64-51*, 1964.

7. Oberst, H. and Becker, G. W., "Uber Die Damping Der Biegeschwingungen Dunner Bleche Durch Fest Haftende Belage II," *Acustica*, Vol. 4, 1954, pp. 433-444.

8. Oberst, H. and Bohn, L., "Progress in the Development of Vibration Damping Materials," *WADC Technical Report 59-676*, 1959, pp. 185-196.

9. Ruzicka, J. E., *Structural Damping*, ASME, 1959.

10. Schwarzl, F., "Forced Bending and Extensional Vibrations of a Two-Layer Compound Linear Viscoelastic Beam," *Acustica*, Vol. 8, 1958, pp. 164.

11. Snowden, J. C., "Representation of the Mechanical Damping Possessed by Rubberlike Materials and Structures," *Journal of the Acoustical Society of America*, No. 6, June, 1963.

12. Whittier, J. S., "Rheological Properties of Adhesives Considered for Interface Damping," *WADD Technical Report 60-280*, 1960.

VITA

Britt K. Pearce was born in Greenville, South Carolina, on December 15, 1942, the son of Clarence and Bobbie Pearce. Upon graduation from Greenville High School in 1961, he began his college career at Clemson University in Clemson, South Carolina.

In 1965, he received his BSME degree and was commissioned a second lieutenant in the U. S. Army Reserve. He delayed entry into the service to enter the Graduate Division of Georgia Institute of Technology the following fall. In 1966 he received his MSME degree and continued his work there in pursuit of the Ph.D. degree.

Mr. Pearce was married in July, 1966, to the former Carey Ann Hunter, a graduate of Furman University and a native of Greenville, South Carolina.